SUBMERGED BREAKWATER INFLUENCE ON BEACH HYDRODYNAMICS. A 2DV APPROACH.

Barcelona, July 1996

Laboratori d'Enginyeria Marítima
Universitat Politècnica de Catalunya
Dept. Enginyeria Hidràulica, Marítima i Ambiental

Technische Universiteit Delft
Faculteit der Civiele Techniek
Vakgroep Waterbouwkunde en Geotechniek
Sectie Waterbouwkunde en Offshore

Author: Rosemarijn Dekker
Supervisors
UPC: Ir. J.A. Jiménez
Ir. F.J. Rivero
TU Delft Prof. K. d'Angremond
Dr. Ir. J. Van de Graaff

PREFACE

This paper is the master's thesis of Rosemarijn Dekker at Delft University of Technology. Prepared at Universitat Politècnica de Catalunya in Barcelona, Spain. The exchange took place from December 1995 until June 1996 as part of the ERASMUS/SOCRATES program of the European Union.

The thesis committee consists of the following persons:

UPC:	Ir. J.A. Jiménez
	Ir. F.J. Rivero
TU Delft	Prof. K. d'Angremond
	Dr. Ir. J. Van de Graaff

The author wishes to express her gratitude to the valuable assistance of J. Jiménez. Also thanks to Francisco Rivero, Martin Groenewoud and Jan van de Graaff.

Finally I would like to acknowledge the European Union for their financial support that made this stay possible.

ABSTRACT

This master's thesis is written using data from experiments performed in the framework of the Human Capital and Mobility program of the European Union. Six universities work together to solve some of the unknown aspects related to the use of submerged breakwaters along sandy coasts.

In this study data from 2DV tests carried out in Delft and Barcelona are used, from Delft are taken the morphological data and from Barcelona the velocity measurements. By varying the wave height and the wave period of the incoming wave the influence of these parameters on hydro- and morphodynamics are investigated. To analyse the performance of submerged breakwaters in beach profile morphodynamics the following parameters characterising beach changes are analysed; erosion volume, shoreline retreat, beachface slopes, developed profiles, bottom height change and cross shore transport rate.

The influence of the wave height on the development of the profile is very clear, a larger wave height showing a larger change. The influence of the wave length is less evident and contrary to expected. A larger wave length is causing larger changes. The breakwater is in general reducing the changes of the beach profile, having a larger influence on the steeper and higher incoming waves.

The validity of an energetic transport model (Bailard) and a hydro-morphodynamic numerical model (UNIBEST_TC) is verified for these experiments. The transport volumes calculated from the bottom profile changes measured in Delft are compared with transport volumes calculated from the velocity measurements in Barcelona, using the Bailard formula, and with transport volumes calculated with UNIBEST_TC. The transport volumes measured in Delft are in general larger than the calculated transport volumes. The quantity of the calculated transport volumes is restricted by the maximum values for the transport coefficients applied in the Bailard formula and UNIBEST_TC, taken from the literature.

TABLE OF CONTENTS

PREFACE

ABSTRACT

TABLE OF CONTENTS

CHAPTER 1 INTRODUCTION

1.1 Introduction

A lot of sandy coasts all over the world have to contend with erosion. There has been looked for different solutions to stop or reduce this erosion. This is especially important if the hinterland has a large economic importance. In several countries a common method to undo this erosive effects is to compensate the lost sediment by beach nourishment. As this is an expensive method and it has to be repeated endlessly there has been searched for other solutions. One of these is the application of submerged shore parallel breakwaters. The aim of these breakwaters is to reduce or stop the erosion by influencing the wave characteristics of the incoming waves while they pass over the breakwater and forming an impassable barrier for particles moving on the bottom.

In the framework of the Human Capital and Mobility program of the European Union six universities work together to solve some of the unknown aspects related to the use of submerged breakwaters along sandy coasts. Several experiments have been performed to investigate the influence of a submerged breakwater on hydrodynamical and morphological processes.

1.2 The 'dynamics of beaches' project

This master's thesis is written with the use of data obtained in experiments performed as part of the Dynamics of Beaches project. The Dynamics of Beaches project is a part of the HCM-framework. This particular project is a co-operation of six European universities, viz.:

- Aristotle University of Thessaloniki (Greece)

- University of Gent (Belgium)

- University of Liverpool (United Kingdom)

- University College of Cork (Ireland)

- Delft University of Technology (The Netherlands)

- Universitat Politècnica de Catalunya (Spain)

The objectives of the Dynamics of Beaches project are to improve the existing knowledge on physical processes pertaining to the nearshore region (including the surfzone), without and with a submerged breakwater by generating high quality data.

At different universities have been performed tests concentrating on a certain aspect of the investigations. In this master's thesis data from 2 DV tests carried out in Delft

and in Barcelona are used. In Delft the main aim was looking at the morphological response of the profile applying wave fields with different characteristics and repeating the tests for the case without and with breakwater. In Barcelona the hydrodynamic characteristics have been measured, applying wave fields with the same characteristics as in the Delft experiment and performed as well for the case without and with breakwater.

1.3 Aims of this study

To analyse the performance of submerged breakwaters in beach profile morphodynamics using experimental data. To do this different parameters characterising beach changes are analysed (erosion volume, shoreline retreat, beachface slopes, developed profiles, bottom height change and cross shore transport rate).
An additional objective is to analyse the performance of an energetic transport model (Bailard) to predict 'real' transport rates. Additionally this was also done with a full model (including wave propagation and hydrodynamics) UNIBEST_TC.

1.4 Layout

In the next chapter the effectivity of a submerged breakwater and the in these experiments used breakwater is described. The experimental set-up of the experiments in Delft and in Barcelona and the performed measurements are given in Chapter three. In Chapter four the in Delft obtained morphological data are analysed using the following parameters; erosion volume, shoreline retreat, beachface slopes, developed profiles, bottom height change and cross shore transport rate, concentrating on the effect of the submerged breakwater. A short description of existing types of cross shore profile models is given in Chapter five, finishing with a more extensive description of the here used model UNIBEST_TC. In Chapter six a description and the results of the carried out analysis comparing the cross shore transport volumes is given. This comparison is done using transport rates derived from the morphological Data in Delft, from the calculation with the Bailard formula using the velocity data from Barcelona and from the application of UNIBEST_TC. In the last chapter (seven) conclusions are drawn and recommendations are given.

CHAPTER 2 SUBMERGED BREAKWATERS

2.1 Introduction

This chapter will start with a short description of the type of breakwater relevant for the experiments. Which is an offshore breakwater parallel to the shore. The influence of the breakwater on the hydraulic performance of the waves with the energy balance of Powell and Allsop (1985) will be mentioned in the first paragraph. In the second paragraph the effectiveness of submerged breakwaters and the influence of the different parameters on this effectiveness is described and the chapter will conclude with a description of the breakwater as was used during the experiment.

Offshore breakwaters parallel to the shore can be useful if the cross-shore sediment transport mode prevails. They can be used to protect the beaches from strong eroding wave action. They influence the profile because the wave characteristics change while passing them and as well because they form an impassable barrier for particles moving on the bottom. The functionality of a breakwater is its capacity for dissipating the energy of the incident wave. The higher the hydraulic efficiency of the structure, the lower will be the amount of energy transmitted to the protected zone. Of these breakwaters there are two types: submerged or reef breakwaters and emerging breakwaters.

The advantages of submerged breakwaters are:
- Their influence on the waves is depending on the size of the waves, the influence is larger on the larger waves. During normal weather circumstances, with low energy waves, the waves can pass and there will be a better water exchange between the inner and outer zones of the submerged breakwater, which reduces the waterlogging area.
- Because the water can pass over them, they can be built as continuous structures, thus avoiding the gaps in which there will be a strong seadirected flow. This is a theoretical point, since when this is put in practice the expenses rise too much.
- They do not spoil the aesthetic aspect of the beach.
- They may result more economic than emerging structures.

The disadvantages of submerged breakwaters are:
- They can only be used in areas with small tidal changes, the effectivity depends largely on the freeboard.
- The influence on the waves is smaller, behind these breakwaters higher levels of wave activity lare noted.

2.2 The hydraulic performance

An exact analysis of the interaction mechanisms between the breakwater and wave motion is very complex, because of the different processes which take place while the waves pass the breakwater, e.g. breaking, friction, transmission through the structure. It is difficult to detect which effect is caused by which mechanism due to the mutual interactions occurring among them.

Powell & Allsop (1985) investigated stability of the structure and the reflection, transmission and dissipation of wave energy. They considered the following energy balance:

$$E_i = E_d + E_r + E_{to} + E_{tt} \qquad (2.1)$$

where E_i is the incident wave energy
E_d is the dissipated wave energy
E_r is the reflected wave energy
E_{to} is the transmitted wave energy by overtopping, and
E_{tt} is the transmitted wave energy through the structure,

and defined the corresponding coefficients:

$$K_r = \frac{H_r}{H_i} = \sqrt{\frac{E_r}{E_i}} \qquad K_{to} = \frac{H_{to}}{H_i} = \sqrt{\frac{E_{to}}{E_i}} \qquad K_{tt} = \frac{H_{tt}}{H_i} = \sqrt{\frac{E_{tt}}{E_i}}$$

$$K_d = \sqrt{\frac{E_d}{E_i}} \qquad K_t = \sqrt{K_{to}^2 + K_{tt}^2} \qquad (2.2)$$

For submerged and permeable structures shorter waves will propagate above the breakwater while longer waves will pass partly above the structure and partly through it, depending on the relative freeboard (F/H_i), the breakwater permeability, the water depth and the wave period. Increasing the crest width above that needed for stability, has little effect on the wave transmission.

- Reflection

Some proportion of the incident wave energy will be reflected on the structure. The amount of reflected energy is related to the permeability of the structure, the height of the structure and the wave characteristics. In general the less permeable and higher the structure and the longer the incident wavelength the larger the amount of reflected energy. The highest content of reflected energy is to be found at the lowest frequency of the spectrum (Damiani (1995)). Shorter or steeper waves may dissipate more of their energy at the structure and reflect a lower proportion. The most significant erosion is found in front of impermeable barriers.

- Friction

Flowing over the structure, some energy will be dissipated in turbulent friction. The amount of dissipated energy depends on the width of the berm and the wave characteristics. The larger the berm width and the longer the wave period, the more energy will be dissipated. Longer period waves are likely to dissipate energy and short period waves can pass over relatively unchanged.

- Breaking

Depending on the crest freeboard and the incident wave conditions energy might be dissipated by breaking on the structure. The original wave will be changed in one or more waves with a smaller height and a shorter period. The amount of dissipated energy depends strongly on the incident wave period and wave height. The shorter and steeper the waves, the more they will break on the structure and the larger the amount of dissipated energy. The breaking type is generally plunging, breakwaters are usually so designed as to force this kind of breaking to avoid that the eddy flows produced by breaking may cause undesired erosion at the landside toe of the breakwater.

- Transmission

If the breakwater is permeable some wave energy might be transmitted through the structure. This amount of transmitted energy depends strongly on the permeability and the wave characteristics. The longer the waves and the more permeable the construction, the larger the amount of transmitted energy. Transmission is negligible for short period waves, but may be of importance for porous structures subjected to long waves.

- Set-up

Because the water can not flow freely back to the sea the set-up increases behind the submerged breakwater in comparison to the situation without breakwater. This set-up causes a withdrawal of the waterline (Damiani (1995)).

2.3 The effectiveness of submerged breakwaters

This section is a bit short, caused by the limited availability of articles on this subject in the literature. Until now there has been done more research on emerging breakwaters. The effectiveness of submerged breakwaters depends on the shape, berm width, submergence of the barrier, the tide movement and the incident wave characteristics. The shoreline retreat is more or less the same comparing experiments with and without breakwater, the breakwater only slows down the process of the backing of the shoreline (Chiaia et al. (1992)).

- Barrier height

With an increasing barrier height, the transmitted wave height is reducing. The height of the barrier does not have a significantly influence on the waterparticle velocities at the offshore foot of the structure. If there will be deposition of sediment or scouring at the onshore foot is depending on the barrier height and the wave height; for small barrier heights there is a depositing behaviour. The amount of set-up caused by the barrier is strongly related to the height of the structure and the wave height (Aminti et al. (1983)). The level of reflection is low in cases of higher submergence. The set-up is very sensitive to the variations in submergence (Damiani (1995)).

- Berm width

The wave attenuation and the barrier produced set-up increase as the berm width increases. In order to force wave breaking on the structure berm its width should be at last 7-9 times the submergence (Aminti et al. (1983)). The effect of the change of the berm width on the waves is much smaller than the effect of the barrier height.
The influence of the width of the berm on breaking, which is the major cause of dissipation in cases with a low value of submergence, is small. The berm width influences more the amount of friction, the dissipation of energy is relatively consistent for high values of submergence. The berm width does not seem to be determinant for the reflection. The variation of the berm width hardly influences the set-up (Damiani (1995)).

- Offshore face slope

The offshore face slope seems not to have evidence influence on the wave transmission.

- Effect of roughness

As the roughness increases, the energy dissipation and the wave attenuation increase as well (Aminti et al. (1983)). The roughness has less effect on the wave transmission than the barrier height and the berm width.

2.4 Breakwater cross-section in the experiment

The following is taken from the Test Definition Report. The experiments were conducted with a small scale model of a submerged breakwater. The proto-type was designed in accordance with the steps outlined below.

1. The breakwater has been designed with a permeable core, but it is constructed with an impermeable core for simplicity. From the hydrodynamic point of view
   this has been shown by several authors to be a reasonable approach (Van der Meer and Daemen (1994) and Davies and Kriebel (1992)).

2. The armourlayer, consisting of 2 layers of rock stones, has been designed according to the formula presented in Van der Meer (1990):

   $$\frac{h_c}{h} = (2.1 + 0.1 * S)\exp\left(-0.14 * N_s^*\right) \qquad (2.3)$$

   where the spectral stability number N_s^* is defined by Ahrens (1987) as

   $$N_s^* = \frac{H_s}{\Delta D_{n50}} s_p^{-1/3} \qquad (2.4)$$

   and S = damage level (here chosen as 2, corresponding to start of damage), Δ = buoyant mass density (here 1.573), D_{n50} = nominal diameter, and

s_p = local wave steepness. Although the formula presents some uncertainties, mainly due to the scatter in the data to which it was fitted, it is normally presented as being on the safe side. From the test matrix (see table 3.1) it can be seen that the ratio between the crest height and the water depth at the seaward toe is constant for all experiments, that is h_c /h = 0.75. Two local wave steepnesses are being investigated: a design wave height of 4.0 m and corresponding wave periods of 8 and 9 s, respectively. The calculations lead to an average rock weight of w_{50} = 1.416 ton and D_{n50} = 0.812 m, for a rock density of 2.65 ton/m^3.

3. the crest width was chosen as 3 * D_{n50} and the thickness of the armour layer as 2 * D_{n50}.

4. the gradation of the stones for the armour layer followed the log-linear relationship:

$$W_y = W_0 \left(W_{100} / W_0 \right)^{y/100} \qquad (2.5)$$

where the mass of the lightest block is W_0 = 1 ton, and the mass of the heaviest block is W_{100} = 2 ton. W_y gives for a certain y (percentage of stones) the maximum mass.

The resulting proto-type design is shown in Figure 2.1.

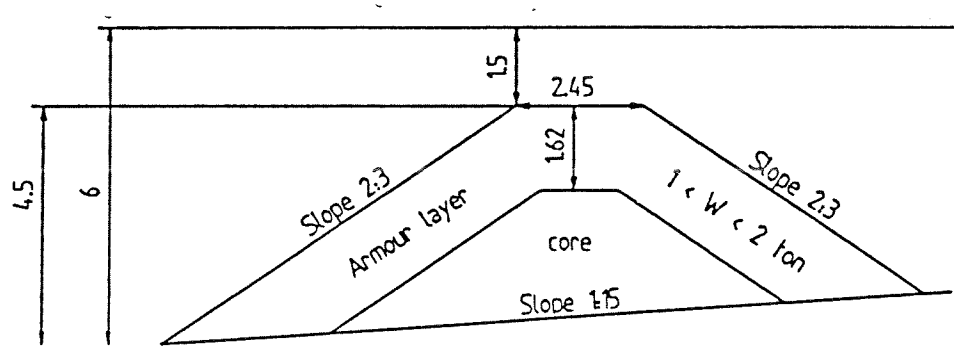

Figure 2.1 *Submerged breakwater cross-section, proto-type values; all dimensions are given in meters*

CHAPTER 3 EXPERIMENTAL SET-UP

In this chapter an overview of the characteristics of the experiments used in this study will be presented. The experiments were performed in the framework of the 'Dynamics of Beaches' project, which is part of the European Union Human Capital and Mobility Programme. In the second and the fourth paragraph consecutively the measurements performed at the Delft University of Technology (DUT) and at the Universitat Politècnica de Catalunya (UPC) are described and the scaled down wave parameters are mentioned. In the third paragraph the in this thesis used measurements of the beach profile development obtained in Delft and the way they are calculated from the data are explained. In the last paragraph a short description of the in Barcelona performed velocity measurements are given.

3.1 Prototype test matrix

The following test matrix was used for the experiments (see Table 3.1). The ideas behind the different combinations of parameters in the test matrix will be explained in the following section taken from the Test Definition Report.

Test-	F/H_s	H_s/L_{0p}	T_p	H_s	h	F	H_s/L_p
case	-	%	(s)	(m)	(m)	(m)	%
A	1.00	1.50	8.0	1.5	6.0	1.5	2.61
B	1.00	2.67	6.0	1.5	6.0	1.5	3.67
C	1.00	3.84	5.0	1.5	6.0	1.5	4.66
D	0.75	2.61	7.0	2.0	6.0	1.5	4.06
E	1.50	2.56	5.0	1.0	6.0	1.5	3.01

Table 3.1 Prototype Test Matrix for all experiments (HCM-programme). Prototype scale

with:
F = freeboard ($F = h - h_c$)
H_s = significant wave height
L_{0p} = offshore wave length for peak period T_p
T_p = spectral peak period
h = waterdepth at toe of structure
h_c = crest height
L_p = local wave length associated with the peak period (Airy wave theory)

Two non-dimensional parameters have been considered to be the most significant for the hydrodynamic behaviour of a submerged breakwater: a wave parameter (the wave steepness) and a geometry parameter (the relative freeboard, F/H_s). In the following

the wave steepness is defined by H_s/L_{0p}, which relates to the Irribarren number, $(\tan\alpha)/\sqrt{H/L_{0p}}$. The correct local wave steepness at the position of the breakwater is also calculated for comparison.
To cover a reasonable range of normal wave steepnesses, that is from moderately long waves with low steepness to relatively short and steep waves, H_s/L_{0p} is suggested to vary within the range 1% to 4%. Likewise the relative freeboard must be chosen so that the submerged breakwater affects significantly wave transmission without acting as a non-submerged breakwater. F/H_s is suggested to vary within the range 0.75 to 1.5.

The general idea is to cover a reasonable range of variation of the aforementioned variables with 5 test cases: a central case and 4 additional test cases, in which H_s/L_{0p} is increased and decreased for a fixed value of F/H_s and vice versa (i.e. defining a diamond shaped set of test conditions). As the two non-dimensional parameters, F/H_s and H_s/L_{0p} consist of 3 dimensional parameters (two wave parameters and one geometry parameter) the possible solutions are:

1. Fixing L_{0p} (i.e. T_p) and varying H_s and F (i.e. h)
2. Fixing F (i.e. h) and varying H_s and L_{0p} (i.e. T_p)
3. Fixing H_s and varying L_{0p} (i.e. T_p) and F (i.e. h)

It was decided to fix the breakwater cross-section in all experiments. Therefore a variation of F should be obtained by varying h. In theory this is not a problem, but it is generally a more reasonable solution to fix the water depth for all experiments for practical reasons, e.g. the tuning of the active absorption limit for reflected waves and the time consuming process of adding or removing water especially in the large scale wave flumes. Hence, it was decided to carry out the experiments for a wave matrix following solution 2.
The proto-type test matrix which applies to all experiments to be conducted is shown in Table 3.1. This matrix provides a nearly regular 'diamond pattern' in the (F/H_s, H_s/L_{0p})-plane, a distorted 'diamond pattern' in the (F/H_s, H_s/L_p)-plane and a vertical line in the (H_s,F)-plane (see Figure 3.1)

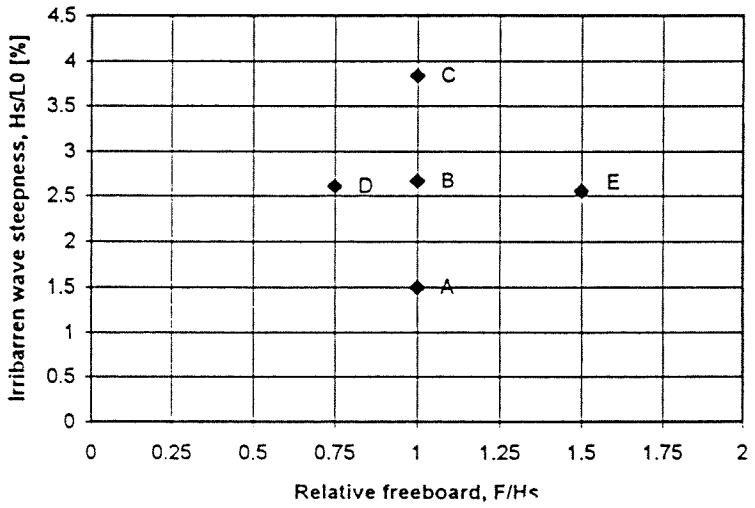

Figure 3.1 Diamond pattern of the Prototype Test Matrix

3.2 Experimental set-up in the Laboratory of Fluid Mechanics at DUT

In what follows a basic description of the characteristics of the experiments performed at the Laboratory of Fluid Mechanics at DUT will be presented. A full detailed description can be found in Claessen and Groenewoud (1995). The experiments where carried out at the DUT 'Lange Speurwerkgoot', a 32 m long, 1 m high and 0.8 m wide wave flume (see Figure 3.2), using an experimental scale of 1:15.

The waveboard can generate irregular waves and absorb only the reflection of the long waves. Considering the dimensions of the wave flume the experiments were performed at scale 1:15. According to the testprogram tests were done without and with breakwater with an 1 in 15 slope and a movable bed. The bed consisted of sand with a D_{50} = 95 μm (D_{10} = 76 μm, D_{90} = 131 μm). The particle fall velocity (w_s) is approximately 0.01 m/s. The first part of the slope is a non-movable bed made out of concrete.

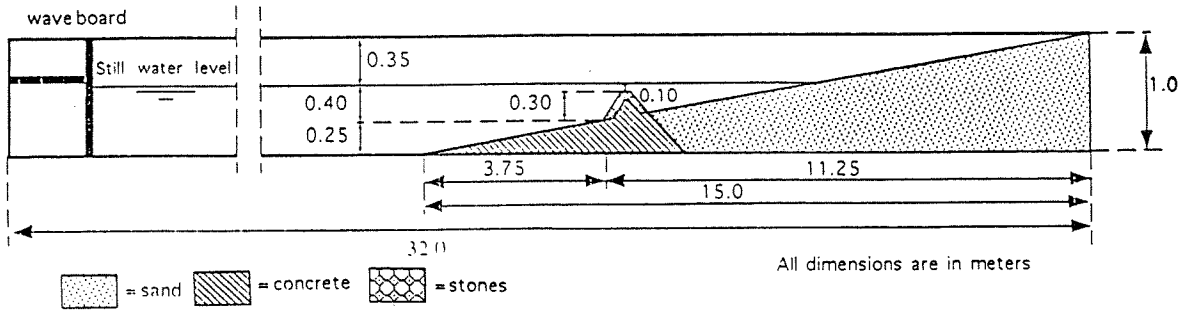

Figure 3.2 *The 'Lange Speurwerkgoot' in the Laboratory of Fluid Mechanics at Delft University of Technology (DUT)*

3.2.1 Test matrix for the scale model

The prototype wave conditions prescribed in the Test Definition Report had to be scaled down to match the scale of the model in the wave flume (1:15). The resulting experimental conditions can be seen in Table 3.2.

Test-	F/H_s	H_s/L_{0p}	T_p	H_s	h	F	H_s/L_p	L_{0p}
case	-	%	(s)	(m)	(m)	(m)	%	(m)
A	1.00	1.50	2.07	0.1	0.4	0.1	2.61	6.69
B	1.00	2.67	1.55	0.1	0.4	0.1	3.67	3.75
C	1.00	3.84	1.29	0.1	0.4	0.1	4.66	2.60
D	0.75	2.61	1.81	0.133	0.4	0.1	4.06	5.12
E	1.50	2.56	1.29	0.067	0.4	0.1	3.01	2.60

Table 3.2 *Model Test Matrix experiments at DUT*

3.2.2 Duration of the experiments

Each experiment lasted for 7.5 hours. It occurred that after 7.5 hours of exposing the bottom profile to waves enough bottom profile evolution has taken place to draw conclusions. This period of 7.5 hours was divided into four intervals, viz.:

Interval 1	from t = 0.0 hours till t = 0.5 hours	Δ t = 0.5 hours
Interval 2	from t = 0.5 hours till t = 1.5 hours	Δ t = 1.0 hours
Interval 3	from t = 1.5 hours till t = 3.5 hours	Δ t = 2.0 hours
Interval 4	from t = 3.5 hours till t = 7.5 hours	Δ t = 4.0 hours

Before the start of Interval 1, between the intervals and after Interval 4 the bottom profile has been measured. The duration of each following interval doubles. This is done because morphological processes often happen on a logarithmic time scale. During the different intervals wave height, velocity and sediment concentration measurements have been performed.

3.2.3 Wave spectra

The generated wave spectra were of the Jonswap-type with a peak enhancement factor γ equal to 3.3. The time duration of each generated wave spectrum was 15 minutes.

3.3 Performed measurements in Delft

Four types of measurements have been carried out; profile measurements, wave height measurements, velocity measurements and sediment concentration measurements. Only the profile measurements will be discussed here since these measurements are used in the present study.

3.3.1 Measurements of the beach profile development

The profile is measured in two different ways. The PROFO (= electronic profile-follower) measurement started at the beginning of the slope at the position x = 0.00 m and ended near the shoreline at position x = 9.20 m in the experiments without breakwater and started at the position x = 5.00 m and ended at the position x = 9.20 m in the case with breakwater. This instrument needs a certain depth to register the correct values, so from x = 9.25 m until x = 12.00 m the depth is measured using a scale which was attached to the side of the wave flume. The jump in the bed in the profile graphs is caused by the fact that there is a difference in profile development over the width of the wave flume, the side walls cause boundary effects. The visual profile measurement taken of the bed at the side wall is a bit lower than the PROFO measurement taken of the bed in the middle of the flume.

During one experiment five times a profile measurement was performed:
Profile measurement no. 0 at t = 0.0 hours (before Interval 1)

Profile measurement no. 1 at t = 0.5 hours (after Interval 1)
Profile measurement no. 2 at t = 1.5 hours (after Interval 2)
Profile measurement no. 3 at t = 3.5 hours (after Interval 3)
Profile measurement no. 4 at t = 7.5 hours (after Interval 4)

3.3.2 Conversion of the profile measurements

The profiles are calculated from the original measurements.

- PROFO measurements

The electronic profile follower (=PROFO) measures the bed height in Volts. This signal is registered by a computer. Afterwards these measured Volt values have to be translated to bed heights (y-value [m]) and to a corresponding position in the wave flume
(x-value [m]).

The relation between measured Volt values and bed heights is derived from the calibration of the PROFO meter. In this calibration a few points at different heights in the flume are measured. At these points the real height is known and the corresponding Volts can be measured. In all the experiments the measured calibration values were the same, so the same formula can be used for every measurement.
'height' = (('volt'-0.2)/0.236)*5/100 [m].

The PROFO meter takes a sample every 50 μs. Because of irregularities in the rails the trolley, to which the PROFO meter was attached, didn't move across the profile in exactly the same time period every measurement, therefore the PROFO measurements contained a different amount of samples. These measurements all covered the entire bed. It is not possible to compare profile measurements with a different number of samples, therefore all the measurements were resampled to 1840 samples (in case of no breakwater present).

In case of a test with breakwater present, the length of the bed measured with a PROFO is much shorter (total length = 4.20 m), because only the bed landwards of the breakwater is measured. In this case a different number of samples was measured as well. These measurements are resampled to 840 samples. In both cases the input files are resampled to a sampling distance of 0.005 m.

- Visual measurements

The visual measurements are read from a scale attached to the side of the wave flume and written down in a Table. To convert these values measured in centimetres to bottom height values, the following formula is used:
height = ((value*39/40)+45.5)/100 [m]

3.4 Experimental set-up at LIM / UPC

In the following a short description of the at the UPC performed experiments is given. They were carried out in the Canal de Investigación y Experimentación Marítima, a wave flume with a length of 100 m, a width of 3 m and a height of 5 m, of the Laboratorio de Ingeniería Marítima at la Universitat Politècnica de Catalunya (UPC) (see Figure 3.3).

The waveboard can generate irregular waves and absorbs all the reflected waves. Considering the dimensions of the wave flume the experiments were performed at scale 1:4. According to the testprogram tests were done without and with breakwater with a 1 in 15 slope. The slope is made out of concrete, the last part is composed of rocks to reduce the reflection of the waves.

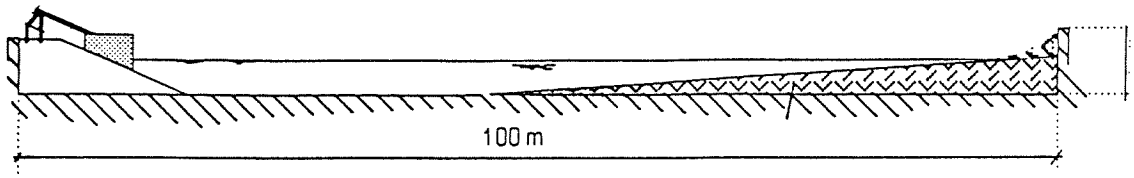

Figure 3.3 *The 'Canal de Investigación y Experimentación Marítima' of the Laboratorio de Ingeniería Marítima at la Universitat Politècnica de Catalunya (UPC)*

The prototype wave conditions prescribed in the Test Definition Report had to be scaled down to match the scale of the model in the wave flume (1:4). The resulting experimental conditions can be seen in Table 3.3. Each experiment lasted for 7.5 hours. The created spectra were Jonswap 3.3 spectra.

Test-	F/H_s	H_s/L_{0p}	T_p	H_s	h	F	H_s/L_p	L_{0p}
case	-	%	(s)	(m)	(m)	(m)	%	(m)
A	1.00	1.50	4.0	0.38	1.5	0.38	2.61	24.98
B	1.00	2.67	3.0	0.38	1.5	0.38	3.67	14.05
C	1.00	3.84	2.5	0.38	1.5	0.38	4.66	9.76
D	0.75	2.61	3.5	0.50	1.5	0.38	4.06	19.13
E	1.50	2.56	2.5	0.25	1.5	0.38	3.01	9.76

Table 3.3 *Model Test Matrix experiments at UPC*

3.5 Short description of the performed measurements in Barcelona

At both sides of the wave flume a rail is attached on top of the walls. A carriage can be driven along the wave flume and moved along the canal. To this carriage several measuring-instruments are attached, it is positioned at the different verticals along the wave flume to be able to measure the desired values (see Figure 3.4). At each vertical the experiment and measurements are repeated.

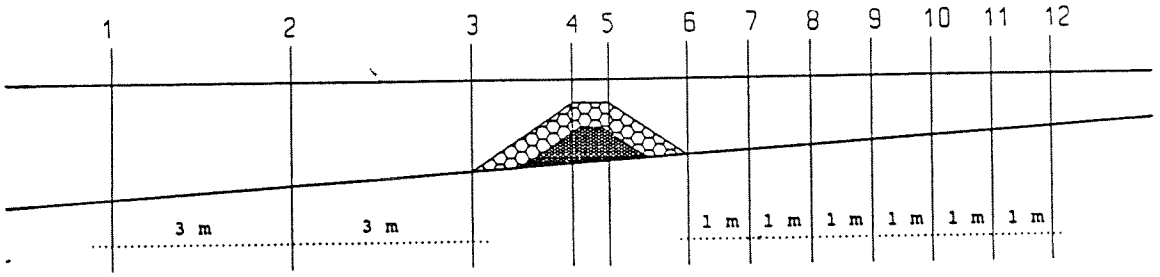

Figure 3.4 Vertical positions of measurements at UPC (scale 1:4)

Three types of measurements have been carried out; wave height measurements, pressure measurements and velocity measurements. Only the in this study used velocity measurements are briefly mentioned. To measure flow velocities use was made of electromagnetic fluid-velocity meters (supplied by Delft Hydraulics with a S-40 sensor). In every vertical the velocity is measured at five different heights spread evenly over the depth. As an example the measuring positions are given at vertical 7 in the experiment with breakwater (see Figure 3.5).

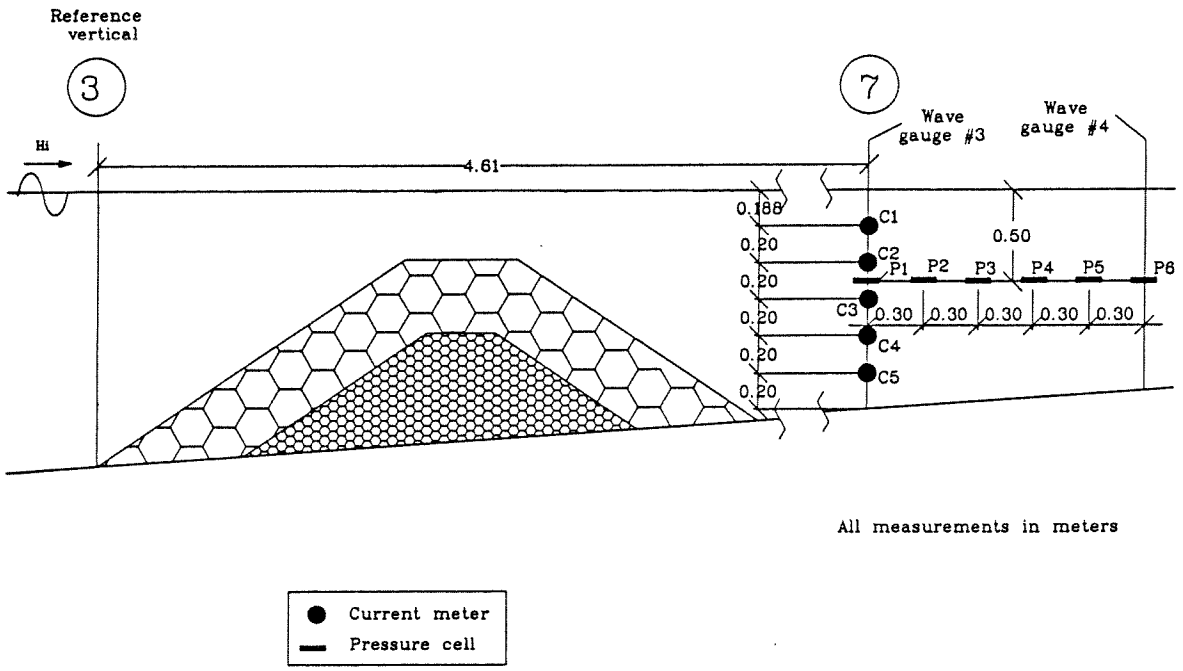

Figure 3.5 Measuring positions at vertical 7 in the experiment with breakwater at UPC (scale 1:4)

CHAPTER 4 BEACH PROFILE MORPHODYNAMICS

4.1 Introduction

In the following main experimental results regarding profile morphodynamics are presented. Profile changes have been characterised using a set of parameters (erosion volume, shoreline movement, beachface slope, profile shape, bottom changes and cross-shore transport rates) covering most of the state of the art 'engineering control variables'. To analyse the breakwater efficiency from a practical point of view, experimental results are presented for the two test situations, 'without' and 'with' breakwater.

One common aspect for all the tests is that their duration was not long enough to reach an equilibrium profile. Due to this, observations and conclusions about beach profile development must be considered as strictly valid for the initial and intermediate states. Any extrapolation of the experimental results to compare the final profile state without and with breakwater must be only considered as indicative (qualitative value) at the best. Another common aspect for all the tests is that they are erosive, so the main differences for the tested conditions is due to the magnitude of the observed erosion and not in the direction of the change (erosion or accretion).

In the next paragraph the data from the experiments in Delft are applied on from the literature obtained criteria, in which erosional and accretional cases are separated. In the following paragraphs consecutively the following characteristics of the developed profiles are described and the relation between the experiments and the influence of the breakwater are mentioned; erosion volume, shoreline movement, beachface slope, profile shape, bottom changes and cross-shore transport rates.

4.2 Application of prediction parameters for erosive/accretive profile response

4.2.1 Introduction

In the following several theories used to distinct erosional from accretive profiles are applied on the data obtained from the experiments in Delft. The predictors used to forecast the profile change can be divided in two types: those who are not including the beach face slope and those who are. It should be noted that the experiments in Delft are small-scale experiments and then, threshold values for criteria separating erosive and accretional cases should be selected according to this. The objective of this comparison is to see if the experimental results agree with many other existing experimental data sets. This can be used to show the validity of the data.

The applied criteria are taken from two different studies, one by Jiménez et al. (in press), where the parameters are plotted with the erosion/accretion volume and the criterion is given as a constant value of the parameter. And the other by Kraus et al. (1991) where the data are plotted in a plane of two parameters and the criterion is given as a relation between the applied two parameters.

The following dimensionless parameters are calculated:

$$G_0 = \frac{\pi w}{gT}$$ parameter introduced by Dean (1973) (4.1)

$$D = N_0 = \frac{H_0}{wT}$$ 'fall speed parameter' or 'Dean number' (4.2)

$$S_0 = \frac{H_0}{L_0}$$ wave steepness in deep water (4.3)

$$F_0 = \frac{w}{\sqrt{gH_0}}$$ a Froude-type number (4.4)

$$P = \frac{g}{w^3}\frac{H^2}{T}$$ Larson and Kraus (1989) (4.5)

$$SH = \frac{H}{L_0} m^{0.27} \left(\frac{L_0}{d_{50}}\right)^{0.67}$$ Sunamura and Horikawa (1974) (4.6)

$$HK = \frac{H}{wT} m$$ Hattori and Kawamata (1980) (4.7)

$$SG = m \frac{H^{0.5}}{(d_{50} L_0)^{0.25}}$$ Sayao and Graham (1991) (4.8)

$$JS = \left(\frac{H}{wT}\right)^{0.5} m$$ Jiménez and Sánchez-Arcilla (1992) (4.9)

w = sediment fall speed
g = gravity
T = wave period
H = wave height
L = wave length
m = beach slope
d_{50} = median sediment grain size

The dimensionless parameters with subscript '$_0$' refer to deep water wave characteristics and they are calculated only using the significant wave height. The other parameters without subscript are calculated using the significant wave height and the hereof derived root-mean-square wave height ($H_s = \sqrt{2} * H_{rms}$ by assumption of a Rayleigh wave height distribution). They are plotted with the erosion volume. Here the erosion volume of the experiments without breakwater is used, as the calculated parameters are the same and the difference between the erosion values obtained in the experiments without and with breakwater are small. For T is taken T_p.

4.2.2 Predictors not including the beach face slope

In Figure 4.1 the data obtained from the Delft experiments are plotted in the S_0-G_0 plane.
Three different criteria are given. Line A ($S_0 = 2.7 * G_0$) is taken from Dean (1973) derived from small scale experiments. Line B ($S_0 = 8.8 * G_0$) is derived by Larson and

Kraus (1989) from large wave tank data. Line C ($S_0 = 184 * G_0^{1.5}$) is introduced by Larson and Kraus (1989) and is a rotation and transformation of the original criterion of Dean. For all the criteria the data are positioned in the erosive part.

Appendix A, Figure A.1 plot the Delft data on the S_0-N_0 plane. Larson and Kraus (1989) found the following relationship between S_0 and N_0; separating erosive from accretive situations $S_0 = M*N_0^3$, in which M = 0.00027 is an empirical coefficient determined from visual fitting, as is the exponent 3. Also applied to this plane is the following criterion obtained by Kraus et al. (1991); $N_s = 3.2$ pertaining to significant wave height. In the graph can be seen that the experimental data agree with the given criteria.

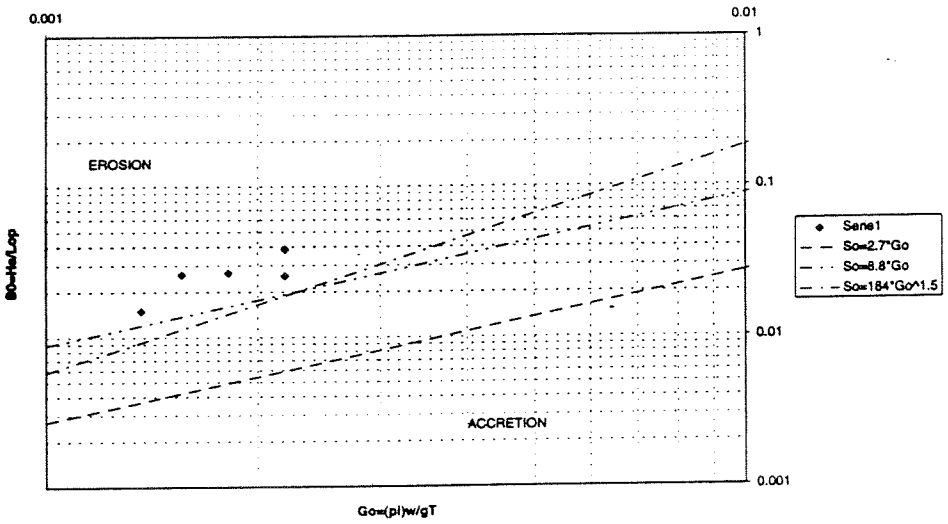

Figure 4.1 Small scale data Delft, S_0-G_0 plane

In appendix A, Figure A.2 the data are reproduced in the S_0-F_0 plane and in appendix A, Figure A.3 in the N_0-F_0 plane. The criteria separating the erosive from the accretive cases are derived from the criterion $S_0 = M*N_0^3$, used in the S_0-N_0 plane, combined with other relationships between the parameters. The criterion in the S_0-F_0 plane is $S_0 = 3.3e09*F_0$ and the one in the N_0-F_0 plane is $N_0 = 22900 * F_0^2$. In both graphs the Delft data are situated in the erosive area.

In appendix A, Figure A.4 the Delft data are, calculated with the Dean parameter, printed with the accretion/erosion volume. The model is based on the assumption that the offshore transport of the sediment mostly takes place in suspension. Supposing that when the waves break the sediment particles are put into suspension. Once suspended it is depending on the fall velocity in relation to the wave period if the net movement will be on or offshore. A relative small fall velocity will induce a landwards movement and a relative large fall velocity an offshore movement. The criterion D = 2.7 separating the erosive and the accretional cases is taken from Jiménez et al. (in press) applicable on deep water. All the data agree with this criterion.

In appendix A, Figure A.5 the from the Delft data calculated dimensionless Dalrymple (1991) P-values are plotted with the erosion volumes, all the data are according to the criterion P = 9500.

4.2.3 Predictors using the beach face slope

In appendix A, Figure A.6 the dimensionless parameter of Sunamura and Horikawa (1974) is applied on the Delft data. This parameter is obtained from a semi-emperical analysis based on the hydrodynamics in the breaker zone. Non of the data is in line with this criterion according to the by Jiménez at all derived criterion SH = 20. If the data are calculated with for the wave height the significant wave height, the difference is smaller. However Jiménez et al. (in press) made this fit using large scale experiments. If the original threshold value of Sunamura and Horikawa is used (SH = 4) all the experiments fall in the erosive area.

In appendix A, Figure A.7 the parameter of Hattori and Kawamata (1980) is printed for the Delft data. This parameter uses the same relationship between the forces caused by the wave movement putting the sediment in suspension and the gravity force as the Dean parameter, only the beach face slope is added. The data are all situated in the erosional plane, HK > 0.12.

The equation derived by Sayao and Graham (1991) is plotted in appendix A, Figure A.8 It is shown that the criterion, SG > 0.10, separating erosion/accretion is applicable.

The parameter derived by Jiménez and Sánchez-Arcilla (1992) to predict erosion/ accretion for beaches from large scale data is plotted in appendix A, Figure A.9. This parameter is similar to the Dean parameter, but the relationship is not linear. All the Delft data is situated in the erosive plane, JS > 0.09.

4.2.4 Conclusions

Although the Delft data are acquired from small scale experiments and the criteria are obtained for large-scale experiments, nearly all the criteria are applicable to the data. Only the large scale criterion of Sunamura and Horikawa did not agree with the data, so it had to be converted to small scale to satisfy the conditions.
From this analysis it can be assumed that the observed beach profile behaviour is in agreement with the existing criteria delimiting erosion/accretion. From the behaviour point of view the data set can be considered as 'correct'.

4.3 Erosion volumes

The erosion volumes are calculated for every time step in relation to the original profile (t0 = 0 hours). The erosion volume is calculated as the eroded volume in the inner part of the profile (see Figure 4.2).

4.3.1 Erosion volumes in experiments without breakwater

In all the experiments the erosion volume is continuously increasing (see Figure 4.3), even during the last stages. This indicates that in none of them an equilibrium profile is reached.

Looking only at the physical effects on the erosion volumes the following is noticed: The most important parameter controlling erosion volumes (from the tested conditions) is the incident wave height. Thus the largest erosion volume corresponds to the test with the highest wave height (experiment D) whereas the smallest erosion volume is generated during the experiment with the lowest wave height (experiment E) (see Figure 4.3). Between this range of erosion volumes lay those observed for intermediate wave heights (experiments A, B and C). For these, although with a similar wave height, different volumes are produced.

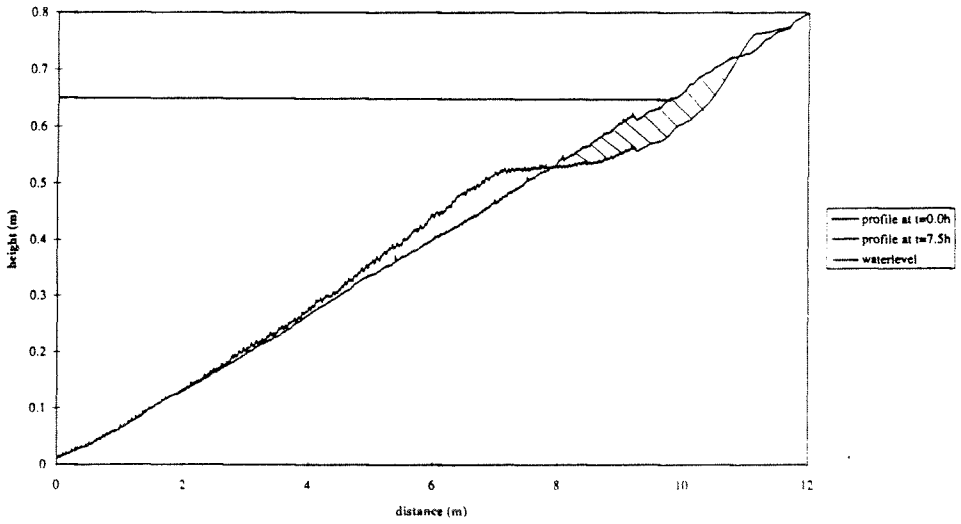

Figure 4.2 Calculation of erosion volume

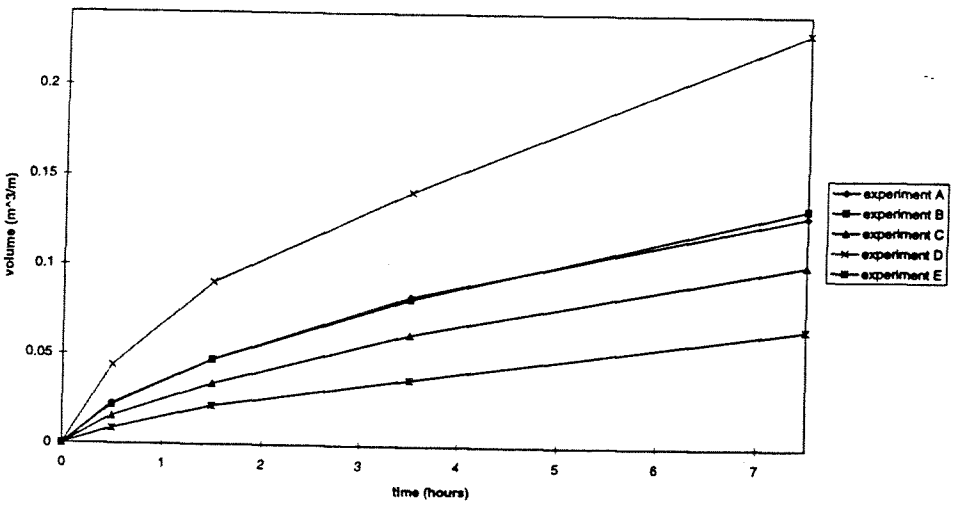

Figure 4.3 Erosion volumes in experiments without breakwater

The different behaviour during experiments A, B and C has to be associated with the difference in wave periods since the other parameters are nearly equal (H, w, tan β). Wave periods for these experiments have a decreasing sequence of A, B, C which produce an increasing sequence of steepness (H/L) of A, B, C. According to this and, for instance, looking at any of the analysed predictors in the previous section it would be expected that erosional behaviour would increase from experiment A to C.
However looking at the experimental results (fig 4.3) the observed sequence is the opposite, i.e. experiment C presents the smallest erosion volume whereas experiments A and B present a higher and nearly equal one.
Moreover, when the analysis of the influence of wave steepness is extended to the other two experiments, this 'non-expected' behaviour is more marked. Thus, it is observed that experiments B, D and E with a nearly equal wave steepness give results completely different. In order to stress this it has to be observed that the experiment with the largest erosion volume (experiment D) and the one with the smallest (experiment E) have the same wave steepness.

As a result of this and for the tested conditions (sediment characteristics and wave characteristics) the main parameter to control erosional behaviour (regarding erosion volumes) is the wave height. Moreover, when wave steepness is considered the observed relationship is in the opposite of the expected one.

4.3.2 Erosion volumes in experiments with breakwater

In all experiments, except experiment B during the last interval, the erosion volumes are increasing (see Figure 4.4) for each consecutive timestep in a similar way to the one observed for the 'without' breakwater tests. This shows that the profile is not in an equilibrium state after the last time step.

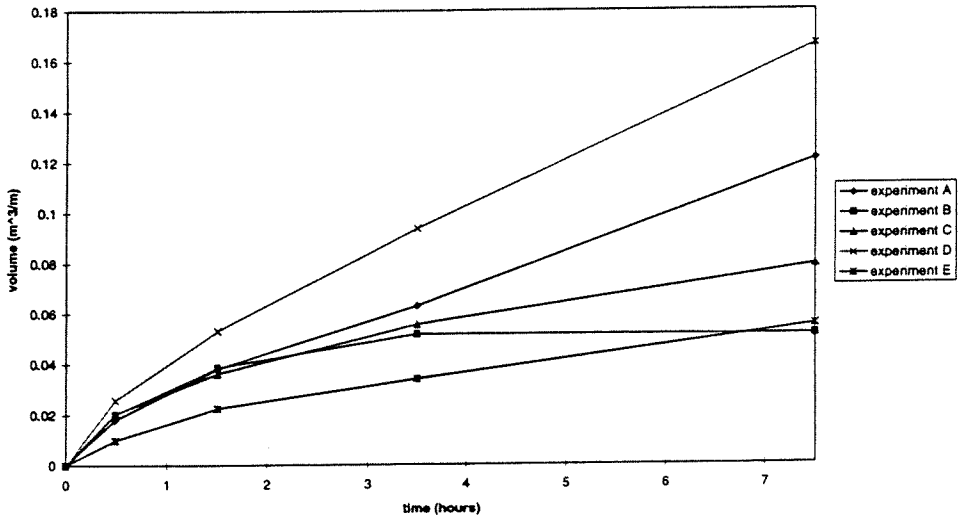

Figure 4.4 Erosion volumes in experiments with breakwater

Concentrating on erosion volumes, the following aspects arise from the analysis:
The observed behaviour is similar to the one observed for tests without breakwater. In other words, these experiments reproduce the earlier identified influences of wave height and steepnesses on erosion volumes. The main difference is observed in experiment B which seems to reach a 'stable' situation at the last stage of the test, given the smallest final erosion volume.

4.3.3 Comparison between experiments without and with breakwater

In Figure 4.5 the ratios between the experiment without and with breakwater regarding the erosion volumes are plotted. As expected, it can be seen that the erosion volume is larger in the experiments without breakwater than in the experiments with breakwater. Only in experiments C and E during time intervals 1 and 2 the erosion volume is larger in the experiment with breakwater, but the differences are very small, at the end of both tests the erosion volume in the experiment without breakwater is larger.

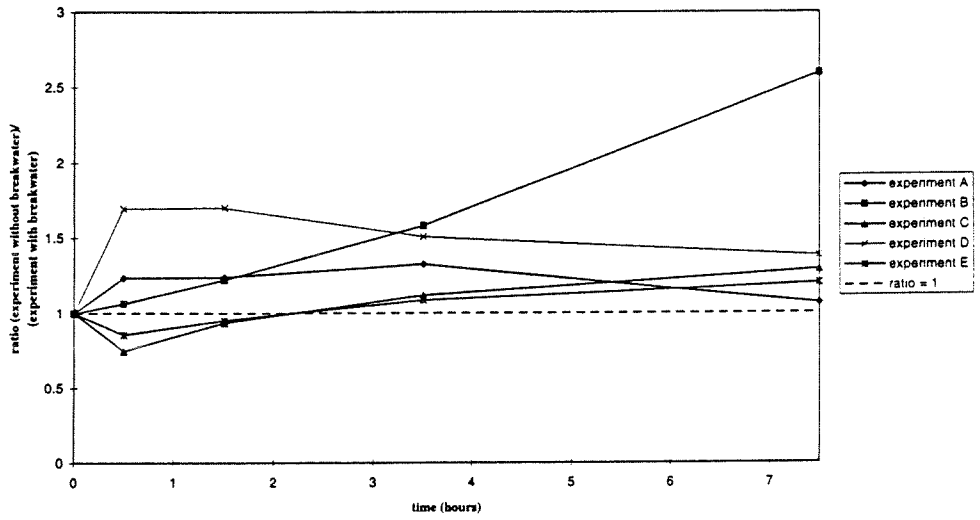

Figure 4.5 *Ratio between the erosion volumes of the experiment without and the experiment with breakwater*

Characterising the efficiency of the breakwater on the reduction of erosion volumes and leaving out test B (which shows a different behaviour from the other ones) the following sequence (from the most efficient experiment to the least one) is observed: D, C, E and A, with a reduction in erosion volumes of 28%, 23%, 17% and 6% respectively. The most important reduction corresponds to the case with the highest wave height (D). This is in agreement with the expected submerged breakwater performance: higher waves will be affected by the breakwater inducing its breaking, filtering part of the incoming wave energy. In general this efficiency can be put in terms of dimensionless freeboard (F/H_s), i.e. for lower values of F/H_s higher efficiency in filtering incoming wave energy will be obtained and then, smaller

erosion volumes would be expected. This is true for experiments D, C and E, although experiments B and A do not fulfil the rule. It can be 'outliers' but due to the limited number of experiments it is not possible to generalise it.

4.4 Shoreline retreat

The shoreline is defined as the horizontal position of the intersection of the profile and the Still Water Level (h = 0.65 m for all tests).

4.4.1 Shoreline changes in experiments without breakwater

Figure 4.6 shows the time evolution of shoreline changes for the experiments without breakwater. As it was previously mentioned, all the experiments resulted in shoreline retreat and, moreover, from the observed changes it is clear that profiles do not reach an equilibrium state.
In all the cases the shoreline changes show an exponential form with a relatively rapid response during the first part of the experiment (0.0-1.5 hours) and decreasing change magnitudes as the profile evolves towards an hypothetical equilibrium state.

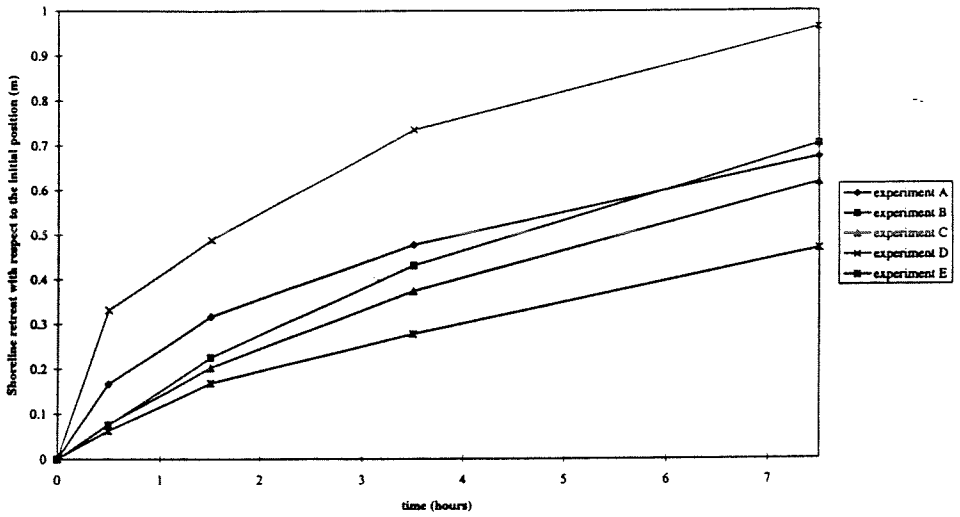

Figure 4.6 *Shoreline retreat with respect to initial position in the experiments without breakwater*

Looking at the first stage of the tests (t < 2 hours) a clear classification of tests as a function of the observed response can be done. Thus, for this phase and using the observed shoreline recession, three 'groups' are identified: test D, the most erosive one, test A an intermediate case and tests B, C and E with a similar behaviour.
During the second part of the experiment (t > 2 hours) test B, C and E leave their initial similarity in magnitude, showing a greater difference in the final recession than the expected, looking only at the initial stage.

Although the physical explanation of the observed behaviour must be done considering all the controlled variables, some points arise from the shoreline change analysis.
As it was observed for erosion volumes, for the range of tested conditions it seems that the main parameter controlling shoreline erosion is the wave height. Thus, the largest retreat corresponds to the experiment with the largest wave height (experiment D). Whereas the smallest retreat corresponds to the smallest wave height (experiment E). As it was observed for the erosion volumes the effect of wave period or steepness seems to play a secondary role or, at least, different to the expected one. Thus, the experiment with the largest steepness is not the most erosive one (in shoreline recession terms), being exceeded in shoreline-retreat for all the experiments (with steepnesses much more lower) with the exception of experiment E. For experiments with the same initial wave height, the variations in the wave period (for the used range) do not produce significant changes in shoreline retreat and, even, the observed changes are not in agreement with the sequence in the corresponding steepness.

4.4.2 Shoreline changes in experiments with breakwater.

In the shoreline movement graph (Figure 4.7) can be seen that in all experiments the shoreline is retreating. The general retreat curve is similar to that observed in the 'without' tests, a rapidly retreat in the first stages to be slowly attenuated at the latter periods. Nor was an equilibrium situation reached during these tests.

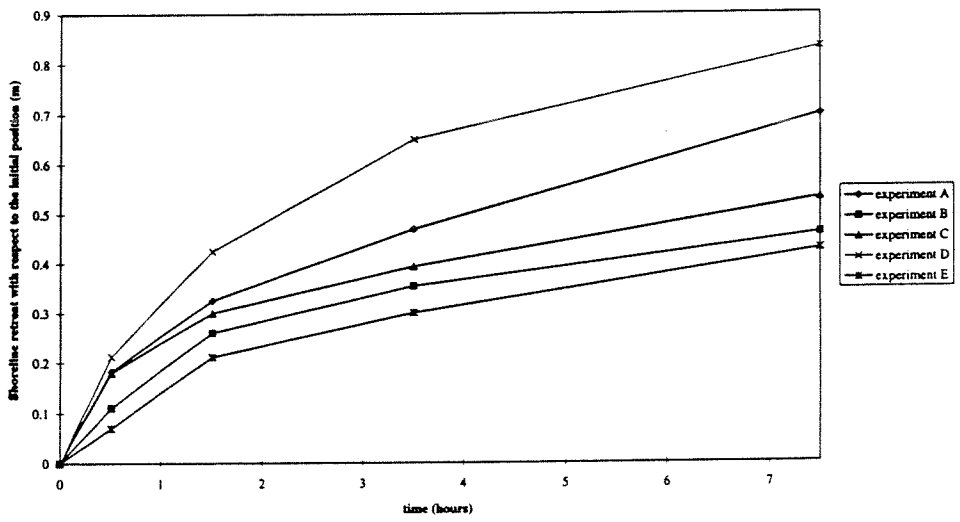

Figure 4.7 *Shoreline retreat with respect to initial position in the experiments with breakwater*

There is a similar behaviour as in the experiment 'without'. The wave height is the most important characteristic influencing the shoreline retreat. Giving the largest retreat for the experiment with the largest wave height (experiment D) and the smallest retreat for the experiment with the smallest wave height (experiment E). In

the comparison of the experiments with the same wave height (A, B and C), it is expected that the experiment with the highest wave steepness (experiment C) will show the largest shoreline retreat. But here the shoreline retreat is much larger in the experiment with the smallest wave steepness (experiment A). This development is the same as in the experiment without breakwater and according to the earlier found results in the erosion volumes.

4.4.3 Comparison between experiments without and with breakwater

In Figure 4.8 the ratio between the experiment without and with breakwater regarding the shoreline movements are plotted. In general it can be seen that the shoreline retreat at the end of the experiment in the experiments without breakwater is approximately a factor 1.1 larger than in the experiments with breakwater.

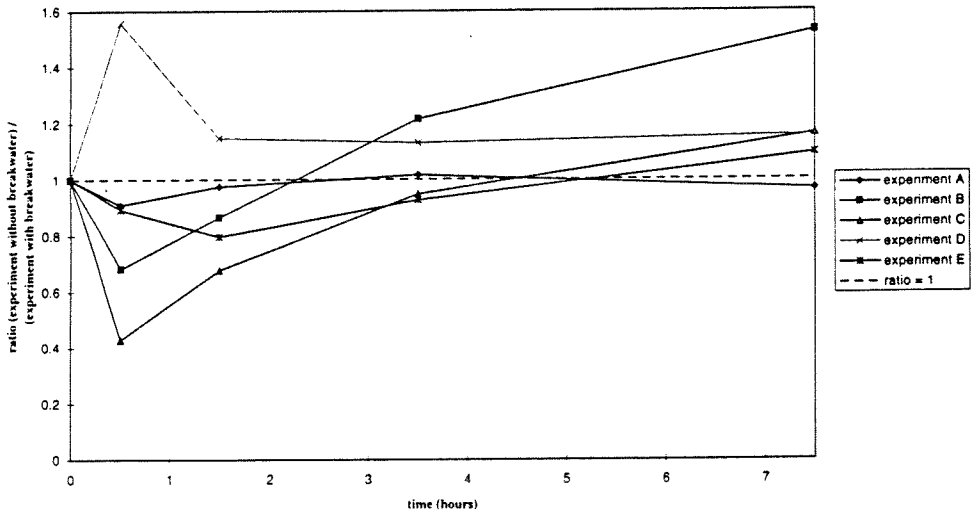

Figure 4.8 *Ratio between the shoreline movements of the experiment without and the experiment with breakwater*

At the start of the experiment the retreat of the experiments with breakwater is larger than in the ones without breakwater and at the end of the experiments vice versa. This fact was also observed for erosion volumes although only for two tests (C and E) and it appears as if the inclusion of the structure produces a perturbation in the system at the beginning of the experiment to be afterwards attenuated. Only in experiment D during the whole experiment the experiment without breakwater has a larger shoreline movement than the experiment with breakwater. In experiment A the differences in shoreline movement between the experiment without and with breakwater are very small during the whole experiment.

The difference of the final retreat (at t4 = 7.5 hours) between the experiments without and with breakwater is in experiments A and E very small. Measuring the efficiency of the breakwater in terms of reducing shoreline retreat, an averaged reduction of

about 10% of the retreat was obtained for the tested conditions. Rating the tests in terms of the efficiency of the breakwater a decreasing sequence was observed: D, C , E and A (leaving out experiment B), which is the same detected while comparing the erosion volumes. Due to this, the use of the dimensionless freeboard (F/H_s) can also be used to explain it.

4.5 Comparison between erosion volumes and shoreline retreat

The ratio between the shoreline retreat and the erosion volume is calculated (see Figure 4.9). The aim of calculating this ratio is to look for a to all experiments applicable relationship between the erosion volume and shoreline retreat. This parameter should serve the same goal for cross shore transport as the constant derived in the single line theory (TOW 1980) for longshore transport.

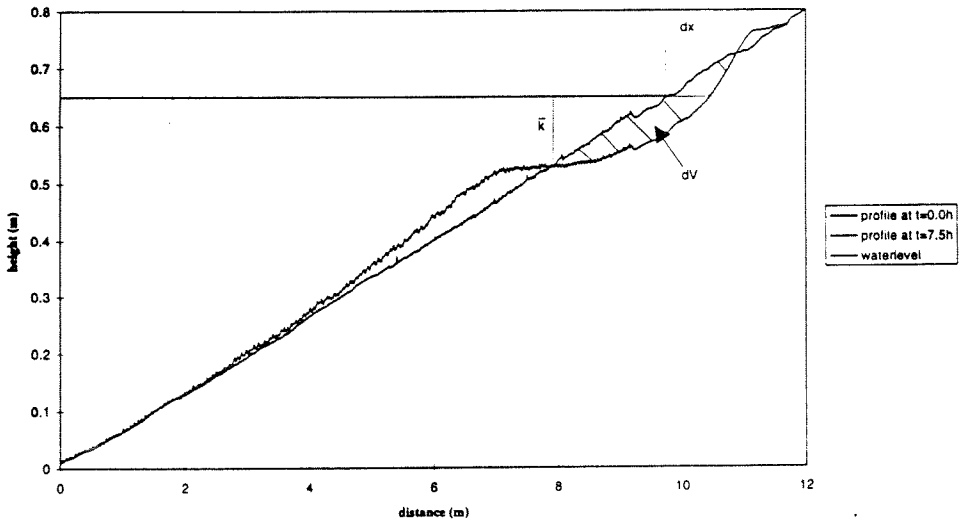

Figure 4.9 *Determination of the relation between the shoreline retreat and the erosion volume*

In most experiments, the ratio obtained at the first stage of the test is different to the ones obtained during the remaining period, which is in line with the other controlled parameters and it represents the initial response of the 'unnatural' profile. After this moment the ratio is more or less steady indicating a homogeneous (in time) response. For all the experiments the ratio is larger for the experiment without breakwater. This implies that the erosion volumes reduce in relation with the shoreline retreat for the experiment with breakwater in comparison with the experiment without breakwater. It can be concluded, assuming that the shoreline is not increasing, that the influence of the breakwater on the erosion volumes is larger than on the shoreline retreat.

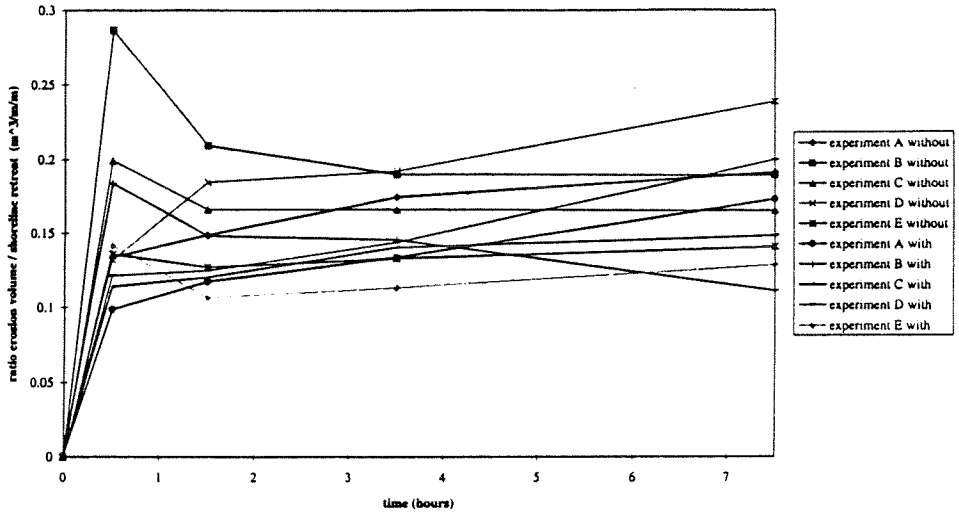

Figure 4.10 The ratios between the erosion volume and the shoreline retreat for all experiments

4.6 Beachface slopes

4.6.1 Introduction

The beachface slope ($\tan\beta$) is calculated taking the bottom profile values 0.2 m seawards and 0.2 m landwards of the shoreline position, they are subtracted and divided over 0.4 m.
The original slope of the profile is 1:15. The slope at t0 = 0 hours should have this value and should be the same for all measurements, this is not the case. This can be caused by:
- the difficulty to straighten out the bed to the right slope
- the way of measuring (the shoreline is always positioned in the area where the bottom height is measured through the wall of the flume)

The measured beach face slopes are compared with the by Kriebel et al. (1991) obtained relationship. They derived a best fit relationship from the field data of Sunamura (1984):

$$m = 0.15\left(\frac{wT}{H}\right)^{1/2}$$

In which m is the beach slope, w is the fall velocity, T is the wave period and H is the wave height. The Delft data (at t4 = 7.5 hours) are plotted on the H/wT-m plane (see fig 4.11), with the best-fit relationship obtained by Kriebel et al. (1991). This relationship is not applicable on the data, the data have a steeper slope in relation with the H/wT than the predicted one. The Delft data are measured before the equilibrium state is reached. Looking at the development of the beach face slopes in time it can be expected that they will increase towards the equilibrium state (see Fig. 4.12). The

different behaviour of the Delft experiments can be associated with the fact that all the data used to derive this relationship are from field experiments and large scale flume data. Moreover, another point to be considered is that the used sediment grain size is quite fine compared with the 'natural beaches' one used to build the relationship.

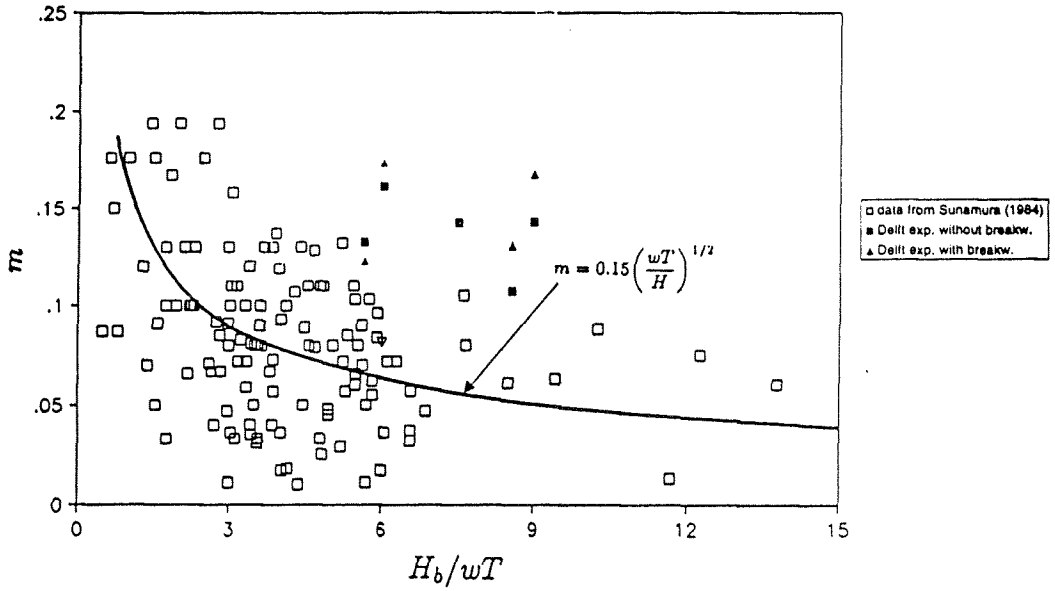

Figure 4.11 Dependence of beach face slope on sediment fall parameter according to Kriebel et al. (1991). Beach face slopes Delft taken at t4 = 7.5 hr

4.6.2 Beachface slopes in experiments without breakwater

Looking at the graph of the beach face slopes in the experiments without breakwater (see Figure 4.12) it can be noticed that at the start of the experiment the beach face slopes change rapidly and afterwards are attenuated for the last stages. This is because at the beginning of the experiments the initial slope is quite far away from the 'equilibrium' one.

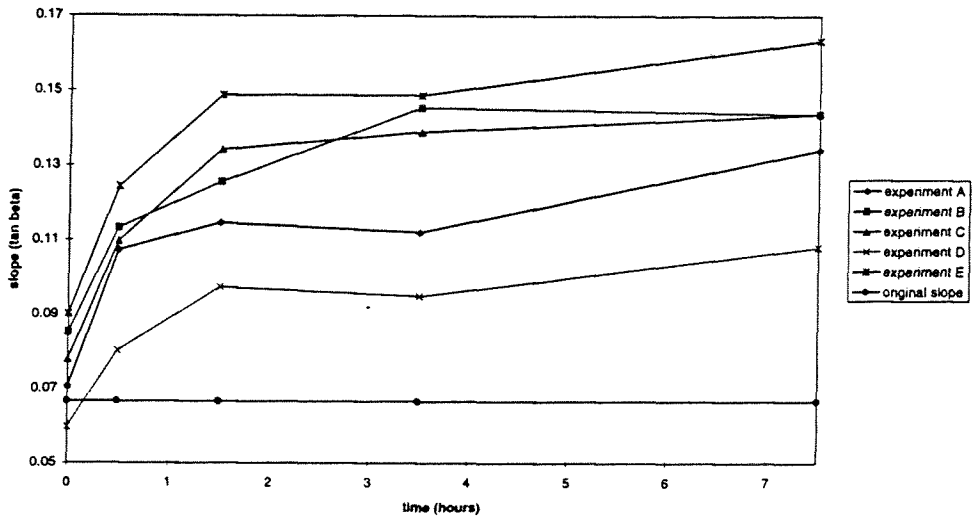

Figure 4.12 Beach face slopes in the experiments without breakwater

Experiment D always has the most gentle beach face slope and experiment E always has the steepest beach face slope. The beach face slopes of experiment A, B and C are laying in between the ones of experiment D and E. In general the beach face slope in experiment A is the steepest of the three and experiment B and C have in turn a steeper beach face slope.

Only concerning the beach face slope the following can be concluded about the influence of the difference in the applied wave fields.
- The parameter which influence is the most clear on the beach face slope is the wave height. The steepest slope occurs in the experiment with the lowest wave height and the most gentle slope in the experiment with the highest wave height. Combining this with the earlier described erosion volume it can be seen that the experiment with the largest erosion volume has the most gentle slope and with the lowest erosion volume the steepest.
- The experiments with the same wave height and varying wave length (A, B and C) do not show a clear influence of the wave length on the beach face slope.

4.6.3 Beachface slopes in experiments with breakwater.

In general the same can be seen in the graph of the beach face slopes in the experiment with breakwater (Figure 4.13) as in the graph of the experiment without breakwater (Figure 4.12). The largest changes take place during the first interval, caused by an original slope very different to the equilibrium one at the start of the experiments, and is further on attenuating in time.

On the whole experiment E has the steepest beach face slope and experiment D has the most gentle beach face slope, except during the last interval where experiment A has the most gentle beach face slope. The beach face slopes of the experiments A, B and C are changing in relation to each other during the whole experiment.

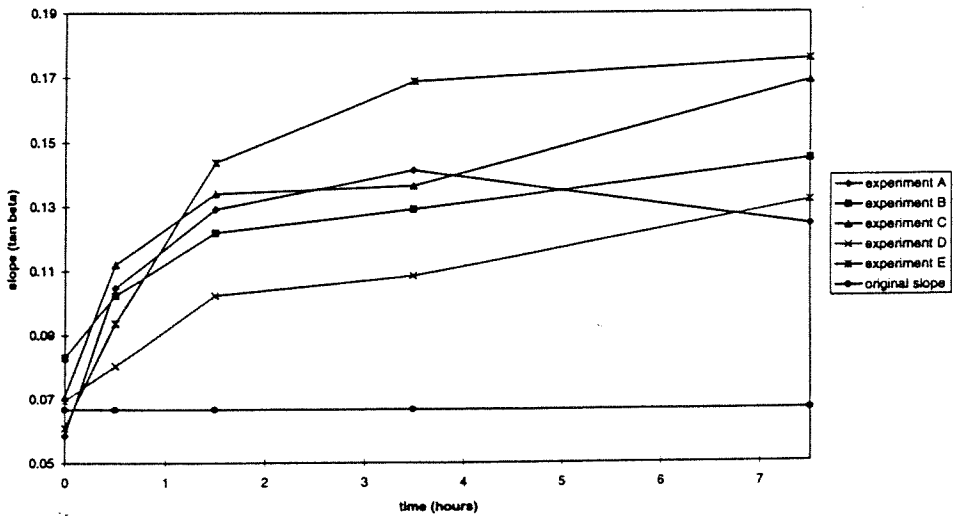

Figure 4.13 Beach face slopes in the experiments with breakwater

Looking at the calculated beach face slopes only in relation to the wave input parameters, the following can be noticed.
- The relation between the wave height and the beach slope is less clear than in the experiment without breakwater. On the whole the steepest beach face slope is formed in the experiment with the lowest wave height (experiment E) and the most gentle in the experiment with the highest wave height (experiment D). This is according to the state of the art, the larger the wave height, the milder the slope. Combining this with the noticed characteristics comparing the erosion volumes for the different experiments the same can be noticed as in the experiment without breakwater, showing a more gentle slope for the experiment with the largest erosion volume and a steeper slope for the experiment with the steepest slope.
- There is no relation visible between the wave length or wave steepness and the beach face slope.

4.6.4 Comparison between experiments without and with breakwater

In Figure 4.14 the ratio between the experiment without and with breakwater regarding the beach face slope are plotted. Not taking into account the measurements during the first two intervals in general it can be seen that the slope in the experiments with breakwater is steeper than the slope in the experiments without breakwater.

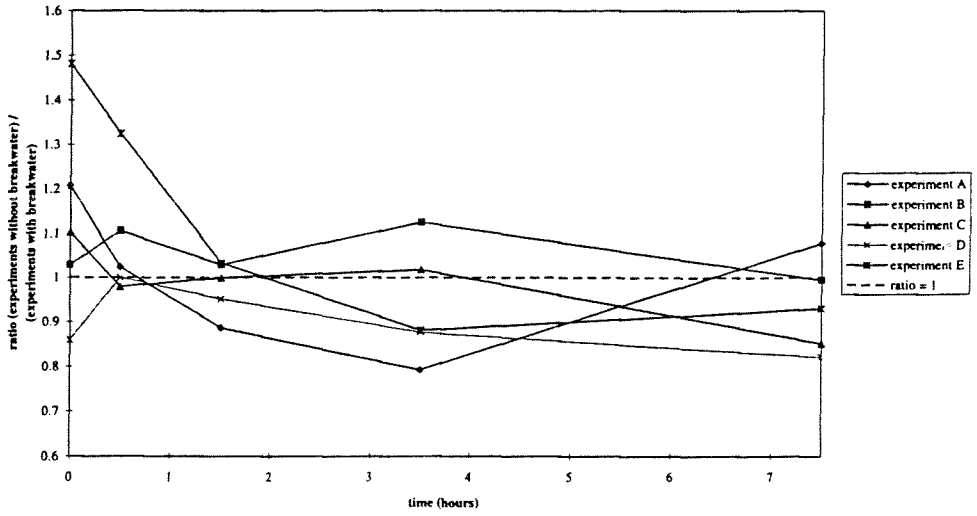

Figure 4.14 Ratio between the beach face slopes of the experiment without and the experiment with breakwater

The values of the experiments without and with breakwater do not differ much, only during experiment D the difference is rather large at the end of the experiment after 7.5 hours. The steeper slopes obtained in the experiments with breakwater are due to the reduction of the incident wave height by the breakwater. As this reduction is higher for the larger wave heights, this is the reason for the largest increase in slope in experiment D.

4.7 Developed profiles

In Delft the bottom profiles are measured at five consecutive moments in time. These profiles are calculated and plotted in graphs for each experiment and for the experiments without and with breakwater.

4.7.1 Description of developed beach profiles in the experiments without breakwater

An example of beach profile development during the experiments without breakwater can be seen in Figure 4.15 (for full details see Appendix B).

In all the experiments the profile develops in the same way. A bar and a trough are formed and the waterline retreats. With every time step the profile continues developing, the size of the bar and the trough are increasing and the waterline retreats further. In all experiments the changes are rather small after the first interval. There is not really a bar visible. Only the shoreward area of the profile changes, a small bar above the waterline and a small trough are formed. During the following intervals the profile changes in the more seaward area as well. More sediment is transported in the seaward direction and a bar is formed which is moving seawards during the consecutive intervals. The trough is growing in two directions, it is getting deeper and moves more shorewards, as the shoreline retreats.

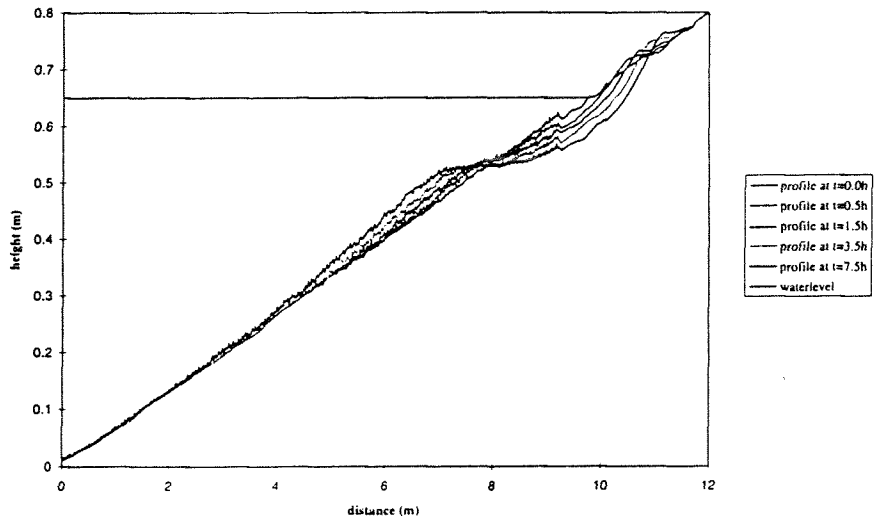

Figure 4.15 Bottom profile development experiment A without breakwater

4.7.2 Comparison of developed beach profiles in the experiments without breakwater

During all the intervals the profile keeps developing. Therefore the differences in the development between the experiments are best noticed after the last interval (at t4 = 7.5 hours) when the distinction of each experiment is the largest and the influence of the different wave characteristics best noticed (see Figure 4.16).

The profiles differ in the position of the bar, the retreat of the shoreline and the amount of transported sediment. In general can be seen that the higher the wave height the larger the changes.

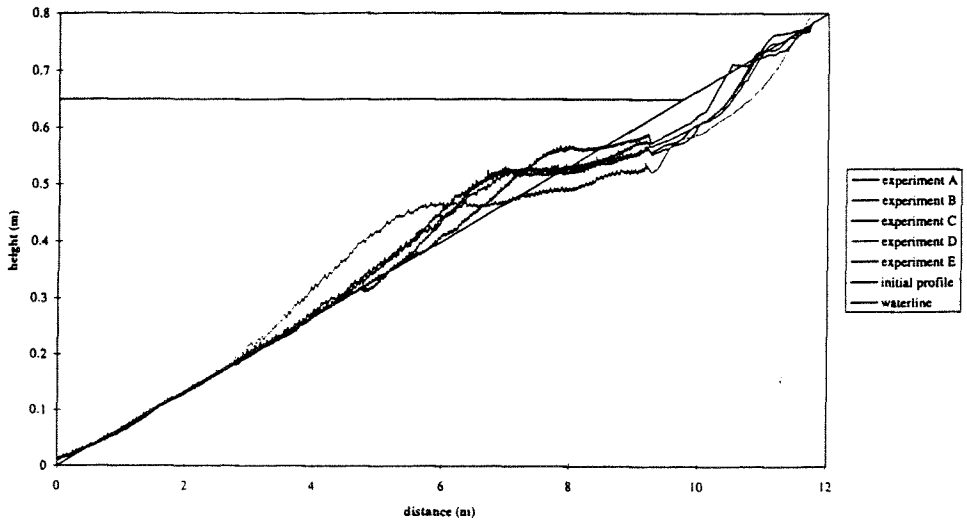

Figure 4.16 Comparison bottom profile development experiments without breakwater

The retreat of the coastline and the size of the trough are the largest and the bar is positioned the most seawards in experiment D, the experiment with the largest wave height, in experiment E, the experiment with the smallest wave height, the retreat of the coastline and the size of the trough are the smallest. This is in line with the state of the art, the larger the wave height the larger the change of the profile. The bar is formed at the breaking point of the waves. As the waves are higher they tend to break in deeper water, and the bar will be positioned more seawards.

In the experiments A, B and C with an intermediate wave height and different wave lengths the height of the bar is more or less the same and it is positioned at the same place. The only difference is the downslope area until which the profile is changed. In experiment A the experiment with the largest wave length the influenced area is the largest. In experiment C the experiment with the smallest wave length the area is the smallest.

4.7.3 Description of developed beach profiles in the experiments with breakwater

An example of beach profile development during the experiments with breakwater can be seen in Figure 4.17 (for full details see Appendix B).

In general there is a shoreline retreat and the trough is increasing for every consecutive time step. Sediment is accumulated at the landside toe of the breakwater,

and this amount of sediment is increasing in time. There is a small quantity of sediment passing over the breakwater.

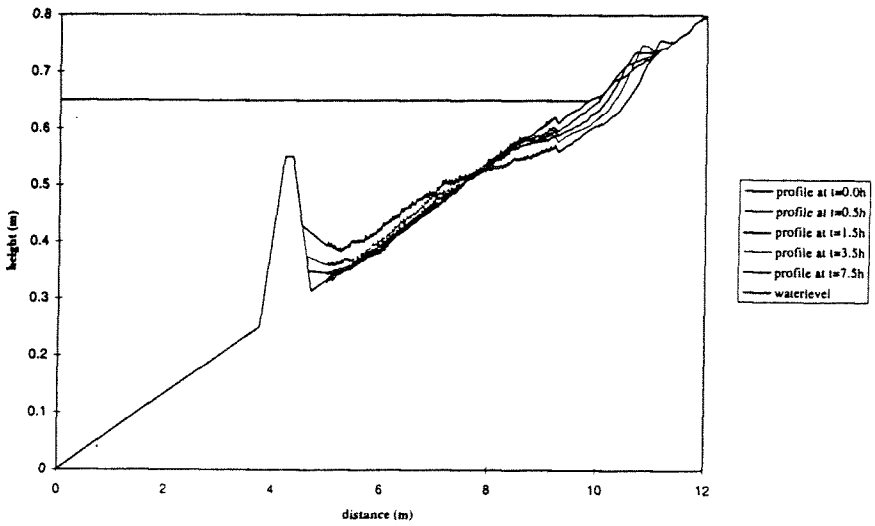

Figure 4.17 Bottom profile development experiment A with breakwater

In experiment B after interval 4 a different development can be noticed (see Figure B.13). In all the other experiments there is a further development of the profile visible, but in this experiment the foregoing changes are not continued. There is still a shoreline retreat, but where normally in the other experiments the trough is enlarged and the bar is moved more seawards, here the last part of the trough is filled with sediment and the bar becomes a little bit smaller. The different wave characteristics of the experiment do not give an explanation for this, as experiment B has an intermediate wave height, wavelength and wave steepness.

4.7.4 Comparison of developed beach profiles in the experiments with breakwater

On the whole the distinction between the developed profiles in the different experiments are the amount of sand deposited at the landside toe, the position of the bar, the volume of the erosion trough and the size of the shoreline retreat. The variation in the position of the bar is smaller than in the experiment with breakwater as the highest waves break while passing over the breakwater, and the difference in wave height between the different experiments is reduced. For this comparison the final measured profiles after the last interval (t4 = 7.5 hours) are used (see Figure 4.18).

The profile of experiment D, the experiment with the largest wave height, changes the most, the whole profile is less steep than the original 1:15 slope, the retreat of the coastline is large. A large amount of sand is accumulated at the landside toe of the breakwater. In experiment E, the experiment with the smallest wave height, the retreat

of the shoreline and the formed bar are the smallest. At the landside toe of the breakwater no accumulation has occurred.

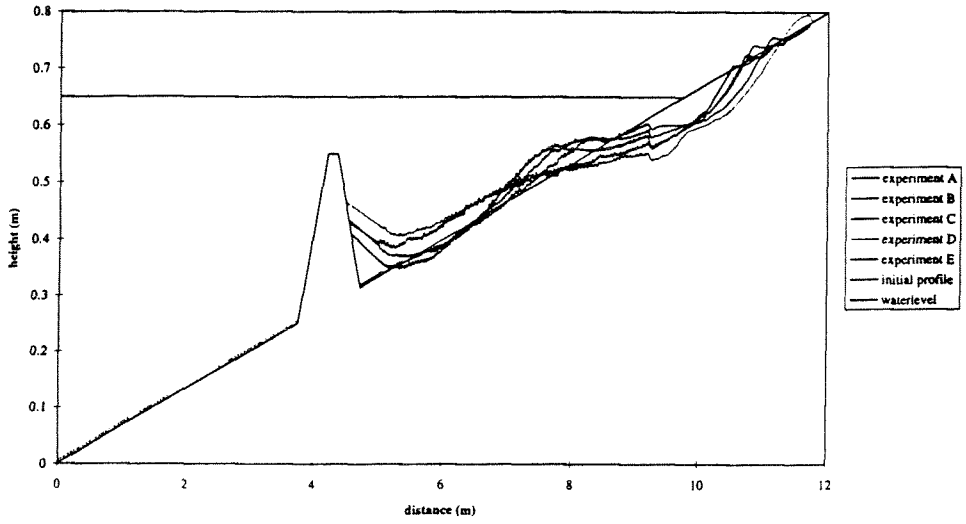

Figure 4.18 Comparison bottom profile development experiments with breakwater

In experiment A, the experiment with the largest wavelength a bar is not really visible, the whole slope has become less steep. In experiment B, the experiment with the intermediate wave height, wavelength and wave steepness, a small bar is formed situated near the shoreline. In experiment C, the experiment with the smallest wavelength, the height of the bar is the largest and the slope of the bar is the steepest. In experiment C there is a second trough formed near the breakwater, this second trough is also formed in the experiments B and E, but is here much smaller.

4.7.5 Comparison of developed beach profiles between experiments without and with breakwater, measured after 7.5 hours

An example of the comparison of the beach profile development between the experiments without and with breakwater can be seen in Figure 4.19 (for full details see Appendix B).

In general in all the experiments without and with breakwater, the shoreline retreat is more or less the same. The profiles differ in the position and the shape of the bar. In the experiments with breakwater the bar is located closer to the shoreline. Another effect of the breakwater is blocking of the sediment transportation over it and the positioning of the bar more landwards. Because the profiles are still changing it is not possible to see what the effects of the breakwater will be in the final situation. The effectiveness of the breakwater is strongly depending on the wave height of the incoming waves.

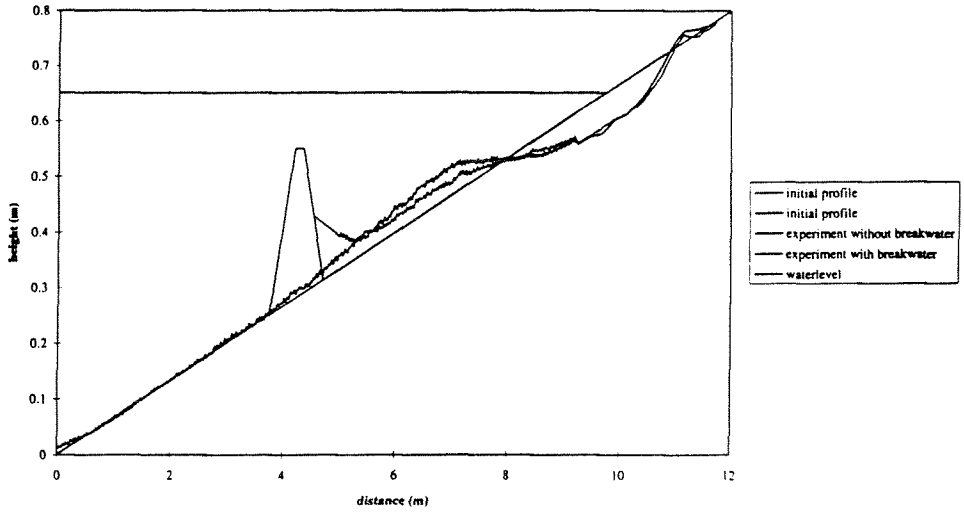

Figure 4.19 Comparison bottom profile development experiments without and with breakwater

In experiment A and D (Figures 4.19 and B.27) the sand which was spread out down the slope in the experiment without breakwater is accumulated at the toe of the breakwater in the experiment with breakwater and the whole slope has become more gentle. In experiments B and C (Figures B.25 and B.26) the bar is bigger and positioned more seaward in the experiment without breakwater. In the experiment with breakwater the distortion of the profile is smaller, there is a smaller bar formed near the shoreline, some sand is transported from the shoreline to the landside toe of the breakwater.
In experiment E (Figure B.28) the differences are very small. In the experiment with breakwater only a small part of the profile changes, a small retreat and a small bar near the shoreline are formed, no sand accumulates at the landside toe of the breakwater. In the experiment without breakwater the retreat of the shoreline is the same and a bit bigger bar further offshore is formed.

The effects of the breakwater are the smallest in experiment E, the experiment with the smallest wave height and wave length and experiment A the experiment with the smallest wavesteepness. The wave field is influenced by the breakwater, depending on the amount of waves that break which is depending on two factors, the wave height in relation with the submergence and the wave steepness.

The main effect of the breakwater on the profile development is that it acts as a physical constraint limiting the domain where the profile will change. Thus, although a similar type of behaviour is observed, the dimensions of the bar/trough system are quite different.

4.8 Bottom changes

By subtracting the consecutive profile measurements, the bottom height change for each time step is calculated. To calculate the total bottom height change, the first (t0 = 0 hours) and the last (t4 = 7.5 hours) measurements are subtracted. Because the calculated values show too much variation the average values over 5 distance steps ($\Delta x = 5 * 0.005 = 0.025$ meter) in the part measured by the PROFO meter are taken. Positive values indicate sedimentation, negative values erosion.

4.8.1 Description of bottom changes in the experiments without breakwater

An example of the bottom height change during the experiments without breakwater can be seen in Figure 4.21 (for full details see Appendix B). In all of the experiments there is generally the same development of the curves visible. The profile can be divided in four zones (see Figure 4.20).

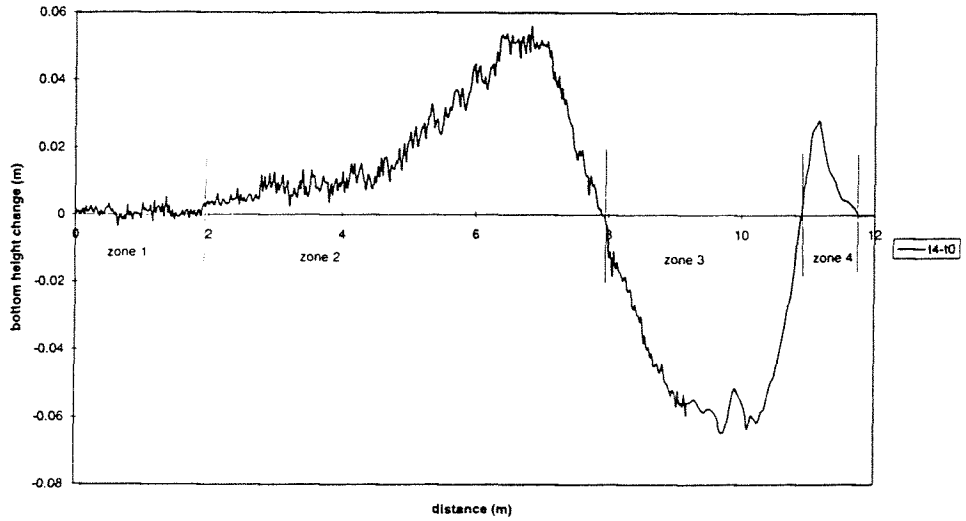

Figure 4.20 Bottom height change between t = 0 and t = 7.5 hr, experiment A without breakwater, division into zones

In zone 1 the profile changes are small. In zone 2 there is sedimentation. During the first interval there is sedimentation and a small bar is formed. In the following intervals the amount of sedimentation increases and the area where the sand is deposited is growing seawards. In zone 3 there is during all intervals erosion. In the consecutive intervals the area in which there is erosion increases. In the shore zone 4 there is sedimentation, the onshore bar is formed. In the consecutive intervals the sedimentation peak moves more shoreward and the slope starts eroding.

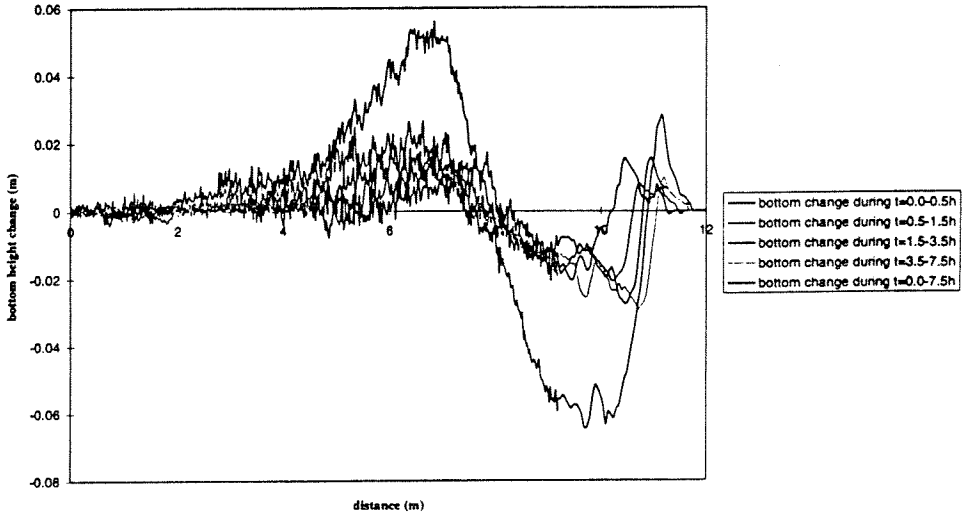

Figure 4.21 Bottom height change experiment A without breakwater

4.8.2 Comparison of bottom changes in the experiments without breakwater

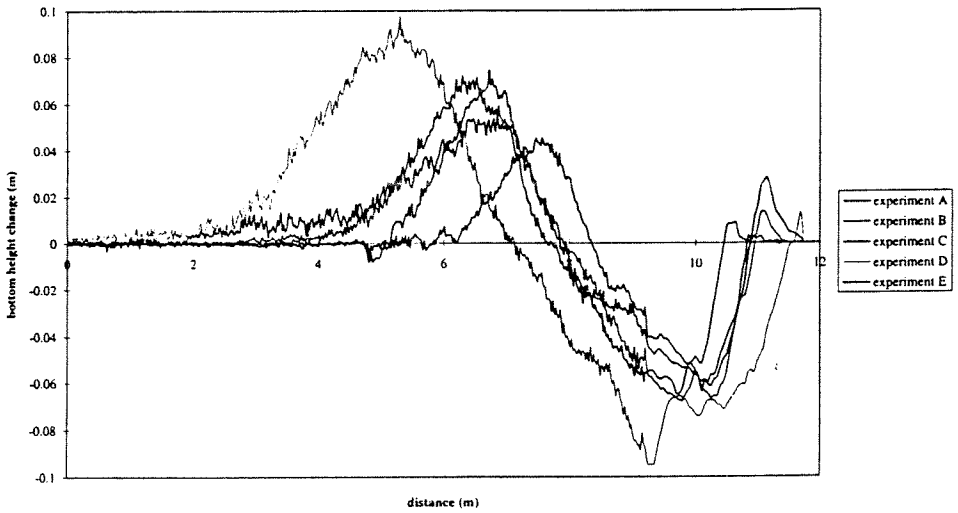

Figure 4.22 Comparison bottom height change experiments without breakwater

The general differences between the experiments are the peak value of the bottom height change, the area over which the bottom height is changing and the position along the profile where the bottom height changes from sedimentation to erosion. The comparison is made using the calculated bottom height profiles after the last interval (t4= 7.5 hours) (see Figure 4.22).

According with the previous analysis (i.e. volume changes, etc.) the experiment with the largest wave height (experiment D) has the largest bottom height change and the experiment with the smallest wave height shows the smallest bottom height change. In experiments A, B and C, with an intermediate wave height, the maximum bottom height changes are between experiment D and E. It was expected that the experiment with the largest wave steepness (experiment C) would show the largest changes and the experiments with the smallest wave steepness (experiment A) the smallest changes. The profile development is not in line with these expectations as was seen in the previous analysis as well.

4.8.3 Description of bottom changes in the experiments with breakwater

An example of the bottom height change during the experiments with breakwater can be seen in Figure 4.24 (for full details see Appendix B). In all of the experiments there is generally the same development of the curves visible. The profile can be divided in five zones (see Figure 4.23).

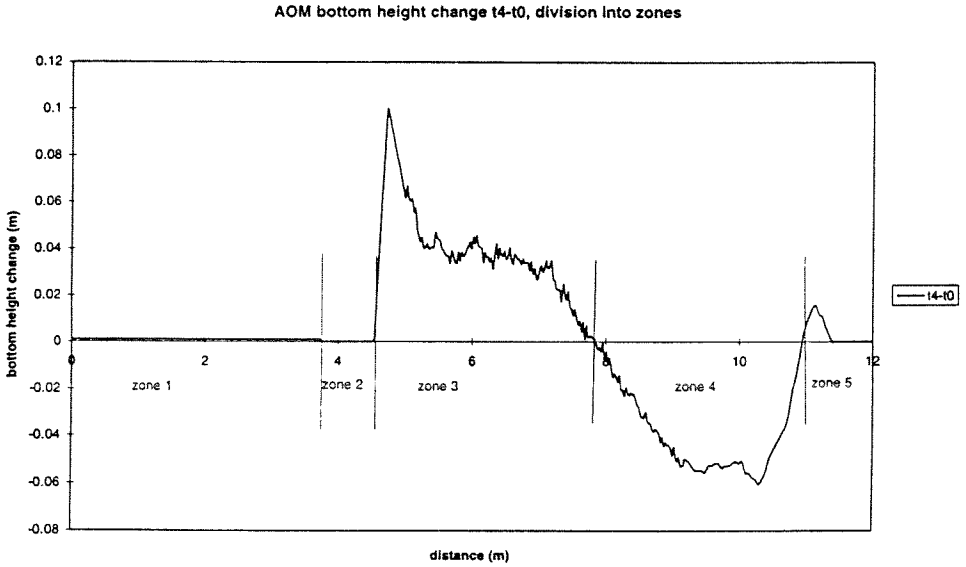

Figure 4.23 Bottom height change between t = 0 and t = 7.5 hr, experiment A with breakwater, division into zones

Zone 1 is the seawards side of the breakwater in which there is in some experiments a small sedimentation. Because the bottom height is not measured at the seawards side of the breakwater it is assumed that the sediment which is found there is spread out evenly over the whole profile seawards of the breakwater.
Zone 2 is the breakwater. Zone 3 is situated immediately landwards of the breakwater. In experiment B and C this zone is very small and two more zones are added, one erosive/zero transport and one accretional, before zone 4 is started. In zone 4 there is erosion in all experiments. Zone 5 is situated above the waterline, this is a small area where sand is deposited .

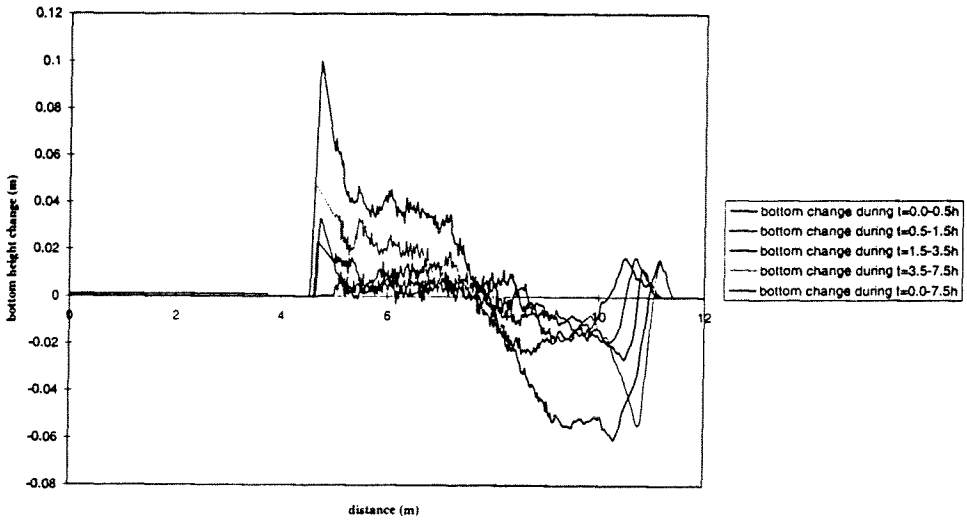

Figure 4.24 Bottom height change experiment A with breakwater

4.8.4 Comparison of bottom changes in the experiments with breakwater

For all experiments it can be seen that the breakwater is nearly completely blocking the sediment transport in seawards direction. The amount of sand which passes over it is negligible. There is at the landside toe of the breakwater a very large value of the bottom height change which reduces to zero or nearly zero passing over the breakwater (see Figure 4.25).

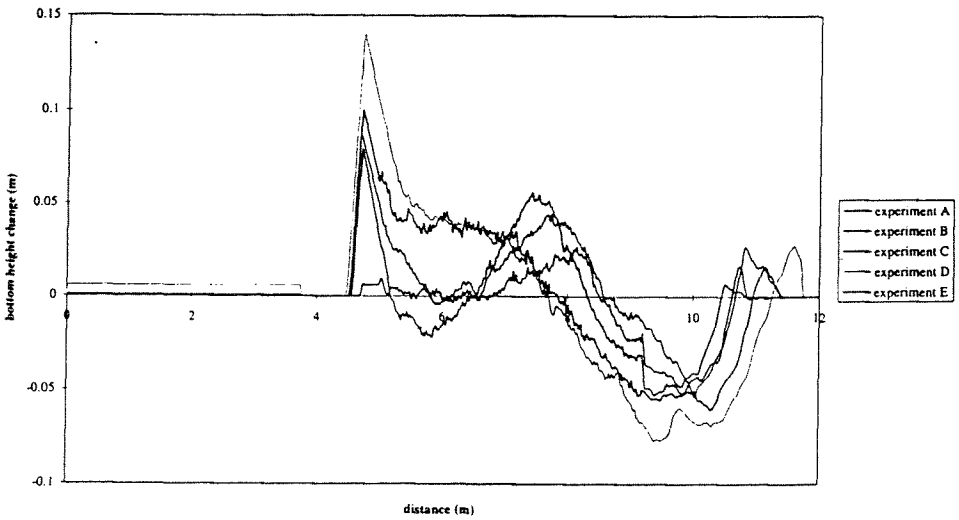

Figure 4.25 Comparison bottom height change experiments with breakwater

The same differences as in the previous analysis can be seen (see Figure 4.25). The wave height is the most important factor distinguishing the bottom height changes of the experiments. The experiment with the largest wave height, (experiment D) gives the largest erosion trough and the largest sedimentation at the landside toe of the breakwater. The experiment with the smallest wave height (experiment E) gives the smallest bottom height changes. The applied wave steepness has a different influence on the bottom height changes then expected from the state of the art, but in line with the before noted characteristics. Here the experiment with the smallest wave steepness / largest wave length shows the largest change in comparison with the experiments with the same wave height and higher wave steepnesses (experiments B and C).

4.8.5 Comparison of bottom changes between the experiments without and with breakwater, measured after 7.5 hours

The breakwater nearly completely blocks the transport downslope. As the slope seawards of the breakwater is made of concrete, the changes downslope in the experiment with breakwater are only caused by the small amount of sand passing over the breakwater and is negligible.
The sand which is transported downslope in the experiment without breakwater is positioned at the landside toe of the breakwater in the experiment with breakwater. This causes in all the experiments except experiment E a large bottom height change in this area.
The bottom height change in the area where the bar and the trough are situated is smaller in the experiment with than in the experiment without breakwater. This is caused by the effect of the breakwater on the wave height. The higher incoming waves break passing over the breakwater and the wave energy reduces causing less bottom height change. This is noted in the before mentioned erosion volume comparison as well.

4.9 Cross-shore transport rate

The cross-shore transport rate is calculated from the bottom height change values. The surface under the curve in the bottom height change graph is calculated starting at $x = 0$ meter and for every x_n ($\Delta x = 0.005$ meter) the surface under the curve from $x = 0$ meter to $x = x_n$ meter is calculated. The here obtained values are positive for an offshore sand transport and negative for an onshore sand transport. In UNIBEST_TC this is opposite and the here calculated sand transports are adapted. In the sand transport rate graphs positive values indicate an onshore and negative values an offshore sand transport rate through the vertical (see Figure 4.26).

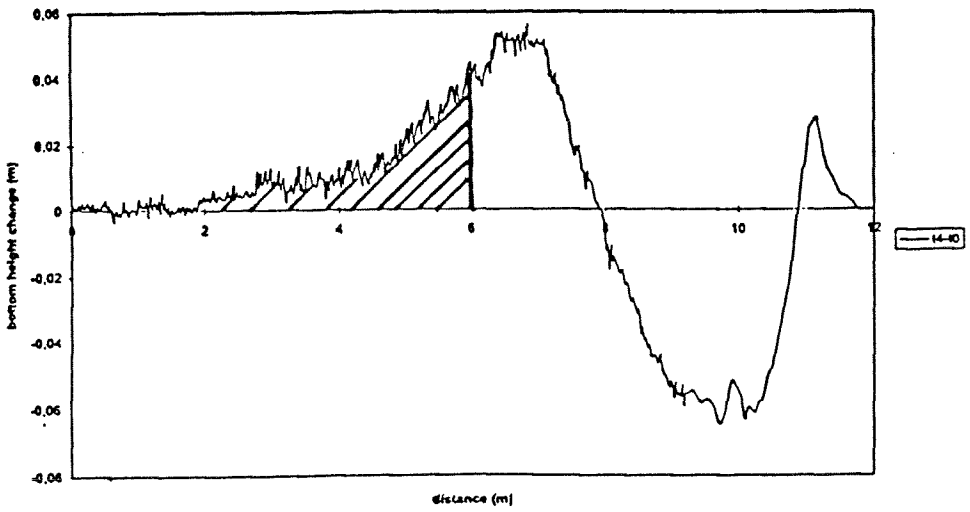

Figure 4.26 Determination of the cross-shore transport rate.

The transport rate at x = 12 meter should be zero, based on the assumption that the amount of sand in the test area is constant. In none of the measurements this is the case. In Claessen and Groenewoud (1995) the following explanation is given for the change of the amount of sand in the test area:

1. inaccuracies of the measuring methods
2. different packing of sand
3. sand is transported through the borders (x = 0 meter and x = 12 meter) of the test area.

ad.1 inaccuracies of the measuring methods.
- the PROFO measures the bed with an accuracy of 0.2 mm.
- the PROFO does not ride across the bed with a constant speed.
- profile measurements around the submerged breakwater were difficult to perform, due to the stones of the breakwater. Sediment was settling between these stones, which was difficult to measure.
- the visual measurements were performed every 5 cm. Between two visual measurements the bed was assumed to be straight. This is not correct, because there were some ripples in the bed.
- it is assumed that the height of the bed is constant over the width of the flume. This is not the case, because due to boundary effects, caused by the sidewalls, profile development is not the same over the width of the flume. During a test the original horizontal bed changes to a slightly hollow- or roundshaped bed.

These are the main reasons for the differences found.

ad.2 different packing of sand.
During a test a lot of particles are stirred up, go into suspension, are transported and settle down elsewhere. There is a good possibility that the pore volume between the sand particles will change during the process. The lost or gained amount of sand is in general too big to be explained by this phenomenon.

ad.3 sand is transported through the borders of the test area.
Case 1: no breakwater present. The profile measurements started at the beginning of the slope and ended landwards of the maximum wave run-up. This means sand can only 'disappear' if it is transported landwards or seawards of these borders. No sand was transported through these borders, through the seaward border only some material with a very small particle diameter was transported, this amount is negligible.
Case 2: with breakwater present. In a test with breakwater the profile measurements did not start at the beginning of the slope, but landwards of the submerged breakwater. This was done because of the following reason. During the first three intervals there was no transport over the breakwater, so there were no profile changes to be measured. Only during the last interval some transport took place over the breakwater. At the end of interval four the average elevation of the bed in this area is calculated by weighing the amount of sand, calculating the volume and dividing this over the total area seawards of the breakwater.

Claessen and Groenewoud (1995) compensated the loss of sediment numerically. Here is chosen to take the measured values. A consequence of this is that a position must be chosen where the cross shore transport rate should be taken as zero. The position of the graphs is depending on this location. Here the transport rate at x = 0 is taken as zero. Positive values represent an onshore transport rate and negative values an offshore transport rate.

4.9.1 Description of cross-shore transport rate in the experiments without breakwater

An example of the cross-shore transport rate during the experiments without breakwater can be seen in Figure 4.27 (for full details see Appendix B). In general the cross-shore transport rate is the highest and concentrated in a smaller area during the first interval, and reduces during the following intervals. The rate continues decreasing, because the profile keeps changing towards the equilibrium profile. This is not reached though, as the rate would be zero for that situation.

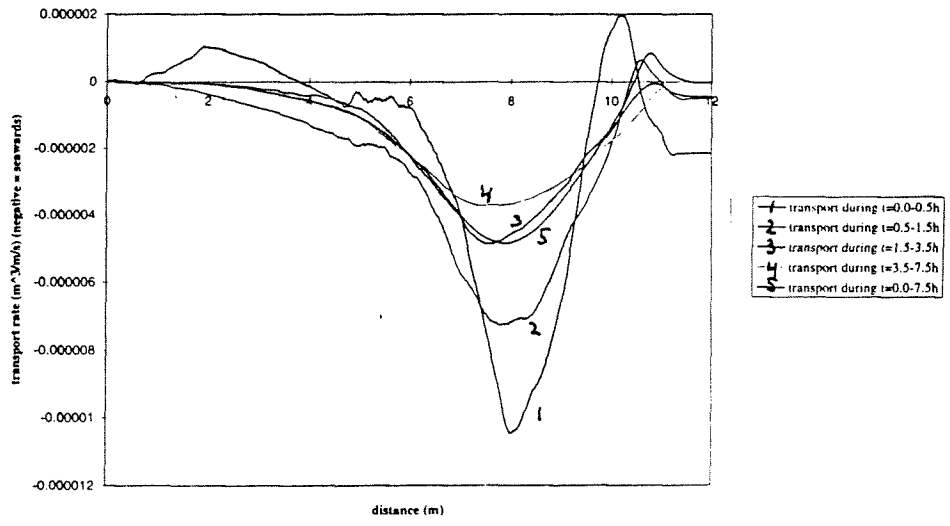

Figure 4.27 Cross-shore transport rates experiment A without breakwater

4.9.2 Comparison of cross-shore transport rate in the experiments without breakwater

As stated in the earlier sections, the wave height is the main characteristic influencing the difference between the development of the profile. Here can be seen as well (see Figure 4.28) that the experiment with the largest wave height, experiment D shows the largest cross-shore transport rate and the experiment with the smallest wave height shows the smallest cross-shore transport rate.
Less evident and contrary to expected is the behaviour caused by the different wave steepnesses. Comparing the experiments with the same wave height and varying wave lengths (experiments A, B and C) it is noted that in the experiment with the highest wave steepness (experiments C) the cross-shore transport rate is significantly smaller than in the experiment with the larger wave steepnesses. This is in line with the previous discussed characteristics, but not in line with existing theories.

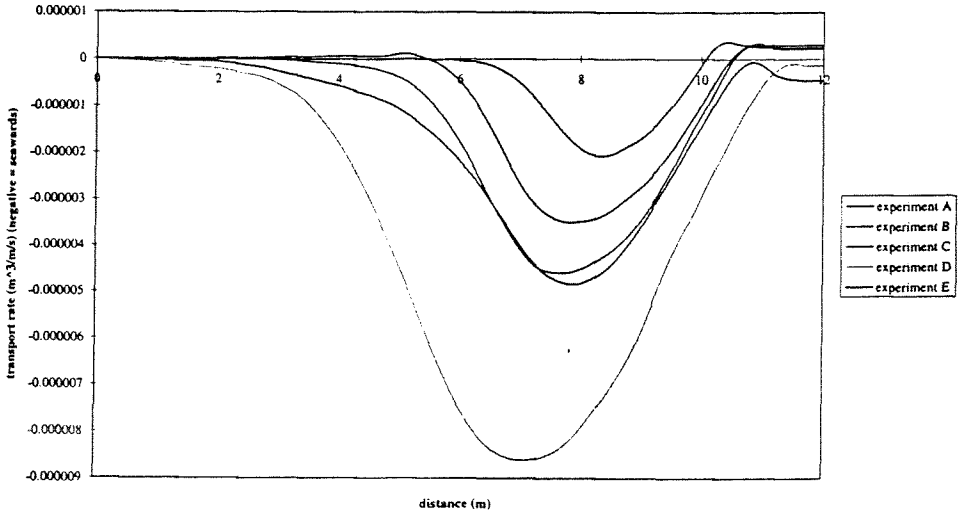

Figure 4.28 Cross-shore transport rates comparison experiments without breakwater

4.9.3 Description of cross-shore transport rate in the experiments with breakwater

An example of the cross-shore transport rate during the experiments with breakwater can be seen in Figure 4.29 (for full details see Appendix B). The same behaviour is shown as in the experiment without breakwater. The largest transport rate occurring during the first interval and a reducing transport rate for the following intervals. The area in which there is a cross-shore transport rate is smaller for the first interval. At the shoreline there is a small landwards transport rate. The larger changes during the first interval are here as well caused by the fact that the shape of the profile at the start of the experiment (1:15 slope) is far from equilibrium.

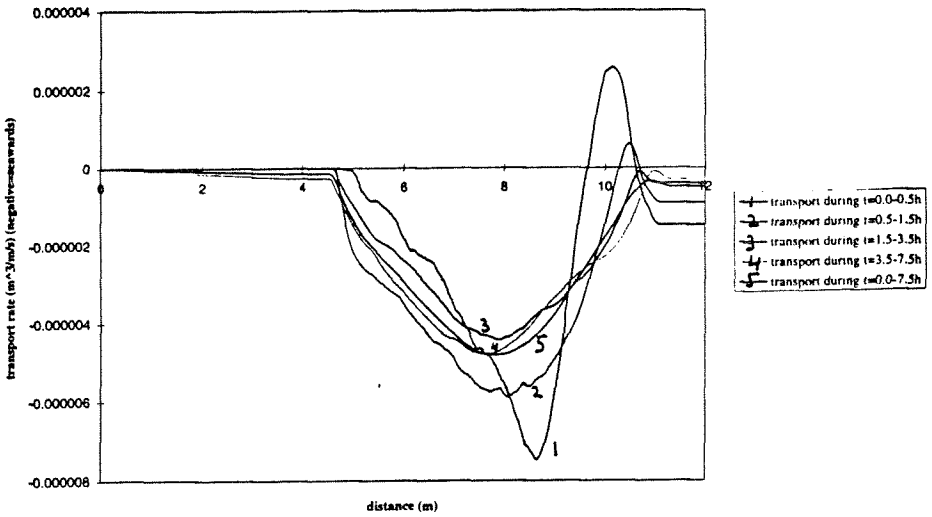

Figure 4.29 Cross-shore transport rates experiment A with breakwater

4.9.4 Comparison of cross-shore transport rate in the experiments with breakwater

The differences in the profile development between the experiments (see Figure 4.30) are comparable to the ones in the experiment without breakwater. A larger wave height causing a larger cross-shore transport rate. The cross-shore transport rates in experiment B, C and E are comparable. Here the influence of the breakwater on the cross-shore transport can be seen, it is causing a reduction of the cross-shore transport in the experiments B and C.

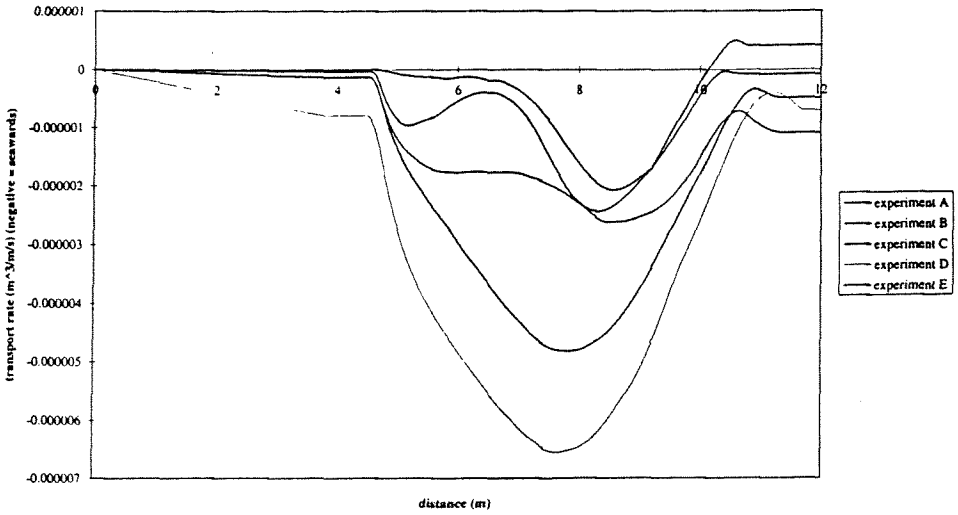

Figure 4.30 Cross-shore transport rates comparison experiments with breakwater

4.9.5 Comparison of cross-shore transport rate between the experiments without and with breakwater measured after 7.5 hours

All the cross-shore transport rates are reduced except in experiment A and E. The amount of breaking of the waves passing over the breakwater is depending on the wave height and the wave steepness. Experiment A with the lowest steepness and intermediate wave height shows hardly any change between the experiment without and with breakwater. The influence of the breakwater on the experiment with the lowest wave height (experiment E) is very small.
The breakwater only serves its goal in reducing the wave energy if the steepness and the wave height of the incoming waves are exceeding a certain value.

4.10 Conclusions

In all the described parameters (erosion volume, shoreline movement, beach face slope, profile shape, bottom height change and cross-shore transport rate) the most important parameter controlling the observed changes is the wave height. The larger the wave height the larger the changes.
The influence of the wave length / wave steepness is less clear. Looking at the results from the experiment with the same wave height and varying wave length / steepness, the general point noted is that the experiment with the largest wave length / smallest wave steepness shows the largest changes in the beach profile development. This is contrary to the state of the art, as for a higher steepness larger changes are predicted considering beach profile changes.

The influence of the breakwater is in general reducing the erosion volume, shoreline retreat, bottom height change, increasing the beach face slope, and blocking the cross-shore transport causing sedimentation at the landside toe of the breakwater for the case with breakwater. The effectiveness is depending on the incoming wave characteristics. The amount of waves which break while passing over the breakwater is depending on the wave height and the wave steepness of the incoming wave. The experiment with the smallest wave height (experiment E) and the one with the lowest wave steepness (experiment A) showing the smallest difference comparing the analysed parameters for the case without and with breakwater. This is as expected as the higher and steeper waves break sooner than the waves with a smaller height and steepness.

CHAPTER 5 CROSS-SHORE PROFILE MODELS

5.1 Review of existing models

There are several types of models to predict beach profile changes caused by changing hydrodynamic conditions or human interference which according to Roelvink and Broker (1993) can be grouped into:

- Descriptive models

In these models the beaches and beach states are classified and a description is given of which parameters influence the state the beach is in. These models are only useful for describing in a qualitative way the parameters which influence the profile development.

- Equilibrium profile models

In these models the developed profiles are described by an equilibrium profile. If the conditions in a certain area do not change significantly, an equilibrium profile can be reached. These models are useful in situations where the wave characteristics do not change a lot and the longshore transport gradients can be neglected.

Dean (1987) derived the following formula for an equilibrium profile model:

$$h = A * x^{2/3} \tag{5.1}$$

where

$$A = 2.25 * \left(\frac{w^2}{g}\right)^{1/3} \tag{5.2}$$

h = local water depth at a distance x from the shoreline
w = sediment fall velocity
g = gravity

- Empirical profile evolution models

These are an extension of the equilibrium profile models, in which only the final stage is described, in the empirical profile evolution models the evolution towards the equilibrium is included as well. This is described in an empirical way, including empirical coefficients to parameterize a large number of processes and therefore they must be determined for every site. These models are useful to give an indication of the occurring transport, the advantage is that a limited computing capacity is required, but the disadvantage is that the empirical coefficients have to be estimated for each site.

- Process-based models

In these models the profiles are not empirically calculated from the shape of the profile, but the different processes which govern the profile development are taken into account. The disadvantage of these models is the relatively large computing

capacity which is needed. UNIBEST_TC is a model of this type and will be used in Chapter 6 to compare its performance to predict transport rates with measured values from experiments.

Basic principles

The processes which are used to calculate the profile in a process based model are the wave propagation and the correlation of the sediment transport to the water movement. The input data are cross-shore profile, sediment properties and seaward boundary conditions such as wave height and period. The rate of change of the bottom level is computed by solving the continuity equation for the sediment volume.

$$(1-n)\frac{\partial z_b}{\partial t}+\frac{\partial \bar{q}}{\partial x}=0 \qquad (5.3)$$

n = pore content of the bed material

During each timestep it is assumed that the boundary conditions and pore content are constant and that the bottom profile change does not influence the watermovement (see Figure 5.1).

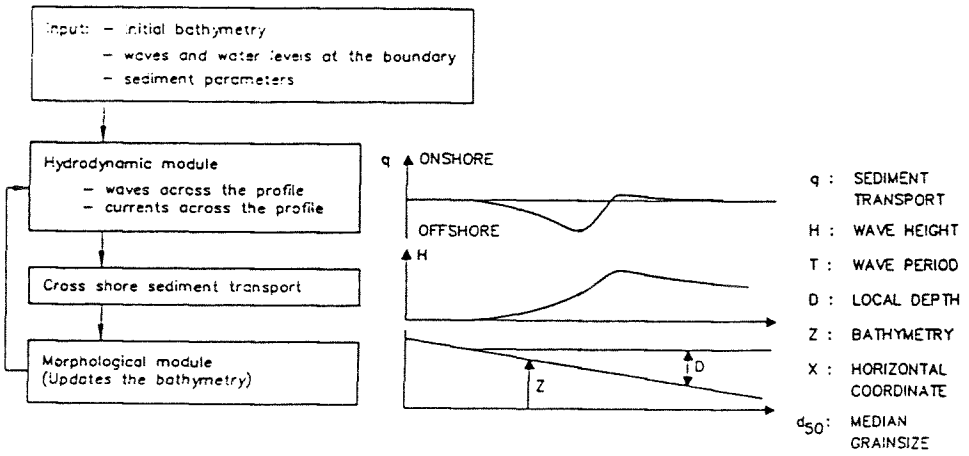

Figure 5.1 Basic structure of the morphological models and definition sketch (Roelvink and Broker (1993))

The time-averaged transport rate is given by:

$$\bar{q}(x)=\frac{1}{t2-t1}\int_{t_1}^{t_2}\int_{z_b}^{z_s}u(x,z,t)c(x,z,t)dzdt \qquad (5.4)$$

u = horizontal velocity
c = volume concentration of sediment.

Because of the complexity of the time scale this equation is schematised and the time scale is split up:

$$u = \bar{u} + u_{lo} + u_{hi} + u' \tag{5.5}$$

$$c = \bar{c} + c_{lo} + c_{hi} + c' \tag{5.6}$$

$\bar{u}, \bar{c}$ = time averaged values
u_{lo}, c_{lo} = caused by low-frequency variation
u_{hi}, c_{hi} = caused by wind-wave frequency
u', c' = caused by turbulent variation

Because only the products of terms with the same time scale can have a non zero value, equation 5.4 can be rewritten as:

$$\bar{q}(x) = \frac{1}{t2 - t1} \int_{t_1}^{t_2} \int_{z_b}^{z_s} \left(\overline{uc} + u_{lo} c_{lo} + u_{hi} c_{hi} + u' c' \right) dz dt \tag{5.7}$$

The in this report used model (UNIBEST_TC) is a time varying total load model, which is characterised by the following two assumptions:
- The vertical integral of the sediment flux is taken as the product of the total load and the velocity at the reference level; assuming that the velocity profile is reasonably uniform over the layer where most of the transport occurs.
- Supposing that the transport is concentrated in the layer near the bottom where the concentration is related to the velocity changes, the total load is taken as a function of the instantaneous reference velocity.

5.2 UNIBEST_TC

Processes shown in Figure 5.1 are calculated or modelled in UNIBEST_TC in the following way (for further details see Appendix C).

5.2.1 Wave propagation model

In UNIBEST_TC the wave energy dissipation (D) is split up in two parts, D_b wave energy dissipation due to wave breaking based on the model of Battjes and Janssen (1978) and D_f wave energy dissipation due to bottom friction. The wave energy decay model of Battjes and Janssen is a model for the dissipation of wave energy in random waves, breaking on a beach.
This model is based on the wave energy balance, written as

$$\frac{\partial P_x}{\partial x} + D = 0 \tag{5.8}$$

in which P_x is the x-component of the time-mean energy flux per unit length, x is a horizontal co-ordinate, normal to the still waterline, and D is the time-mean dissipated power per unit area.

5.2.2 Wave energy due to wave breaking (D_b)

To calculate the wave energy due to wave breaking the wave height distribution and energy dissipation in a broken wave are combined.

- Wave height distribution

For each point with depth (h) a maximum possible wave height (H_m) is defined, and assumed is that all the waves which are breaking or broken at this point have a wave height equal to H_m. Using a probability distribution for the wave height, the probability that at a given point a height is associated with a breaking or broken wave (Q_b) is determined.

$$Q_b = \exp\left[-\frac{1-Q_b}{\left(\frac{H_{rms}}{H_m}\right)^2}\right] \qquad (5.9)$$

The average local energy dissipation rate D is proportional to Q_b.

The value of H_m is based on Miche's criterion for the maximum height of periodic waves of constant form:

$$H_m = 0.88k^{-1}\tanh\left(2\pi h/L\right) \qquad (5.10)$$

To allow for effects of beach slope and of the transformation to random waves H_m is changed into:

$$H_m = 0.88k^{-1}\tanh\left(\gamma kh/0.88\right) \qquad (5.11)$$

in which k is derived from $\left(\frac{2\pi}{T}\right)^2 = gk\tanh(kh)$ (5.12)

and γ is a (slightly) adjustable coefficient. According to Battjes and Stive (1985) the value of γ does not have a strong relation with the bottom slope, but is slightly related to the deep water wave steepness. Under the condition that $\alpha = 1$, as is derived from the determination of the energy dissipation rate (formula 5.17), they stated the following expression for γ.

$$\gamma = 0.5 + 0.4\tanh(33s_{op}) \qquad (5.13)$$

$$s_{op} = H_{rms} / L_{0p} \qquad (5.14)$$

$$L_{0p} = g / (2\pi f_p^2) \qquad (5.15)$$

- Energy dissipation in a broken wave

Following LeMéhauté (1962), the energy dissipation rate in a broken wave is estimated from that in a bore of corresponding height assuming it is a single bore taking place in a uniform flow. Battjes and Janssen apply this to a broken wave which is one of a sequence on a sloping beach with on both sides of the bore a non-uniform flow. The exact formula is changed into an order of sense relationship.

$$D_h \propto \tfrac{1}{4} f \rho g \frac{H^3}{h} \tag{5.16}$$

with f = wave frequency
ρ = mass density of water

This is applied to random waves and the before stated formulas are used; f is replaced by the mean frequency of the spectrum, H is replaced by H_m and the probability of occurrence (Q_b) is added. The factor H_m/h is left out of the relationship as most dissipation occurs in the area where this is in the order of one. The following equation was derived

$$D = \frac{\alpha}{4} Q_b \bar{f} \rho g H_m^2 \tag{5.17}$$

in which α = coefficient of order 1.

5.2.3 Wave energy due to bottom friction (D_f)

For the wave energy due to bottom friction (D_f) the following formula is used.

$$D_f = \tfrac{1}{8} \rho f_w \pi^{\frac{1}{2}} \left[\frac{\omega_r H_{rms}}{\sinh(kh)} \right]^3 \tag{5.18}$$

$$\text{in which } f_w = \exp\left[-5.997 + 5.213 \left(\frac{a_b}{r} \right)^{-0.194} \right] \tag{5.19}$$

in which a_b is the amplitude of the horizontal orbital excursion near the bottom and r is 2.5 * D_{50}.

5.2.4 Wave energy conservation principle

The energy flux is calculated with a linear approximation.

$$P_x = P = E c_g \tag{5.20}$$

in which $E = \frac{1}{8}\rho g H_{rms}^2$ (5.21)

$$c_g = \left[\frac{2\pi \bar{f}}{k}\left(\frac{1}{2} + \frac{kh}{sinh2kh}\right)\right] \quad (5.22)$$

With this determination the system of equations is closed and H_{rms} can be calculated after choosing values for α and γ. The user of UNIBEST_TC has to enter these values as well before running the program.

5.2.5 Momentum balance

The wave induced set up is calculated using the cross-shore momentum equation following Longuet-Higgins and Stewart (1962).

$$\frac{dS_{xx}}{dx} + \rho g h \frac{\partial \bar{\eta}}{\partial x} = 0 \quad (5.23)$$

in which $S_{xx} = \left(\frac{1}{2} + \frac{2kh}{sinh2kh}\right)E$ (5.24)

$h = d + \bar{\eta}$

d = depth of the bottom below still water level

$\bar{\eta}$ = wave-induced set-up

In UNIBEST_TC the wave angle with the shore normal is added as well, but this is not used as the experiments are done in a waveflume (2DV).

According to Roelvink and Stive (1989) there is a deficit in the wave parameters, the H_{rms} wave height, the set up and the energy dissipation, calculated with the model of Battjes and Janssen. In a region just after a point of initial breaking there is a spatial shift between the maximum gradient of wave height and that of the undertow. An explanation for this was found in the time needed to convert organised kinetic and potential energy into small-scale dissipative turbulent motion. To include this phenomenon in UNIBEST_TC the following equation is added to derive the turbulent dissipation.

$$D = D_b - \rho \beta_f \frac{\partial}{\partial x}(k_s hc \cos\theta_w) \quad (5.25)$$

where $D = \rho \beta_d k_s^{3/2}$ (5.26)

k_s = turbulent kinetic energy
θ_w = angle of incidence for waves
β_f = coefficient of order 1
β_d = coefficient of order 1
c = wave propagation/phase speed

5.2.6 Secondary current

The three layer concept (see Figure 5.2) from Stive and De Vriend (1987) is used to describe the secondary current.

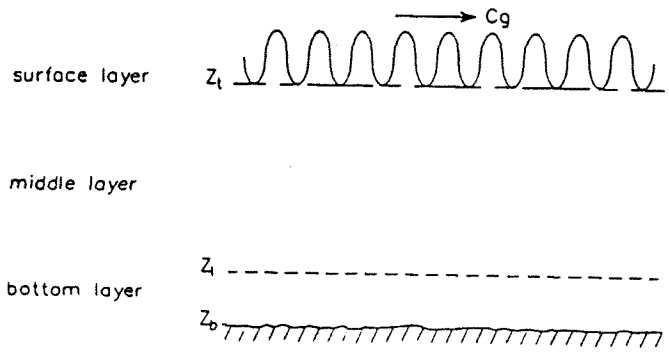

Figure 5.2 Three layer concept

The influence of the surface layer on the middle layer is reduced to an effective shear stress at wave trough level. The secondary current (τ) is composed of two factors. The first is the secondary current caused by non-breaking waves and the second is caused by breaking waves.

$$\tau(t) = \tau_{ts}^{(nb)} + \tau_{ts}^{(bs)} \tag{5.27}$$

$$\tau(t) = \rho\nu_t \frac{u_b^2 k}{c} sinh(2kh) + \frac{D}{c} \tag{5.28}$$

ν_t = eddy viscosity
u_b = near bottom oscillatory velocity amplitude
h = water depth
c = wave phase speed
D = turbulent dissipation

For the non-breaking waves the velocity in the bottomlayer is determined by a relation between the amplitude of the near-bottom orbital velocity, the friction factor and the thickness of the wave boundary layer. This is used as the bottom boundary condition of the middle layer. In case of breaking waves, the shear stress at the bottom is taken as zero. To include a spatial lag between the wave breaking and the offshore directed secondary current the turbulent dissipation (D) is used.

The integral condition of continuity is used, in which the mass flux in the surface layer is compensated by a return current in the lower layers.

$$\int_{z_b}^{z_t} U dz = -\frac{m}{\rho} \tag{5.29}$$

where $m = \left(1 + Q_b \frac{7kh}{2\pi}\right) \frac{E}{c}$ (5.30)

= mass flux in the surface layer due to breaking waves.

5.2.7 Long waves

The random wave-field is represented by a bichromatic wave train with accompanying bound long wave. Under the condition that the surface variance of the random wave corresponds with the surface variance of the schematised wave train.
The near bottom time varying flow due to short and long waves is given by:

$$u_{bi} = \hat{u}_m \cos(\omega_p t) + \hat{u}_n \cos(\omega_p + \Delta\omega)t + \hat{u}_l \cos((\Delta\omega)t + \varphi) \tag{5.31}$$

in which $\Delta\omega = \frac{1}{5}\omega_p$ = beat frequency (5.32)

ω_p = peak frequency
u_l = long-wave velocity amplitude
u_{bi} = bichromatic velocity

5.2.8 Short wave orbital velocity

The model RFWAVE is used to compute the orbital velocities near the bed due to short waves. The model is based on the Fourier approximation of the stream function method as developed by Rienecker and Fenton (1981) and using the wave energy as an input.

5.2.9 Sediment transport

The formula of Bailard (1981) is used to calculate the sediment transport rates. This formula is a total load sediment transport model, applicable to a time-varying flow over a sloping planar bed.

The major part of the sediment suspension in wave conditions is confined to a region close to the bed (within 3 to 5 times the ripple height or the sheet flow layer thickness). The sediment transport is related to the instantaneous fluid velocity and integrated over the complete wave cycle to obtain the net transport rate. It is assumed that the sediment transport takes place by two different mechanisms, bedload sediment and suspended load. From the near-bottom velocities the local near-bottom sediment transport rate is calculated.

Bailard combined the following formulas to compose his sediment transport formula. A slope of cohesionless sediment is subjected to a time-varying flow of water. Assumed is that the phase difference between the near bed velocity and the bed shear stress is negligible. The shear stress is given by:

$$\bar{\tau}_t = \rho c_f |u_t| u_t \tag{5.33}$$

in which ρ = water density
c_f = drag coefficient of the bed
u_t = time varying velocity

and the rate of energy dissipation:

$$\omega_t = \rho c_f |\bar{u}_t|^3 \tag{5.34}$$

For the local immersed weight sediment transport rate is taken a time varying vector quantity:

$$\bar{i}_t = \left(\bar{K}_{B_t} + \bar{K}_{S_t}\right)\omega_t \tag{5.35}$$

$\bar{K}_{B_t}$ = bedload transport rate vector
$\bar{K}_{S_t}$ = suspended load transport rate vector

It is assumed that the bedload transport behaves as a granular fluid shear layer, it consists of two factors the first one in the direction of the instantaneous velocity and the second one is directed downslope.

$$\bar{K}_{B_t} = \frac{\varepsilon_b}{\tan\varphi}\left(\frac{\bar{u}_t}{|\bar{u}_t|} - \frac{\tan\beta}{\tan\varphi}\hat{i}\right) \tag{5.36}$$

in which:
ε_b = bedload efficiency
φ = internal angle of friction of the sediment
$\tan\beta$ = the slope of the stream bed

The suspended transport rate vector is composed of two factors as well, the instantaneous velocity factor and the downslope directed factor. The suspended transport is supported by turbulent diffusion in the stream.

$$\bar{K}_{S_t} = \varepsilon_s \frac{|\bar{u}_t|}{w}\left(\frac{\bar{u}_t}{|\bar{u}_t|} - \varepsilon_s \tan\beta \frac{|\bar{u}_t|}{w}\hat{i}\right) \tag{5.37}$$

ε_s = suspended efficiency
w = fall velocity of the sediment

By combining these formulas and integrating over time the total load transport formula is obtained. The ratio of sediment volume to total volume of the bed material (N) is added, and the water density is substituted by the relative density of the sediment (Δ). This is the way in which the formula is presented in the manual of UNIBEST_TC.

$$\vec{q}_x = \frac{c_f}{\Delta g N}\frac{\varepsilon_b}{\tan\varphi}\left[\left\langle|\vec{u}|^2\vec{u}_x\right\rangle - \frac{\tan\beta_x}{\tan\varphi}\left\langle|\vec{u}|^3\right\rangle\right] + \frac{c_f}{\Delta g N}\frac{\varepsilon_s}{w}\left[\left\langle|\vec{u}|^3\vec{u}_x\right\rangle - \frac{\varepsilon_s}{w}\tan\beta_x\left\langle|\vec{u}|^5\right\rangle\right] \quad (5.38)$$

where:
$c_f = 0.5\ f_w$
$f_w = \exp(-5.977 + 5.213\ (a_b/r)^{-.194})$
$< >$ indicate averaging over time

In the model of Bailard and in UNIBEST_TC the velocity moments are calculated using Taylor series. The velocity moments are expressed in terms of a steady current $\bar{u}$ and an oscillatory wave-induced velocity $\tilde{u}$, combined with the angle between waves and currents. There are two Taylor expansions possible, one with the orbital motion small compared to the steady current and the other vice versa.

5.2.10 Morphology

The bottom level changes are computed from the mass balance (see equation 5.3). Numerical methods to solve these equations can be seen in (Delft, 1992).

CHAPTER 6 DETERMINATION AND COMPARISON OF THE TRANSPORT RATES

6.1 Introduction

As described in Chapter 5, the Bailard transport formula will be used to estimate the transport rates. In the Bailard formula the transport is calculated using several velocity moments of the water movement near the bottom. To verify the validity of the Bailard formula for these experiments the transport volumes calculated from the in Delft measured bottom profile changes are compared with the from the velocity measurements in Barcelona calculated transport volumes, using the Bailard formula, and the with UNIBEST_TC calculated transport volumes.

For the experiments in Delft and in Barcelona the same experimental set-up is used. The difference is the scale of the experiments, in Delft the scale is 1:15 and in Barcelona 1:4, and the material of which the bottom of the wave flume is constructed. In Barcelona an unmovable concrete bed is used and in Delft only the bottom part of the slope is made of concrete and the higher part of the slope is an erodible bed consisting of sand. Another difference is the used waveboard. In Barcelona a waveboard is used which absorbs all the reflected waves, the waveboard in Delft only absorbs the reflected long waves. Because of this contain the waves in Delft more energy. The difference is larger in the experiment with breakwater as in this case the reflection is larger. In the comparison of the transport volumes with UNIBEST_TC the influence of the reflection is included by using the in Delft measured wave height as input parameter.

The velocity measurements in Delft were performed in a difficult situation with the changing bottom profile and were restricted to three positions. Therefore the under better circumstances performed velocity measurements in Barcelona were used and scaled down to Delft scale.

In the following paragraph a definition of the used velocity moments is given. In the section 6.3 the obtained transport rates are described and compared. After an introduction the sediment transport volume calculated from the in Delft measured bottom profile change is compared with the sediment transport volume calculated with the Bailard formula from the in Barcelona measured velocity moments. In the next part the sediment transport volume calculated from the in Delft measured bottom profile change is compared with the sediment transport volume obtained from UNIBEST_TC. In paragraph 6.4 conclusions of the comparison are drawn.

6.2 Transport

6.2.1 Introduction

In the formula of Bailard (equation 6.1) the total transport is split up in two parts; the bottom transport and the suspended transport load. As is unknown for every case how

much of the transport takes place in each mode, for each case the transport coefficients (ε_b and ε_s) have to be set to a certain value.

$$\vec{q}_x = \frac{c_f}{\Delta g N}\frac{\varepsilon_b}{tan\varphi}\left[\left\langle|\vec{u}|^2\vec{u}_x\right\rangle - \frac{tan\beta_x}{tan\varphi}\left\langle|\vec{u}|^3\right\rangle\right] + \frac{c_f}{\Delta g N}\frac{\varepsilon_s}{w}\left[\left\langle|\vec{u}|^3\vec{u}_x\right\rangle - \frac{\varepsilon_s}{w}tan\beta_x\left\langle|\vec{u}|^5\right\rangle\right] \quad (6.1)$$

The transport coefficients are derived using the transport measured in Delft and the calculated transport using the in Barcelona measured velocities. This is done by looking at the ratio between the in Delft measured transport and the with Bailard from the velocity measurements in Barcelona calculated transport after the first time interval (t1 = 30 min) and only using the measurements from the part where the bottom consists of sand (x > 4.72 m). The combination of the bottom transport coefficient and suspended transport coefficient which gave the best values for the ratio in this comparison are applied in UNIBEST_TC. These values are given in Appendix E Table E.2.

6.2.2 Definition of the velocity moments

The velocities are measured at twelve positions. Six of them in the part of the wave flume with an unmovable bottom and the other six in the part with an erodible bottom, all of them situated outside the breaker zone. Only the six measurements in the part with the erodible bottom are used for the transport comparison as the bottom changes at the other six verticals are negligible. The comparison of the transport volumes is made at the Delft scale and therefore the Barcelona velocities have to be scaled down.

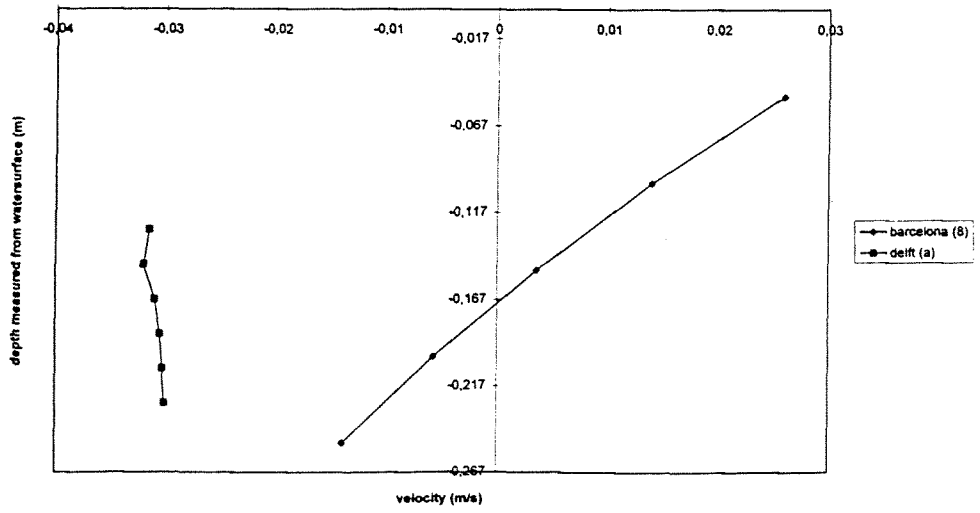

Figure 6.1 Velocity comparison between Delft and Barcelona for experiment A without breakwater

To start with the in Barcelona and in Delft measured velocities were compared. Because of the scale difference the Barcelona velocities were scaled down from a scale 1:4 to a scale 1:15, by multiplying by $\sqrt{(4/15)}$. The comparison was made for two of the Delft verticals with two of the Barcelona verticals which have a more or less comparable vertical position. The differences between the velocities are very large. There were found some discrepancies in the velocity measurements in Barcelona and the validity of the mean velocity measurements was disputed. An example of this velocity comparison is given in Figure 6.1. The velocities in Delft are measured at vertical (a) during timestep 4, and the ones in Barcelona at vertical 8.

- Velocity moments from the velocities measured in Barcelona

Because the velocity measurements in Barcelona were taken outside the breaker zone the assumption is made that the mean velocity is small compared to the orbital velocity.[1]
The transport predicted by the Bailard formula is calculated using only the orbital motion. Before calculating the velocity moments the mean current is subtracted from each measurement.

$$|u|^p = \frac{1}{n}\sum_{n=1}^{i}|u_i - \bar{u}|^p \qquad \text{p=3,5} \qquad (6.2)$$

$$|u|^q u = \frac{1}{n}\sum_{n=1}^{i}|u_i - \bar{u}|^q (u_i - \bar{u}) \qquad \text{q=2,3} \qquad (6.3)$$

- Velocity moments from the calculation in UNIBEST_TC

The velocity moments in the model of Bailard and in UNIBEST_TC are calculated using Taylor series. Because the verticals in which the velocities are measured lay outside the breaker zone, the assumption is made that the mean velocity component is small compared to the orbital velocity. The following Taylor expansion is used, it is simplified because there is only a velocity in the x-direction.

For the odd velocity moments:

$$\langle |u|^2 u \rangle = \langle \tilde{u}^3 \rangle + 3\bar{u}\langle \tilde{u}^2 \rangle + \bar{u}^3 \qquad (6.4)$$

$$\langle |u|^3 u \rangle = \langle |\tilde{u}|^3 \tilde{u} \rangle + 4\bar{u}\langle |\tilde{u}^3| \rangle + 6\bar{u}^2 \langle |\tilde{u}|\tilde{u} \rangle + 4\bar{u}^3 \langle |\tilde{u}| \rangle \qquad (6.5)$$

[1] The obtained results for the mean velocity cannot be used as there were some problems with the velocity measurements during the experiments performed in Barcelona.

and the even velocity moments:

$$\left\langle |u|^3 \right\rangle = \left\langle |\tilde{u}|^3 \right\rangle + 3\bar{u}\left\langle |\tilde{u}|\tilde{u} \right\rangle + 3\bar{u}^2\left\langle |\tilde{u}| \right\rangle \tag{6.6}$$

$$\left\langle |u|^5 \right\rangle = \left\langle |\tilde{u}|^5 \right\rangle + 5\bar{u}\left\langle |\tilde{u}|^3\tilde{u} \right\rangle + 10\bar{u}^2\left\langle |\tilde{u}|^3 \right\rangle + 10\bar{u}^3\left\langle |\tilde{u}|\tilde{u} \right\rangle + 5\bar{u}^4\left\langle |\tilde{u}| \right\rangle \tag{6.7}$$

in which: $\bar{u}$ = mean velocity component
$\tilde{u}$ = time varying velocity component

6.3 Comparison transport volumes

To increase the readability of this section the following abbreviation will be used.

- Sediment transport volume calculated from the in Delft measured bottom profile change = Delft transport.
- Sediment transport volume calculated with the Bailard formula from the in Barcelona measured velocity moments = Bailard transport.
- Sediment transport volume obtained from UNIBEST_TC = UNIBEST transport.

6.3.1 Comparison Delft/Bailard

The transport in the Delft experiments is calculated from the measured bottom profiles (see paragraph 4.9 Cross shore transport rate). To show how the transport is calculated with the Bailard formula an example is given of the calculation of the transport through vertical 9 in experiment A in Appendix D.

When choosing the best data set for the comparison of the transport volumes obtained from the profile measurements in Delft with the transport volumes calculated with Bailard from the velocity measurements (Barcelona), the following contradiction is noted:
- In Barcelona the velocities are measured in a wave flume with a stable bottom, these measured velocities are not influenced by a changing bottom profile. In the Bailard formula the original bottom slope is used. Emanating from this the best possible comparison of the values of the bottom profile transport is made just after the start of the experiment, when the profile has hardly changed.
- In the experiment performed in Delft with the moving bottom profile the relative mistakes are the largest after the first time period, because the profile has not changed a lot and the deviation of the measuring instrument is the same for each experiment, therefore it would be better to use the last measurement to make the relative error the smallest possible.

There has to be made a choice what factor has the most influence on the results; the change in the velocity due to the bottom profile change, or the deviation of the measuring equipment. Here is taken the velocity profile after interval 1 (t1 = 30 min).

In the Bailard formula the velocity moments near the bottom are used. There is not given where exactly they should be taken. The here used value is obtained from an extrapolation until the bottom of the velocity measurements. This might be a source of errors.

To illustrate the correlation between the Delft transport and the Bailard transport graphs are plotted from the Delft transport and the Bailard transport (see Figures 6.2 and 6.3).
The applied values for the transport coefficients are taken within the range used in previously published studies. The maximum applied value for ε_b is 0.2 and for ε_s is 0.03. In general can be seen that the resemblance of the data in the experiment without breakwater is better than in the experiment with breakwater.

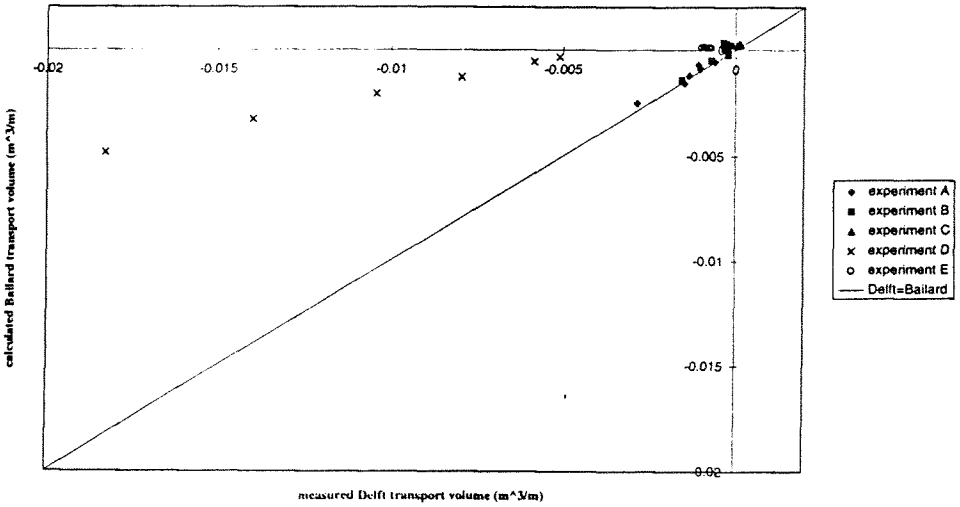

Figure 6.2 *Comparison Delft with Bailard transport volumes, experiments without breakwater*

In nearly all the cases the transport volume calculated with Bailard is smaller than the transport volume measured in Delft. In the experiment without and with there are cases for which the Delft transport is directed in one direction and the Bailard in the opposite. In the graph of the experiments without breakwater (Figure 6.2) can be seen that experiment D, the experiment with the largest wave height and the largest changes in the profile has the largest deviation between the two transport values.
The with Bailard calculated transport values are in general lower than the measured ones. This can be caused by an underestimation of the Bailard formula of the transport, using for the transport coefficients the above mentioned restrictions. More likely is that the used values for the velocities, using only the orbital velocities and neglecting the mean velocity, cause a reduction. Another possible cause of errors is the in the introduction mentioned different type of wave board used in the two experiments causing a higher wave energy in the Delft experiment.

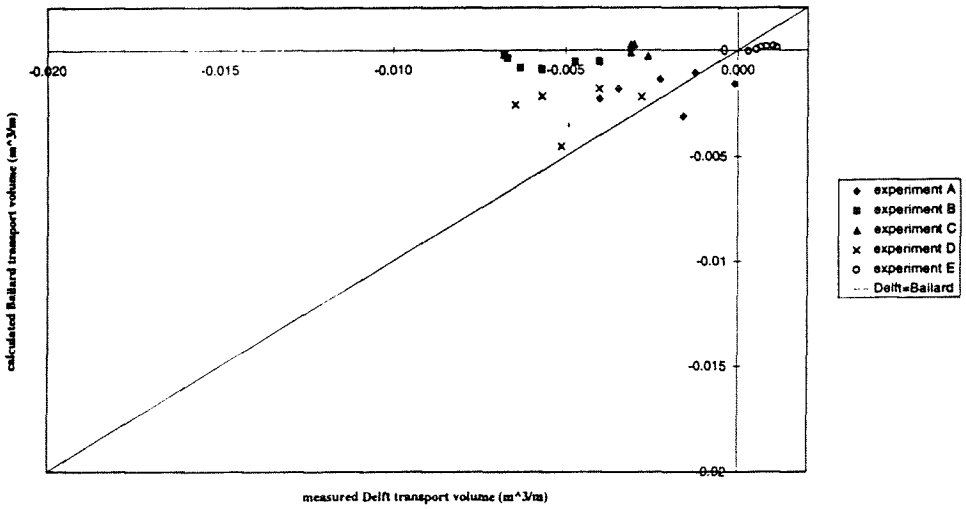

Figure 6.3 Comparison Delft with Bailard transport volumes, experiments with breakwater

Comparing the values obtained in the experiment without and with breakwater it is noted that in the experiment with breakwater the differences between the transport values are larger. This might be caused by the occurrence of a larger mean velocity in the experiment with breakwater which is neglected in the Bailard transport.
The values for the transport coefficients are chosen as the ones giving the lowest ratio comparing the transport measured in Delft and the calculated transport from the in Barcelona measured velocity moments (see 6.2.1 Introduction). For the experiments without breakwater the best set of the transport coefficients (ε_b and ε_s) is different for each experiment, ε_b is laying in the range of 0.10 until 0.20 and ε_s in the range of 0.01 until 0.03. In the experiment with breakwater for all the experiments the maximum values are taken, ε_b as 0.20 and ε_s as 0.03.

6.3.2 Comparison Delft/UNIBEST_TC

For this comparison the six vertical positions of the Delft/Bailard comparison are used and three verticals are added in the shorewards direction to see if the difference between the two transport volumes decreases if the transport volume increases. The input parameters used in UNIBEST_TC are given in Appendix E. The input parameter for the wave height is taken as the by Claessen and Groenewoud (1995) measured wave height at WHM1, which was situated at x = -3 m, the start of the applied profile in UNIBEST_TC. The Delft transport and the UNIBEST transport are plotted in Figures 6.4 and 6.5 to illustrate the relationship between them and the influence of the breakwater on this relationship.

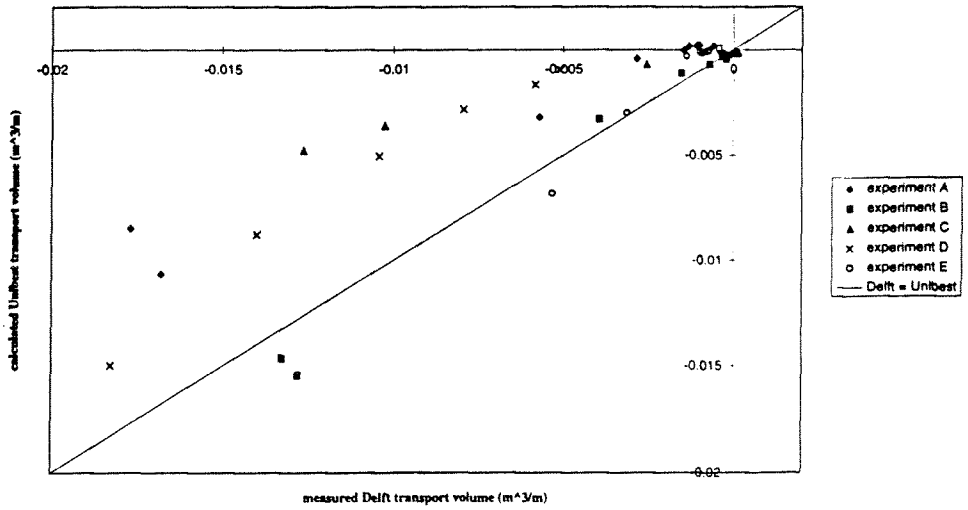

Figure 6.4 Comparison Delft with UNIBEST transport volumes, experiments without breakwater

In UNIBEST_TC for each timestep the cross shore transport rate (S_x [m^3/m/s]) is calculated. The average value from the start of the experiment until the end of the applied interval is calculated and multiplied by the total duration. As the transport coefficients ε_s and ε_b applied in UNIBEST_TC are derived from the comparison of the Delft transport with the Bailard transport it is possible that if other values are taken the difference between UNIBEST transport and Delft transport would be smaller.

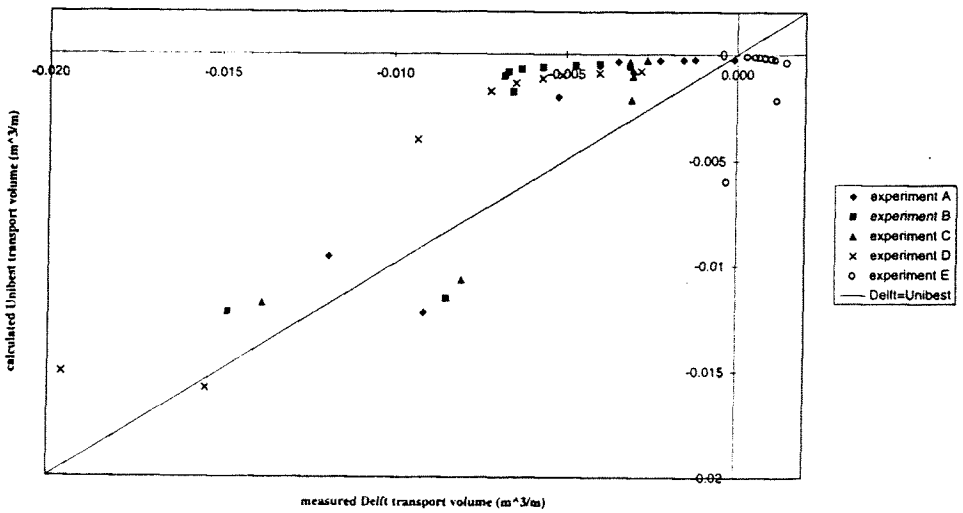

Figure 6.5 Comparison Delft with UNIBEST transport volumes, experiments with breakwater

The values measured in Delft are in general larger than the ones calculated with UNIBEST_TC. This can be caused by an underestimation of the velocities calculated in UNIBEST_TC or an underestimation of the transport volume in UNIBEST_TC (Bailard formula).

In the experiment without breakwater are the differences between the Delft transport and the UNIBEST transport smaller than in the experiment with breakwater. The underestimation of the transport with UNIBEST_TC is much larger in the experiment with breakwater than in the experiment without breakwater, caused by the fact that UNIBEST_TC is unable to calculate the correct transport for a profile with an underwater breakwater.

6.4 Conclusions of the comparison between the measured and calculated transport

The Delft transport is in general larger than the Bailard and the UNIBEST transport. This difference would be smaller for some experiments without breakwater and all of them with breakwater if the applied values for the transport coefficients were not taken within the range used in previously published studies. Here, trying to get the best resemblance possible, the maximum applied value for ε_b is 0.2 and for ε_s is 0.03. Another explanation might be for both cases (comparison with Bailard and with Unibest) an underestimation of the transport in the Bailard formula. For the Bailard transport the other causes might be the negligence of the mean velocities in the calculation of the velocity moments or the smaller absorption capacity of the wave board used in the Delft experiments causing a higher level of wave energy in these experiments. In the comparison with the UNIBEST transport the smaller value of the obtained transport might be caused by an underestimation of the velocity moments in the programme.

In the experiment with breakwater the ratios between the Delft transport and the Bailard transport and the ratio between the Delft transport and the UNIBEST transport are in general larger than in the experiment without breakwater. This might be explained by the following:
- UNIBEST_TC is incapable of calculating the correct transport for a profile with an underwater breakwater. In nature (experiment) the breakwater causes an increase in turbulence and an increase of the average wave frequency. This is not included in the UNIBEST_TC model.
- The velocity development along the depth is influenced by the breakwater. The mean velocity will increase and will be directed seawards. This mean velocity component is not taken into account in the calculation of the velocity moments from the Barcelona velocity data and therefore is the calculated transport smaller than the measured transport.

The ratio between the Delft transport and the Bailard transport and the ratio between the Delft transport and the UNIBEST transport is smaller for the larger transport volumes, caused by a larger wave height and/or wave length and a longer duration of the experiment. There are several possible explanations for this phenomenon:

- As the transport volumes are larger the relative error will be smaller.
- The Bailard formula can underestimate the transport volumes in the deeper water where the waves have not yet start shoaling.
- The in UNIBEST_TC used calculation for the velocity moments may underestimate/ overestimate certain values.

For the experiments without breakwater the best set of the transport coefficients (ε_b and ε_s) is different for each experiment, ε_b is laying in the range of 0.10 until 0.20 and ε_s in the range of 0.01 until 0.03 (see Appendix E, Table E.2). In the experiment with breakwater for all the experiments the maximum values are taken, ε_b as 0.20 and ε_s as 0.03.

CHAPTER 7 CONCLUSIONS AND RECOMMENDATIONS

7.1 Conclusions

The main aim of this master's thesis is to study the influence of a submerged breakwater on the morphological behaviour of the beach profile behind it.
The observed beach profile behaviour is tested and found in agreement with existing predictive criteria for erosion/accretion. The model scale is not affecting these results and the data set can thus be considered as 'correct' from a qualitative point of view.

The following parameters are analysed for the morphological data obtained in Delft; erosion volumes, shoreline retreat, beachface slopes, developed profiles, bottom height changes and cross shore transport rates. The most important parameter controlling beach profile changes is the wave height. The larger the wave height, the larger the changes. The influence of the wave period (wave steepness) is less evident. In general comparing the experiment with equal wave height, larger wave period (smaller wave steepness) produces larger changes in the beach profile development. This is not the expected behaviour, normally the smaller the wave period (the higher the wave steepness) the larger the changes, as far as beach profile morphodynamics is concerned.
The experiments without and with breakwater are compared, the influence of the breakwater is reducing the erosion volume, shoreline retreat, bottom height change, increasing the beach face slope, and blocking the cross shore transport, causing a sedimentation at the landside toe of the breakwater. The effectiveness of the breakwater is depending on the incoming wave characteristics; larger in the experiments with larger wave height (experiment D) and steeper waves (experiment C). This is caused by the larger amount of waves that break over the breakwater. One of the aspects arising from the analysis is that the breakwater has a better effectiveness reducing erosion volumes than shoreline displacements.

The sediment transport volume through certain verticals is calculated in three ways: the first one from the morphological data measured in Delft, the second one using the velocity moments measured in Barcelona in an energetic transport model (Bailard) and the third one applying a numerical model (including wave propagation and hydrodynamics) UNIBEST_TC.
From the comparison of these values it can be noted that the transport values obtained with the Bailard formula and UNIBEST_TC are smaller than the ones obtained from the morphological experiments.

Possible explanations for this phenomenon might be:
- Underestimation of the transport in the Bailard formula. There is a theoretical restriction on the transport coefficients used in the Bailard formula (and in UNIBEST_TC), which is taken from the literature ($\varepsilon_b \leq 0.2$ and $\varepsilon_s \leq 0.03$). With larger values for these constants the differences might be smaller for some tests without breakwater and will be smaller for all the tests with breakwater.
- For the Bailard formula the negligence of the mean velocity will reduce the calculated transport, and the difference in the absorption capacity of the wave

generation system will cause a higher energy level (and a larger transport) in the Delft experiments.
- For UNIBEST_TC the cause might be that the calculated velocities will be underestimated by the programme.

The differences are much larger in the experiments with breakwater. Additionally to the general explanation the following is applicable for the experiments with breakwater.
- UNIBEST_TC is incapable of including a submerged structure and calculating the influence that this structure has on the increase of turbulence and mean wave frequency.
- The velocities applied in the Bailard formula are restricted to the orbital velocities. The breakwater causes an increase in the mean velocity which is neglected here.

7.2 Recommendations

This study is based on just one set of data for each test case (different applied wave characteristics and without / with breakwater), to get more reliable results more experiments should be carried out.
To get more information on the final effect the morphological experiments should have been performed for a longer time period, here there is no equilibrium state reached.
Additionally due to the observed 'wrong' beach profile behaviour in function of the wave steepness, it is proposed to increase a bit the grain size in order to see if the use of very fine sediments is conditioning the results.

The mean velocity measurements were not correct and therefore only the orbital velocities were used. The verticals where the measurements were performed were all positioned outside the breaker zone, the development inside the breaker zone is interesting as well, there is less known about it. The comparison should be made again including the mean velocities and with measurements performed inside the breaker zone as well.

Finally, a very simple recommendation is done, regarding the beach profile measurements: the connection between the PROFO measurements and the 'visual' ones has to be improved because it makes the results non-conservatives.

REFERENCES

Ahrens, J.P., 1987
Characteristics of reef breakwaters
Coastal Engineering Research Center, Technical report CERC-87-17

Aminti, P., Lamberti, A. and Liberatore, G., 1983
Experimental studies on submerged barriers as shore protection structures
Int. conf. on coastal and port eng. in developing countries, Colombo 1983

Bailard, J.A., 1981
An energetics total load sediment transport model for a plane sloping beach
Journal of geophysical research, vol 86, No C11, pp 10938-10954

Bailard, J.A., 1991
Energetics model for cross-shore sediment transport
Coastal sediments '91 workshop cross-shore sediment transport models, 24 june 1991

Battjes, J.A. and Janssen, J.P.F.M., 1978
Energy loss and set-up due to breaking of random waves
Proceedings of 16th international conference on coastal engineering, pp 569-587

Battjes, J.A. and Stive, M.J.F., 1985
Calibration and verification of a dissipation model for random breaking waves
Journal of geophysical research, 1985 (C5), pp 9159-9167

Chiaia, G., Damiani, L. and Petrillo A., 1993
Evolution of a beach with and without a submerged breakwater: experimental investigation
Coastal engineering 1993, proceedings of 23d international conference on coastal engineering, volume 2, pp 1959-1972

Claessen, E.W.M. and Groenewoud, M.D., 1995
Effect of submerged breakwater on profile development
Master's thesis
Delft University of Technology, Faculty of Civil Engineering

Dalrymple, R.A, 1991
Prediction of storm/normal beach profiles
Journal of waterways, ports, coastal and ocean engineering, 118, 2, pp 193-200

Damiani, L., 1995
Experimental analysis on the efficiency of submerged breakwaters
Proceedings of the 3rd international conferenceon the planning design and operation of marinas, pp 359-366

Davies, B.L. and Kriebel, D.L., 1992
Model testing of wave transmission past low-crested breakwaters
Proceedings of 23d international conference on coastal engineering, volume 1, pp 1115-1128

Dean R.G., 1973
Heuristic models of sand transport in the surf zone
Proceedings of the conference on engineering dynamics in the surfzone, pp 208-214

Dean, R.G., 1987
Coastal sediment processes: towards engineering solutions
Procedures coastal sediments 1987, ASCE

Delft Hydraulics, 1992
User's manual UNIBEST_TC version 1.00
Delft, The Netherlands

De Vriend, H.J. and Stive, M.J.F., 1987
Quasi-3D modelling of nearshore currents
Coastal Engineering, 11 (1987), pp 565-601

Hattori, M. and Kawamati, R., 1980
Onshore-offshore transport and beach profile change
Proceedings 17th coastal engineering conference, ASCE, pp 1175-1193

Hogedal, M., Gironella, F.X., Arcilla, A.S. and Rivero, F., 1994
Dynamics of beaches, test definition report
Human capital and mobility program, Barcelona July 1994

Jiménez, J.A. and Sanchez-Arcilla, A., 1992
Simulación de cambios a corto plazo en la línea de costa
Revista de obras publicas, 3315, pp 41-51

Jiménez, J.A., Sanchez-Arcilla, A. and Valdemoro, H.I., (in press)
Prediccion de los cambios en el perfil de playa utilizando parametros adimensionales sencillos

Kraus, N.C., Larson, M. and Kriebel, D.L., 1991
Evaluation of beach erosion and accretion predictors
Coastal sediments 1991, ASCE, pp 572-587

Kriebel, L.K., Kraus, C.K. and Larson, M., 1991
Engineering methods for predicting beach profile response
Coastal sediments 1991, ASCE, pp 557-571

Lamberti, A, Petrillo, A. and Ranieri, M., 1985
A comparative analysis of some types of submerged barriers as beach defence structure
Proceedings 21st congress, international association for hydraulic research, Melbourne August 1985, volume 4, theme C, pp 27-34

Larson, M. and Kraus, N.C., 1989
SBEACH: Numerical model for simulating storm-induced beach change
Report : empirical foundation and model development, Technical report CERC-89-9, Coastal engineering research center, U.S. army engrg waterways expt. Station, Vicksburg, Miss.

LeMéhauté, B, 1962
On non-saturated breakers and the wave run-up
Procedures 8th international coastal engineering conference, Mexico 1962, pp 77-92

Longuet-Higgins, M.S. and Stewart, R.W.
Radiation stress and mass transport in gravity waves, with applications to surf-beats
Journal of fluid mechanics, vol. 13, 1962, pp 481-504

Powell, K.A. and Allsop, N.W.H., 1985
Low-crest breakwaters, hydraulic performance and stability
Hydraulics Research, Wallingford, Report SR 57, July 1985

Rienecker, M.M. and Fenton, J.P., 1981
A Fourier approximation method for steady water waves
Journal of fluid mechanics, vol 104, pp 119-137

Roelvink, J.A. and Broker, I., 1993
Cross-shore profile models
Coastal engineering, 21 (1993), pp 163-191

Roelvink, J.A. and Stive, M.J.F., 1989
Bar-generating cross-shore flow mechanisms on a beach
Journal of geophysical research, vol 94, no C4, pp 2785-4800, april 1989

Sayao, O.J. and Graham, J.E., 1991
On the prediction of beach profiles
Associate committee on shorelines, 5, 1, pp 14-23

Soulsby, R.L., 1995
The 'Bailard' sediment transport formula: comparison with data and models
Advances in Coastal Morphodynamics: an overview of the G8 - coastal morphodynamics project, 1992-1995, Delft Hydraulics 1995, pp 2_48-2_53

Stive, M.J.F. and De Vriend, M.J., 1987
Quasi-3D current modelling: wave induced secondary current
ASCE specialty conference the 'coastal hydrodynamics', Delaware

Stive, M.J.F. and Wind, H.G., 1986
Cross-shore mean flow in the surf zone
Coastal Engineering, 10 (1986) 325-340

Sunamaru, T., 1984
Quantitave prediction of beach-face slopes
Geological Society of America bulletin, vol 95

Sunamaru, T. and Horikawa, K., 1974
Two dimensional beach transformation due to waves
Procedures 14th coastal engineering conference, ASCE, pp 920-938

Tarnowska, M. and Zeidler, R.B., 1991
Offshore breakwaters
Polish-Dutch short course on coastal protection and dredging, Gdánsk, May 1991

Van der Meer, J.W. and Daemen, I.F.R., 1994
Stability and wave transmission at low-crested rubble mound structures
Journal of waterways, ports, coastal and ocean engineering, 1 (1), pp 1-19

Van der Meer, J.W. (1990)
Low-crested and reef breakwaters
Technical report, Delft Hydraulics, DH H-986

Van Rijn, L.C., 1993
Principles of sediment transport in rivers, estuaries and coastal seas
Amsterdam, Aqua publications I11, 1993

Velden, E.T.J.M. van der, 1989
Coastal engineering
Collegedictaat F7, Coastal engineering
Delft University of Technology, Faculty of Civil Engineering

APPENDIX A

- GRAPHS PREDICTING EROSIVE/ACCRETIVE RESPONSE OF THE PROFILE

GRAPHS PREDICTING EROSIVE/ACCRETIVE RESPONSE OF THE PROFILE

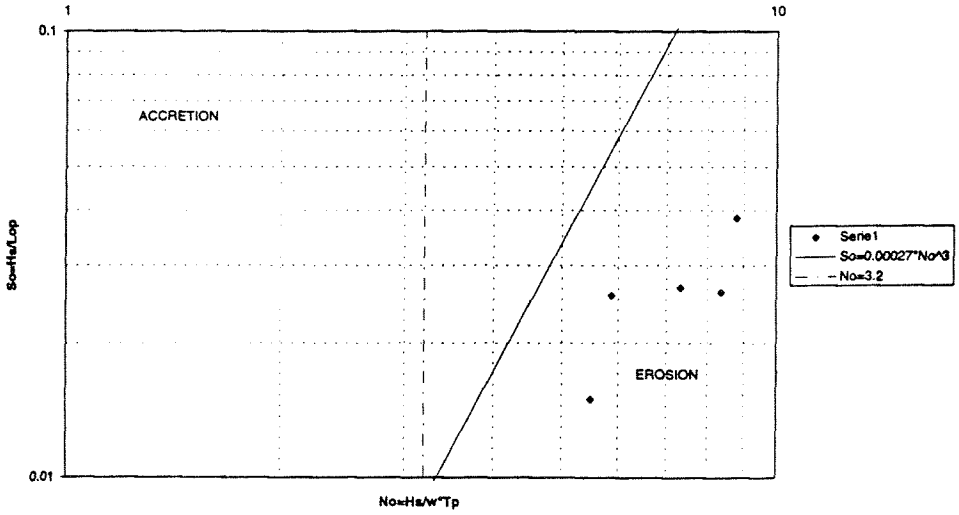

Figure A.1 Small scale data Delft, S_0-N_0 plane

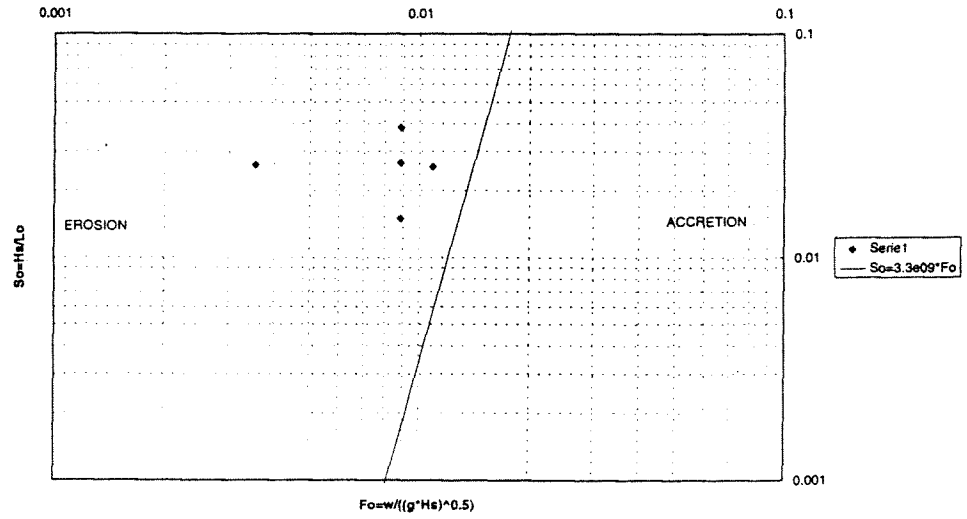

Figure A.2 Small scale data Delft, S_0-F_0 plane

GRAPHS PREDICTING EROSIVE/ACCRETIVE RESPONSE OF THE PROFILE

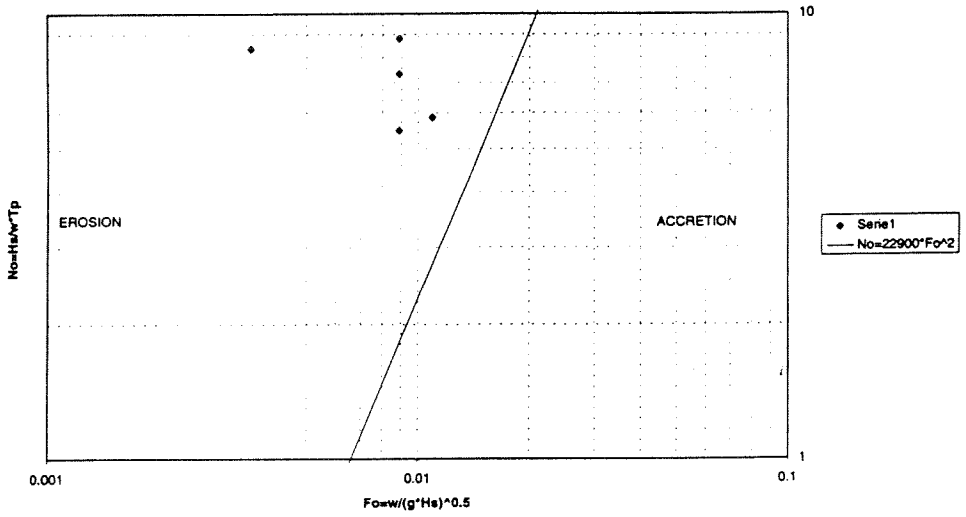

Figure A.3 Small scale data Delft, N_0-F_0 plane

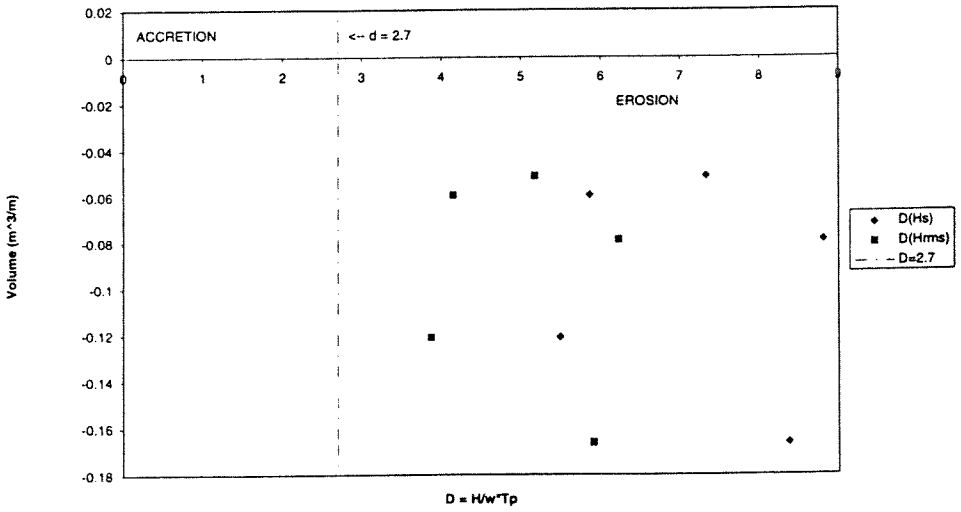

Figure A.4 Erosion and accretion volumes versus D

GRAPHS PREDICTING EROSIVE/ACCRETIVE RESPONSE OF THE PROFILE

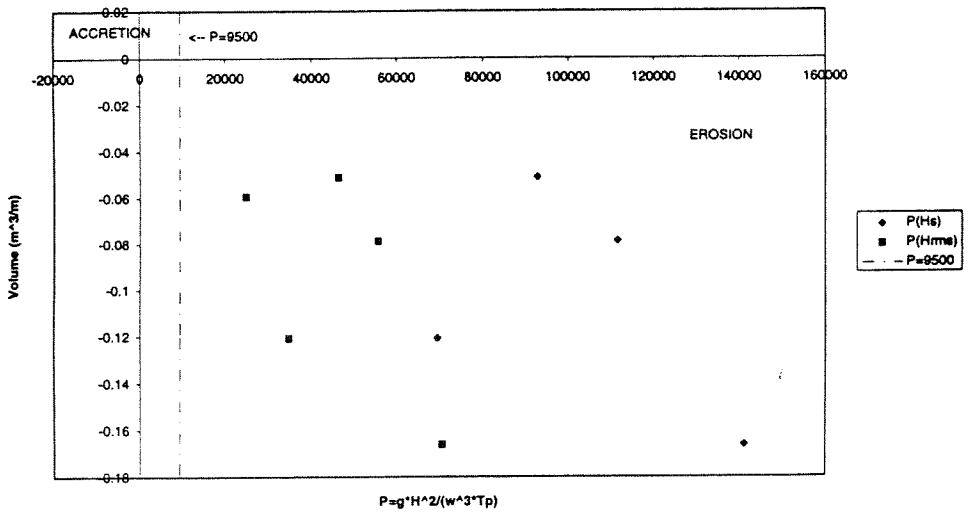

Figure A.5 Erosion and accretion volumes versus P

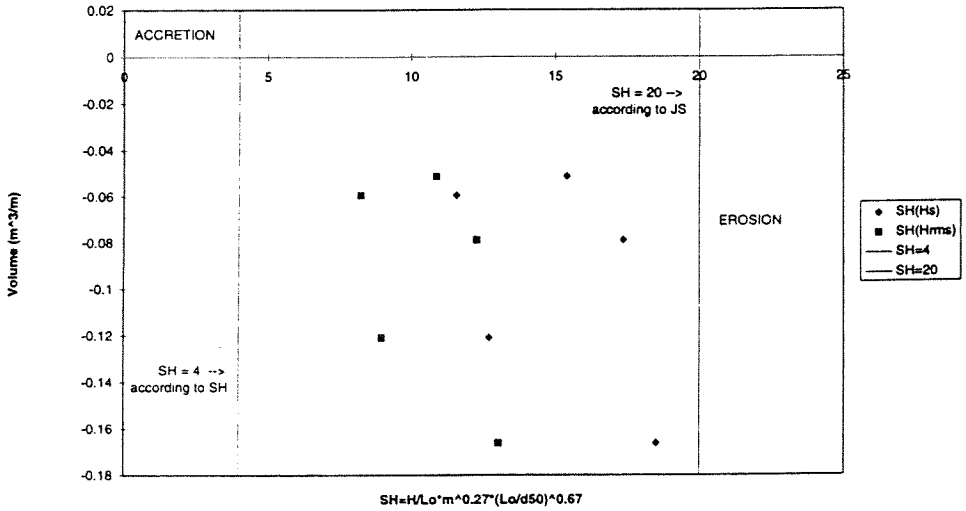

Figure A.6 Erosion and accretion volumes versus SH

GRAPHS PREDICTING EROSIVE/ACCRETIVE RESPONSE OF THE PROFILE

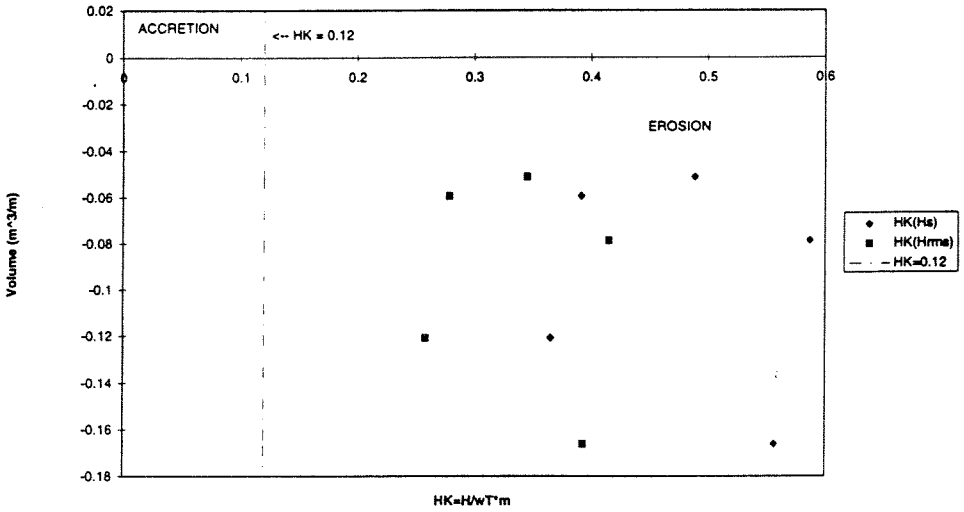

Figure A.7 Erosion and accretion volumes versus HK

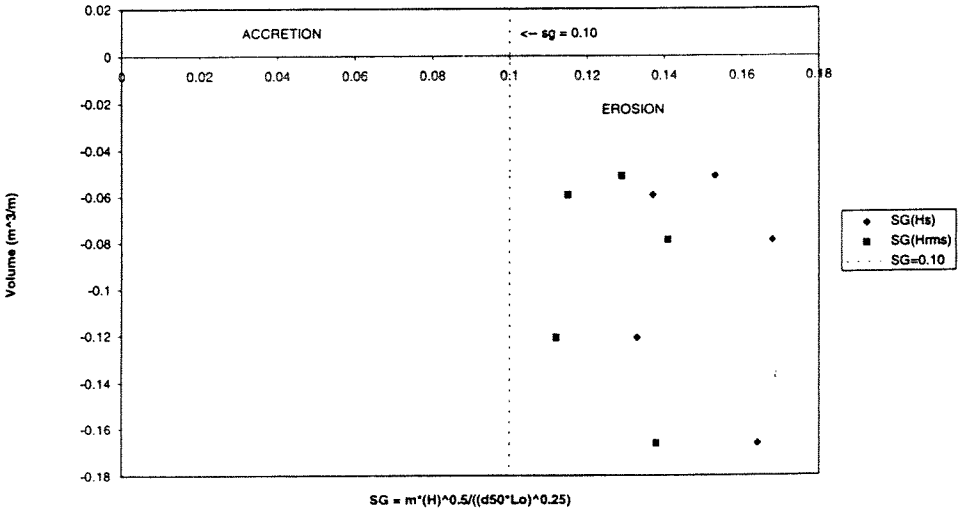

Figure A.8 Erosion and accretion volumes versus SG

GRAPHS PREDICTING EROSIVE/ACCRETIVE RESPONSE OF THE PROFILE

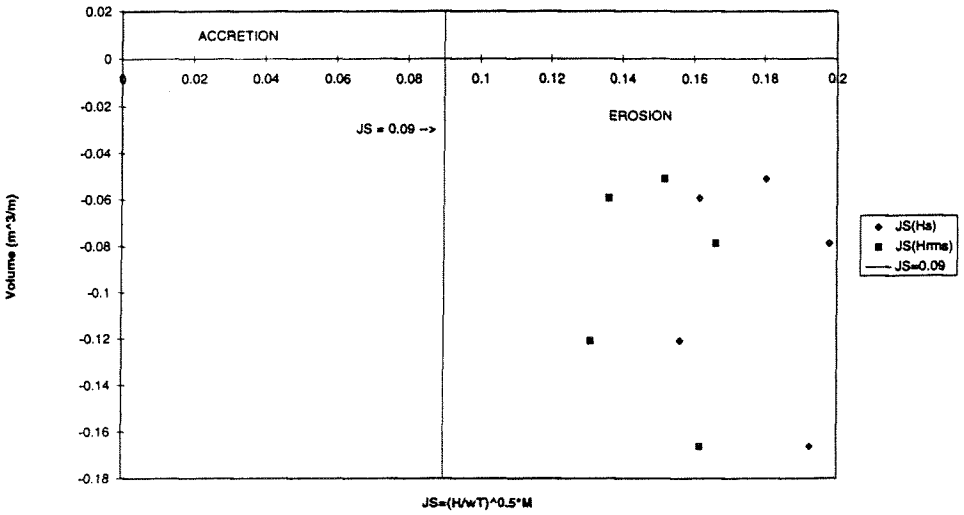

Figure A.9 Erosion and accretion volumes versus JS

APPENDIX B

- BEACH PROFILE RESPONSE EXPERIMENTS B, C, D AND E.

  - Bottom profile development
  - Bottom height change
  - Cross shore transport rate

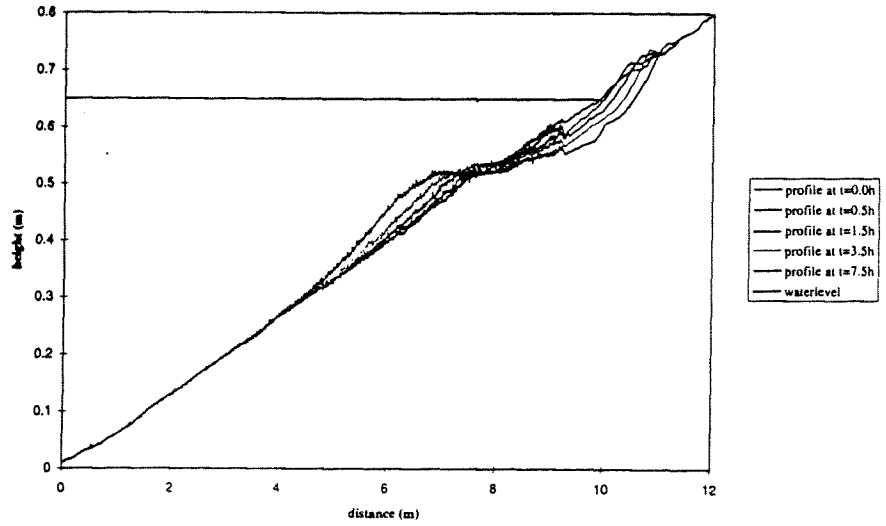

Figure B.1 Bottom profile development, experiment B without breakwater

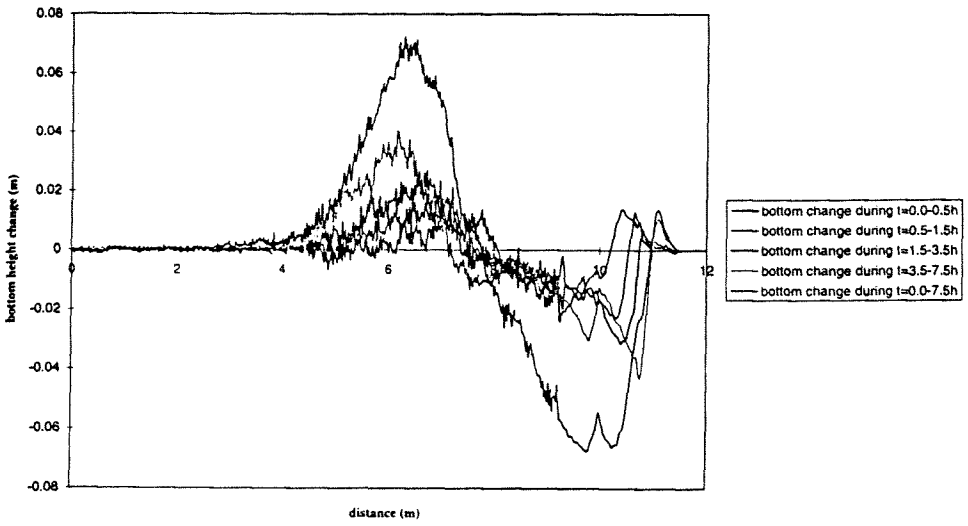

Figure B.2 Bottom height change, experiment B without breakwater

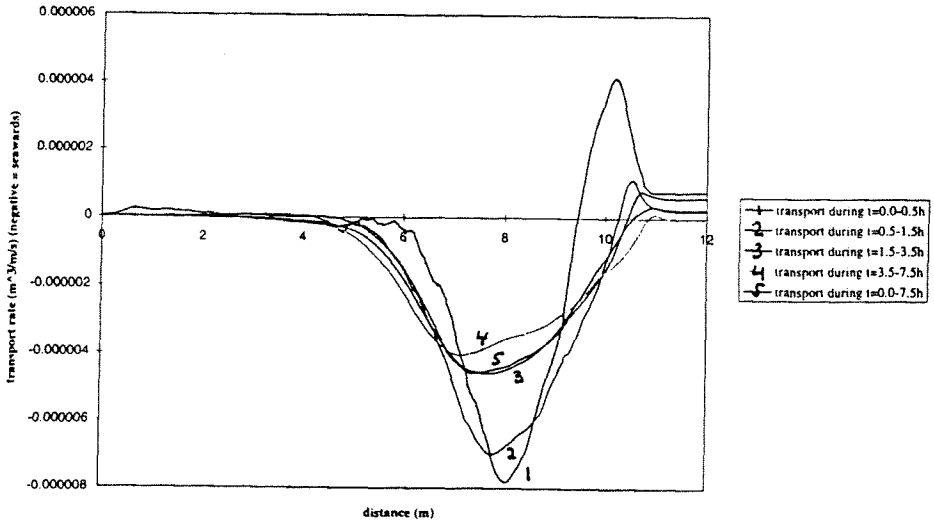

Figure B.3 Cross shore transport rate, experiment B without breakwater

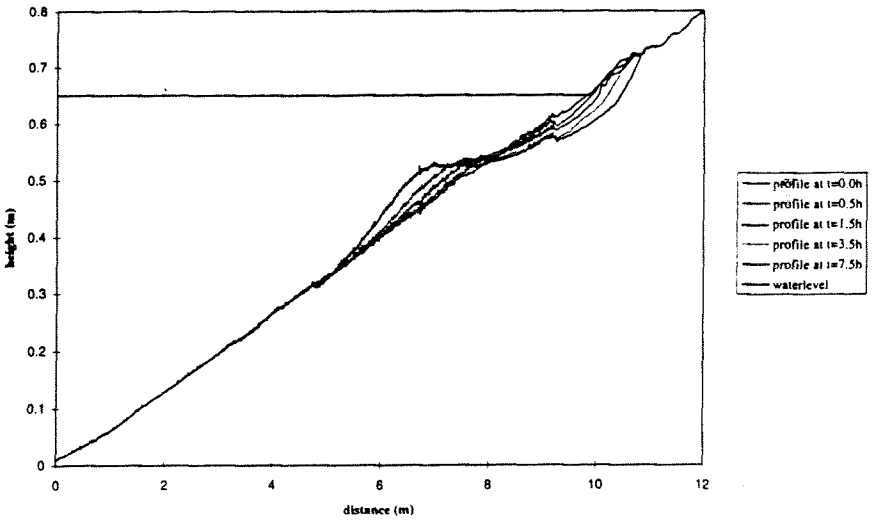

Figure B.4 Bottom profile development, experiment C without breakwater

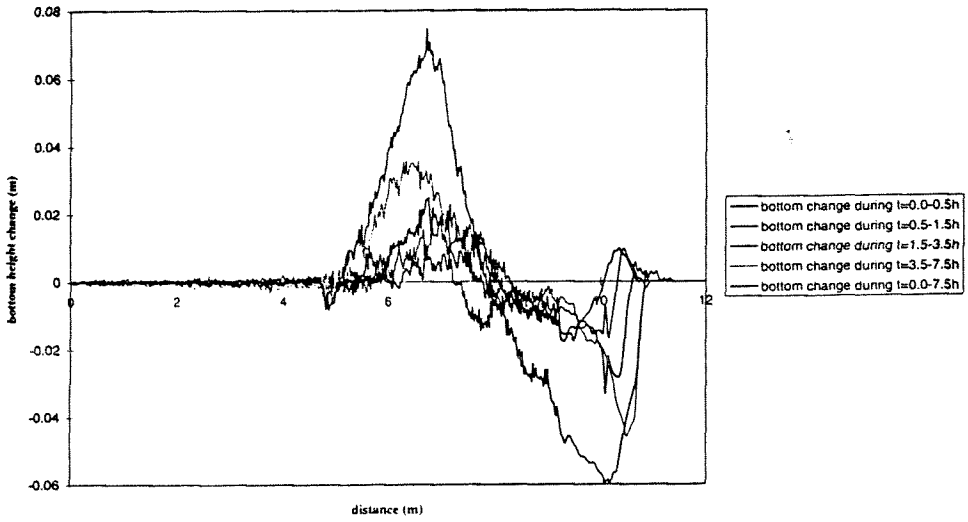

Figure B.5 Bottom height change, experiment C without breakwater

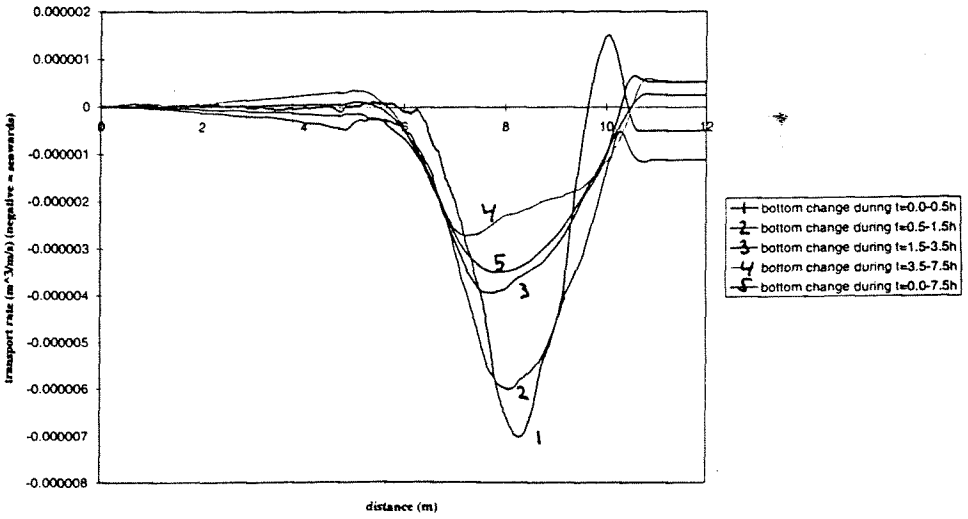

Figure B.6 Cross shore transport rate, experiment C without breakwater

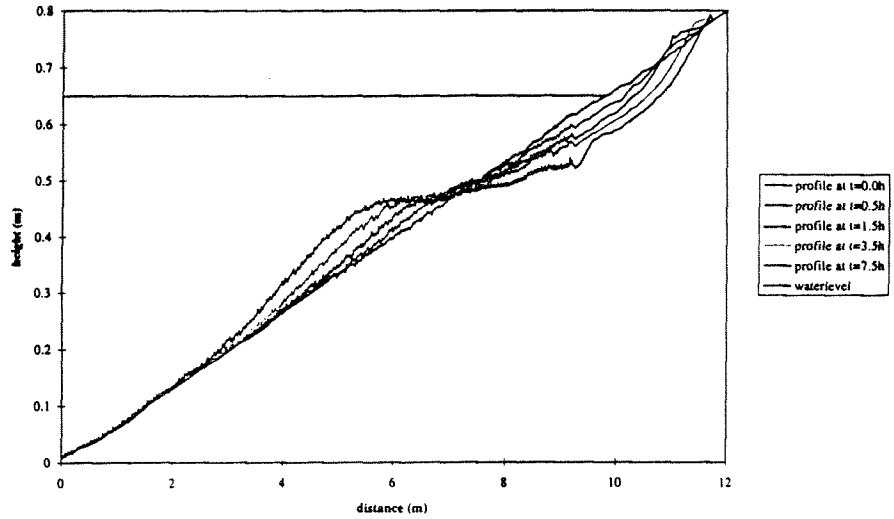

Figure B.7 Bottom profile development, experiment D without breakwater

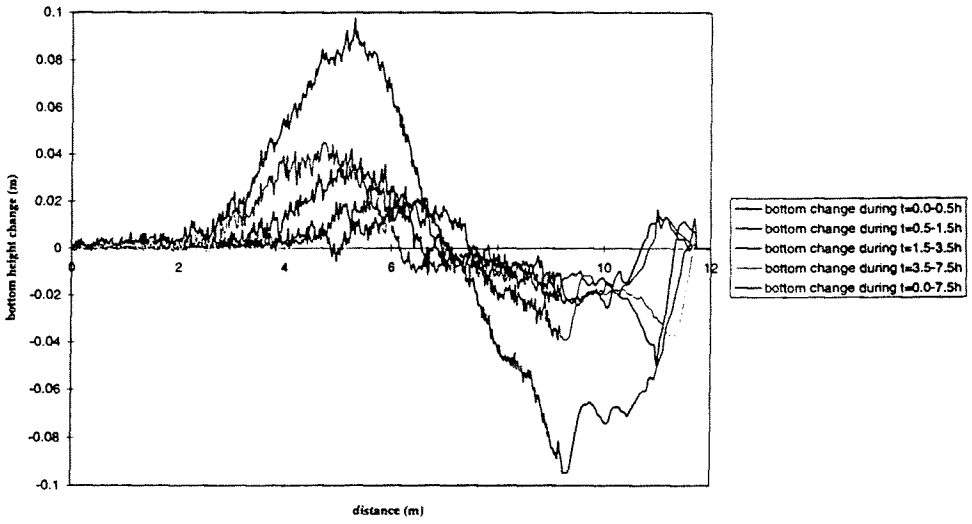

Figure B.8 Bottom height change, experiment D without breakwater

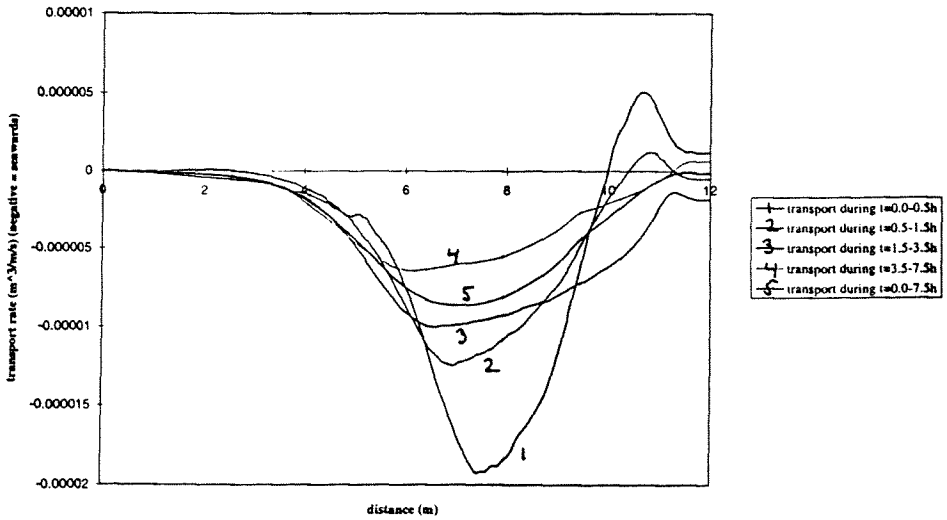

Figure B.9 Cross shore transport rate, experiment D without breakwater

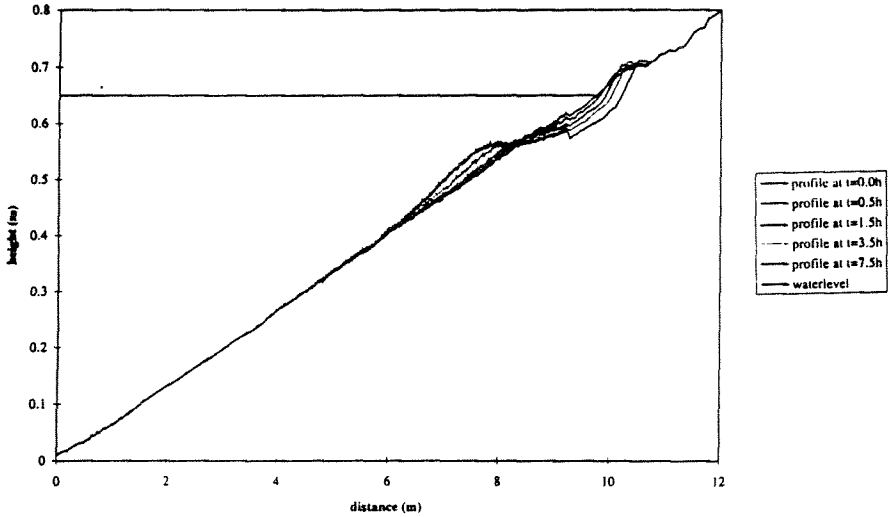

Figure B.10 Bottom profile development, experiment E without breakwater

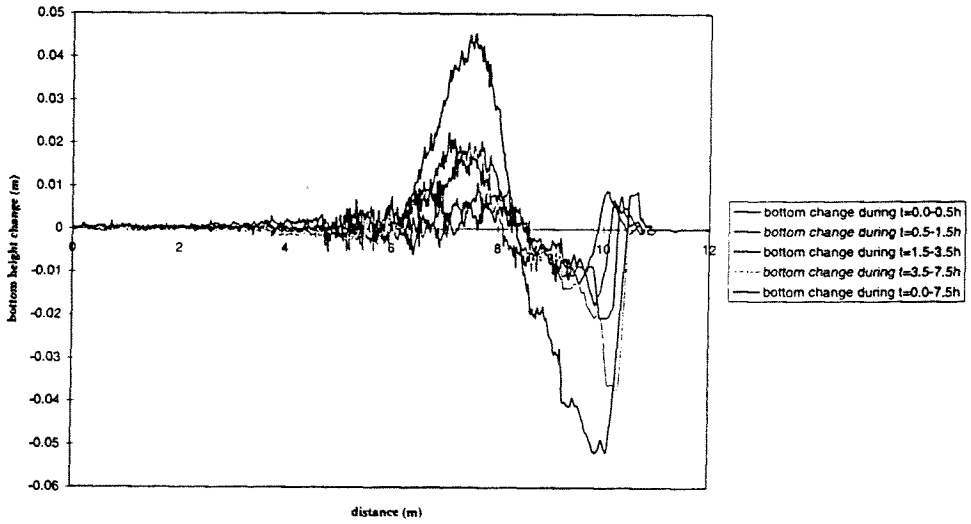

Figure B.11 Bottom height change, experiment E without breakwater

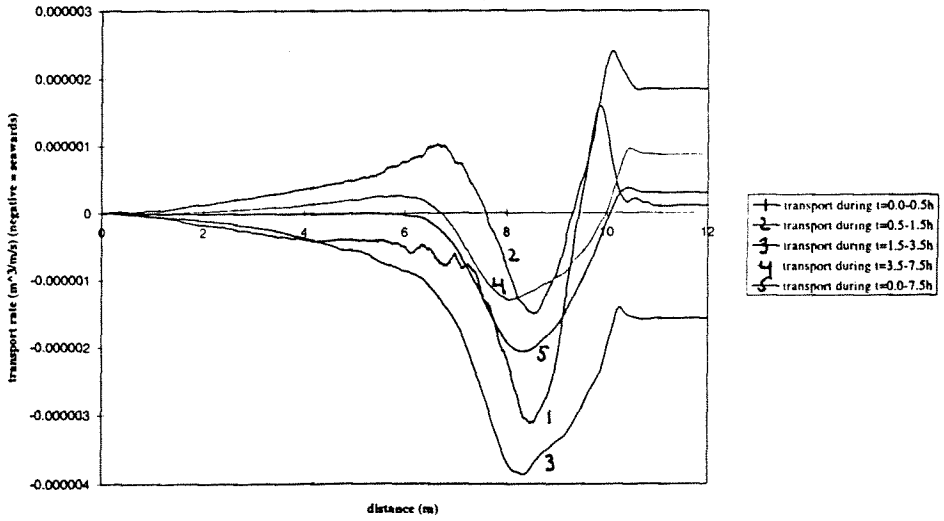

Figure B.12 Cross shore transport rate, experiment E without breakwater

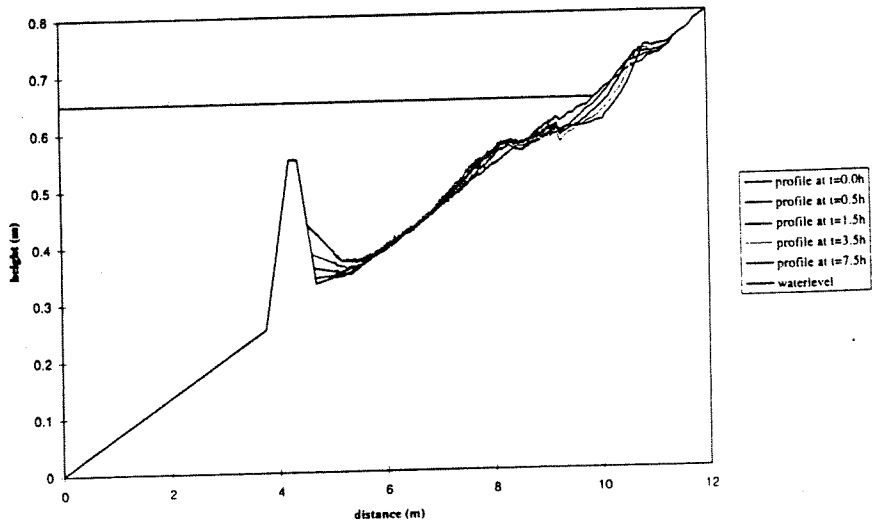

Figure B.13 Bottom profile development, experiment B with breakwater

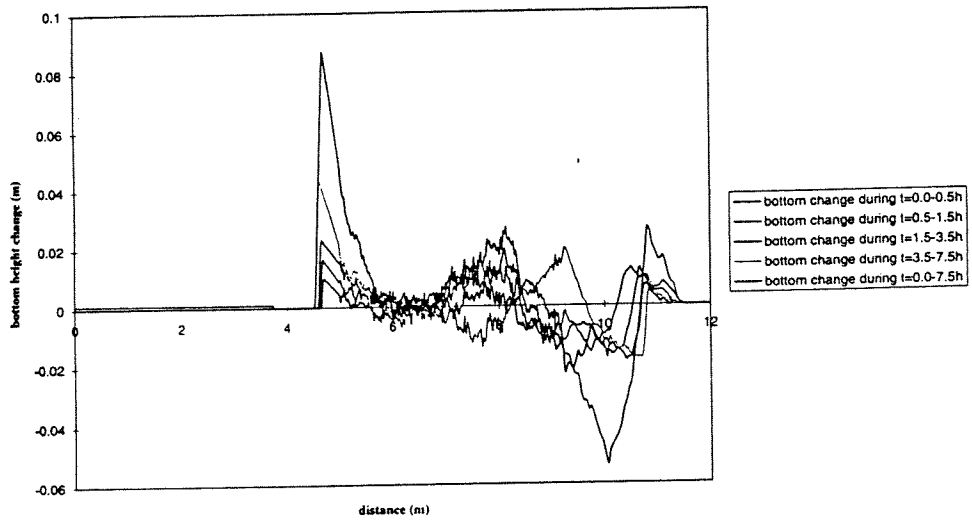

Figure B.14 Bottom height change, experiment B with breakwater

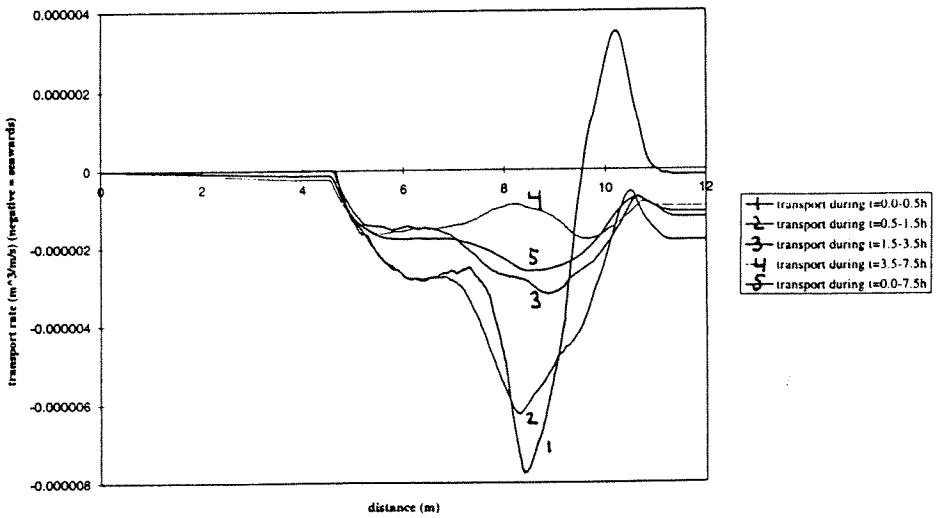

Figure B.15 Cross shore transport rate, experiment B with breakwater

BEACH PROFILE RESPONSE

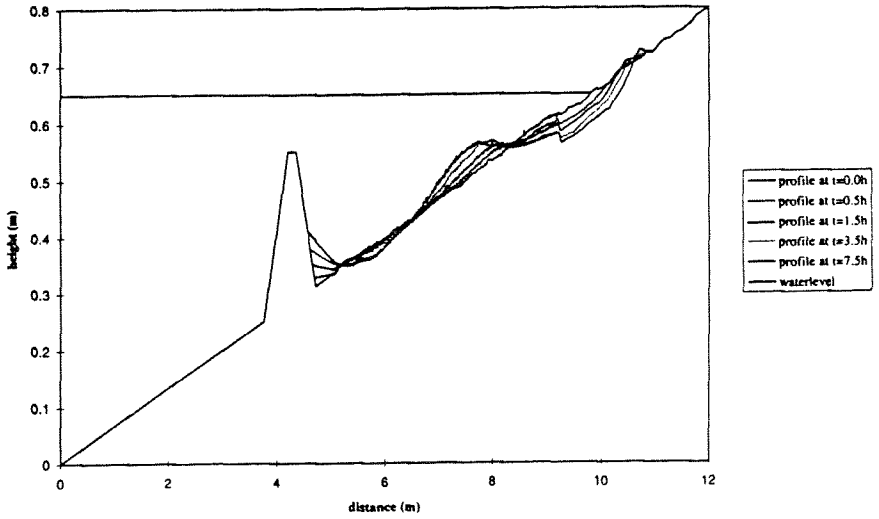

Figure B.16 Bottom profile development, experiment C with breakwater

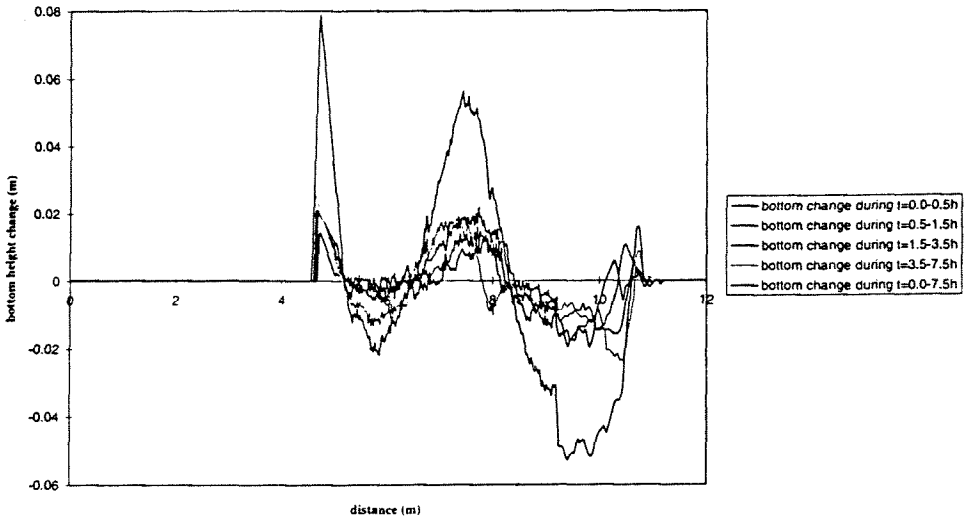

Figure B.17 Bottom height change, experiment C with breakwater

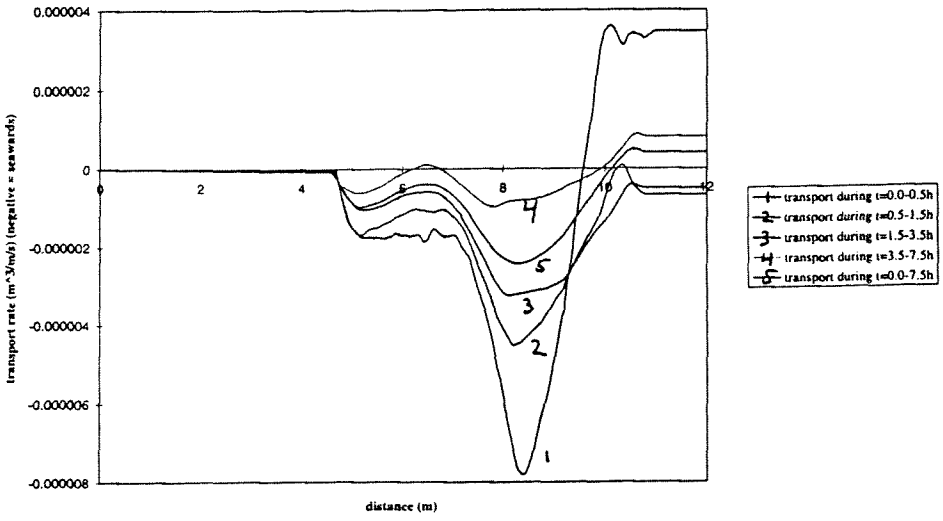

Figure B.18 Cross shore transport rate, experiment C with breakwater

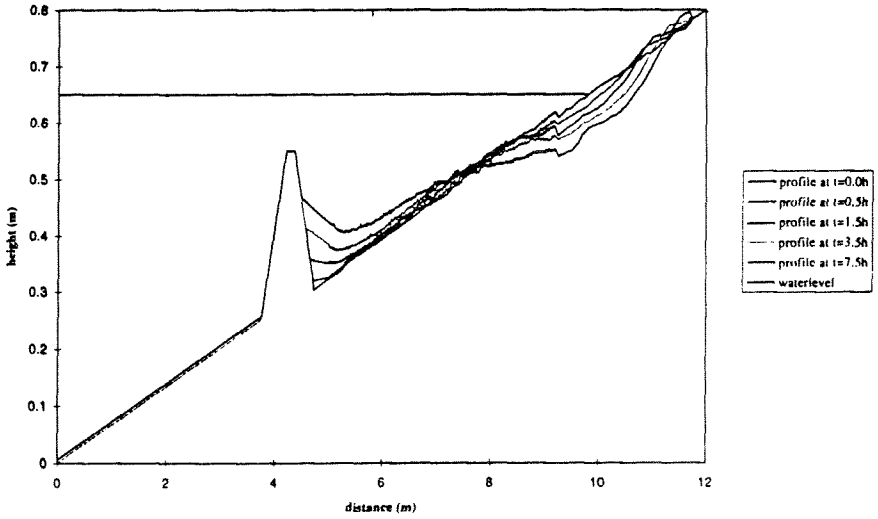

Figure B.19 Bottom profile development, experiment D with breakwater

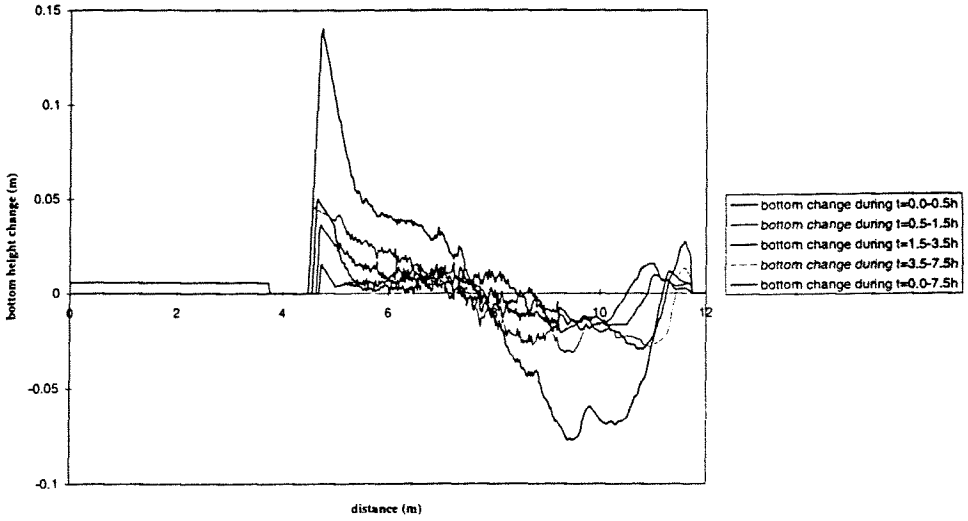

Figure B.20 Bottom height change, experiment D with breakwater

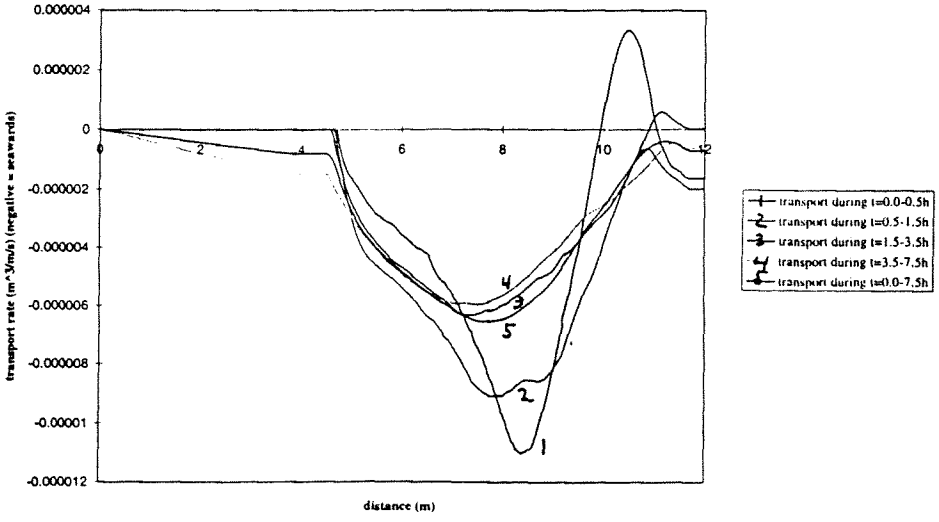

Figure B.21 Cross shore transport rate, experiment D with breakwater

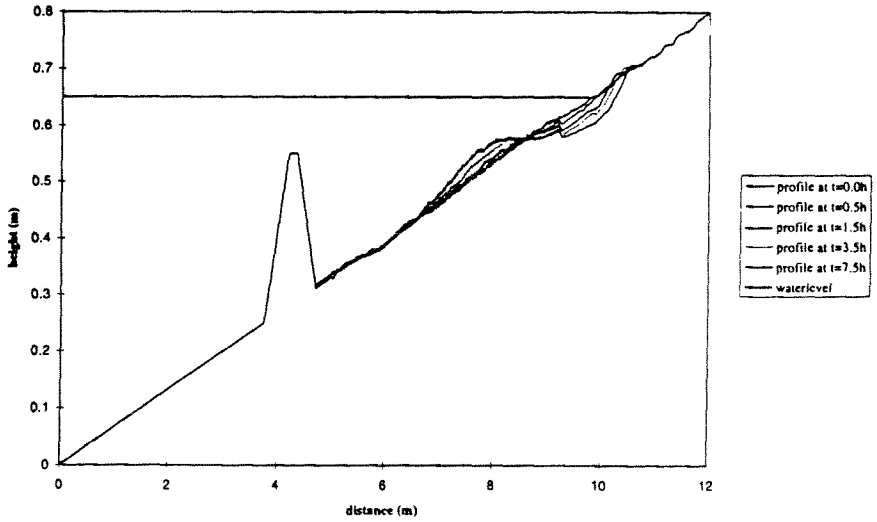

Figure B.22 Bottom profile development, experiment E with breakwater

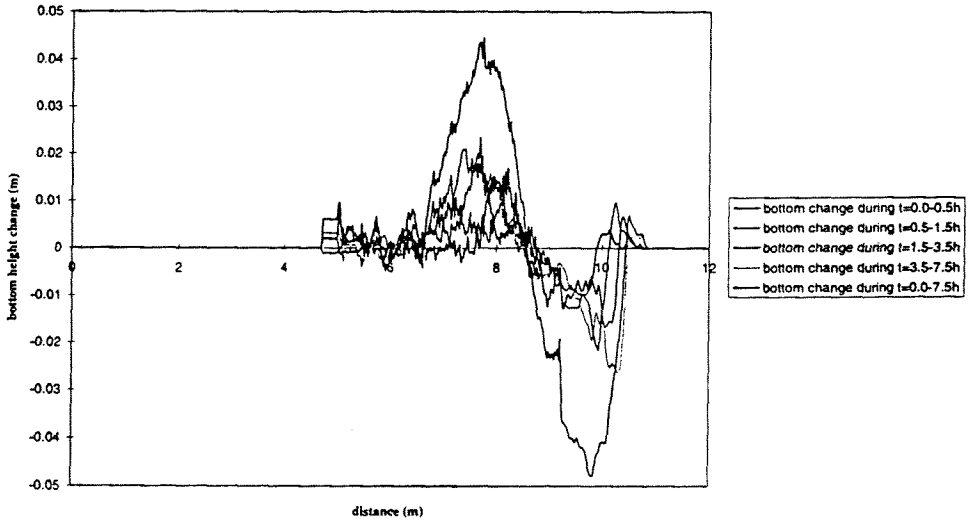

Figure B.23 Bottom height change, experiment E with breakwater

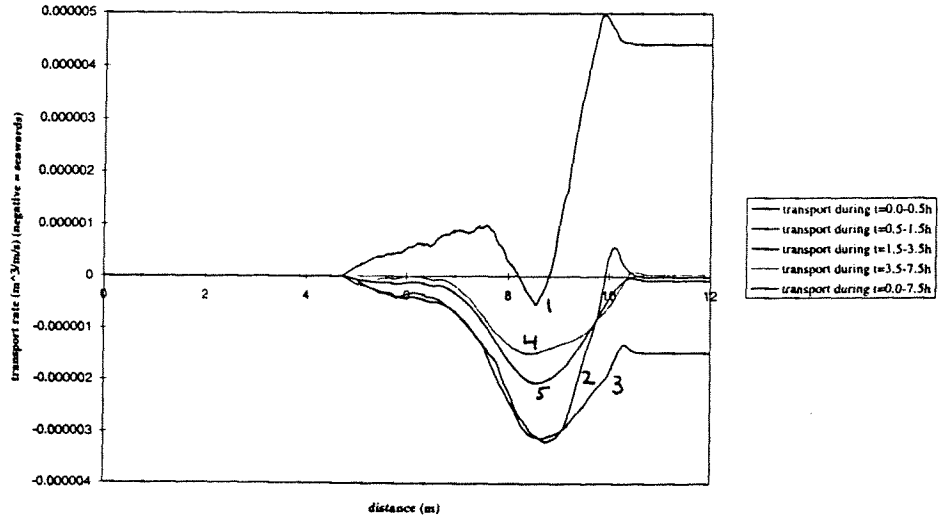

Figure B.24 Cross shore transport rate, experiment E with breakwater

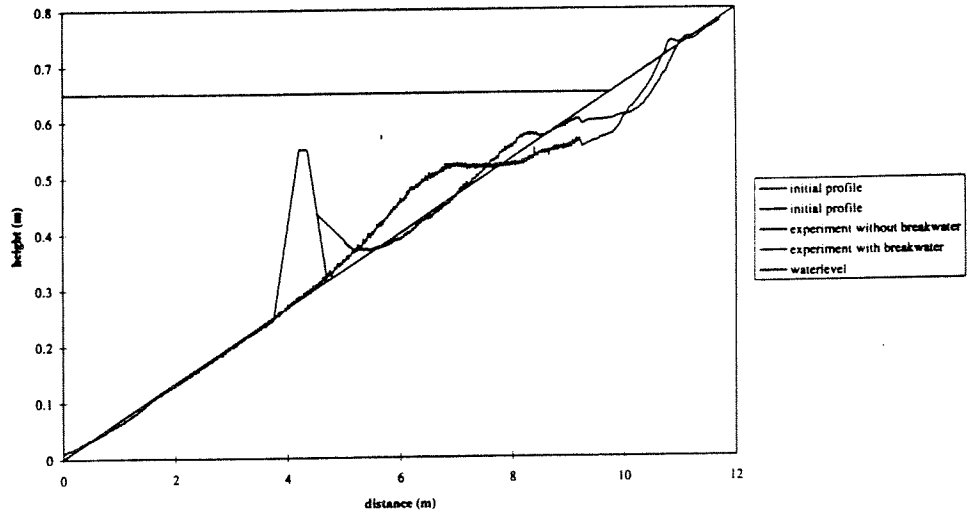

Figure B.25 Comparison bottom profile development experiment B without and with breakwater

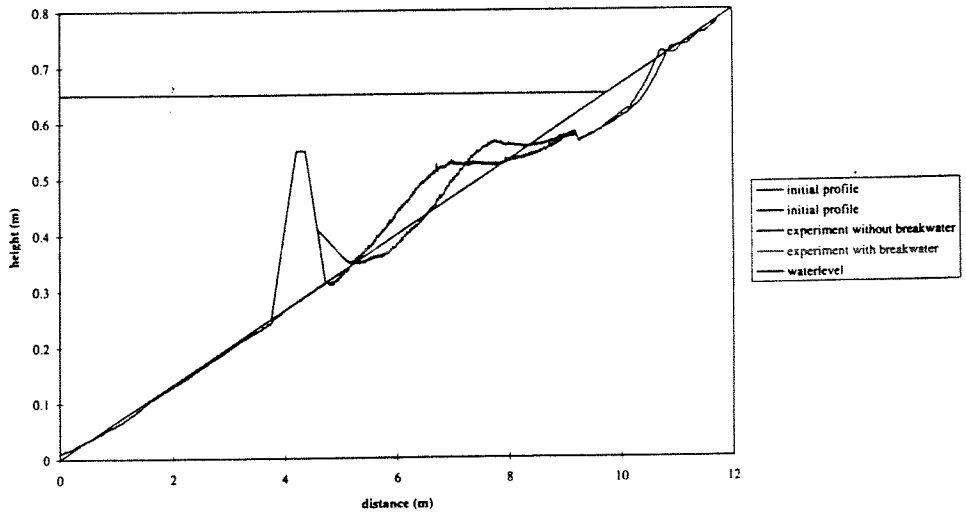

Figure B.26 Comparison bottom profile development experiment C without and with breakwater

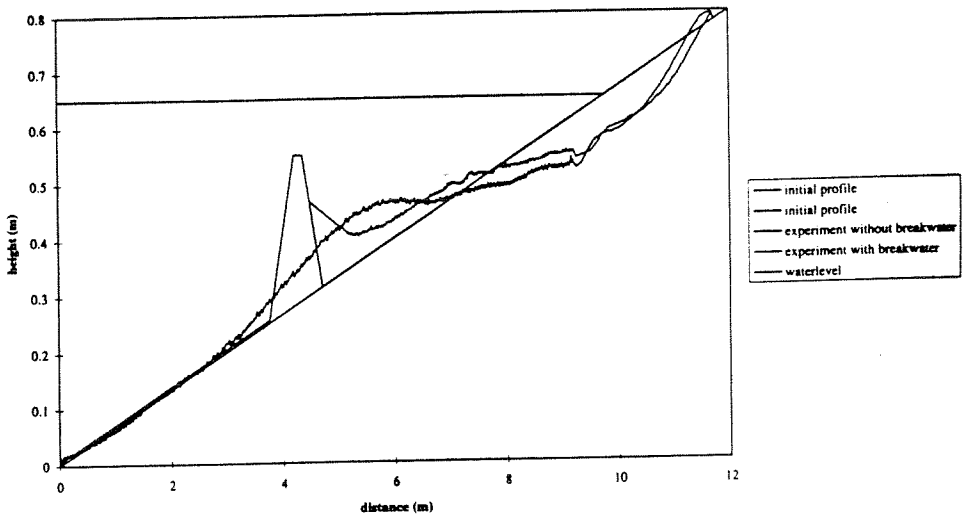

Figure B.27 Comparison bottom profile development experiment D without and with breakwater

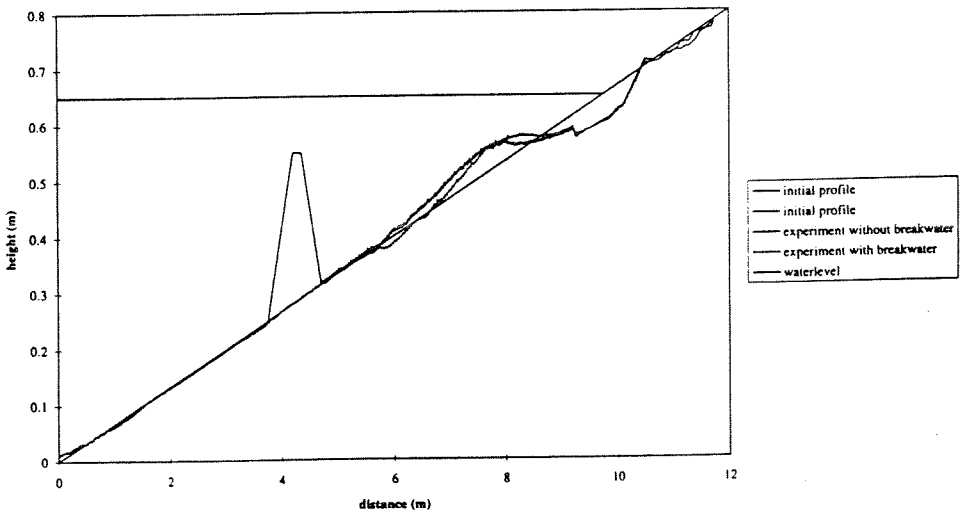

Figure B.28 Comparison bottom profile development experiment E without and with breakwater

APPENDIX C

- THEORETICAL BACKGROUND FROM MANUAL UNIBEST_TC

MATHEMATICAL-PHYSICAL DESCRIPTION

LIST OF SYMBOLS

Wave propagation

E	:	wave energy
ρ	:	density of water
g	:	gravitational accelaration
H_{rms}	:	root mean square wave height
c_g	:	group velocity
ω_r	:	relative wave frequency
k	:	wavenumber in direction of propagation
V	:	alongshore directed depth-averaged velocity
D_f	:	wave energy dissipation due to bottom friction
D_b	:	wave energy dissipation due to wave breaking
Q_b	:	fraction of breaking waves
H_m	:	maximum wave height
f_w	:	friction factor
D_{50}	:	50% grain diameter

Turbulence model

β_f	:	coefficient of order one
β_d	:	coefficient of order one
k_t	:	turbulent kinetic energy

Cross-shore momentum equation

θ_w	:	angle of incidence for waves
S_{xx}	:	radiation stress

Longshore momentum equation

i_y	:	the longshore water-level gradient due to the tide
A	:	calibration coefficient
f_c	:	friction factor due to steady current
$\tilde{U}\|_{H_{rms}}$	:	amplitude of the orbital velocity for H_{rms}

Secondary current

ν_t	:	eddy viscosity
$\tilde{u}_b$	:	near bottom oscillatory velocity amplitude
h	:	water depth
c	:	wave phase speed
D	:	turbulent dissipation
U	:	secondary current
$\tilde{u}$, $\tilde{w}$	:	orbital wave velocities
$<z_s>$	:	wave averaged surface elevation
m	:	mass flux due to breaking waves

Long waves

G_{nm}	:	transfer function [Sand, 1982]
$a_n = a_m$	:	short wave amplitudes
ξ_a	:	long bound wave amplitude
$\Delta\omega$	:	beat frequency
ω_p	:	peak frequency
u_l	:	long-wave velocity amplitude
u_{bi}	:	bichromatic velocity

Sediment transport

x, y	:	two directions perpendicular to each other
$\vec{q}_x$, $\vec{q}_y$	:	transport [m³/m'/s]
$\vec{u}$	:	instantaneous, total velocity vector near the bottom [m/s]
$\vec{u}_x$, $\vec{u}_y$	:	instantaneous velocity component in x and y direction respectively [m/s]
$\tan\beta_x$	:	$\frac{\partial z_b}{\partial x}$, z_b = bottom level, + = upwards
$\tan\beta_y$	:	$\frac{\partial z_b}{\partial y}$
Δ	:	relative density of sediment [-]
N	:	ratio of sediment volume to total volume, bed material [-]
$\tan\phi$	:	angle of internal friction [rad]
w	:	fall velocity [m/s]
c_f	:	friction coefficient = ½ f_w
ϵ_B	:	efficiency factor bottom transport
ϵ_s	:	efficiency factor suspended transport
a_b	:	amplitude of hor. orbital excursion [m]
r	:	2.5 * D_{50}

Velocity moments

$\overline{u}$	:	mean velocity component
$\tilde{u}$	:	wave velocity component
$\tilde{u}_s$	:	short-wave velocity component
$\tilde{u}_l$	:	long-wave velocity component
T_p	:	peak period

Morphology

z	:	bottom level
S_x	:	cross-shore sediment transport

Formulations

The UNIBEST_TC module is a direct descendant of the models OSTRAN [Stive and Battjes, 1984] and CROSTRAN [Stive, 1986]. In Roelvink and Stive [1989], the model is tested against wave flume measurements and improved on some points.In this paper a more detailed description of the mathematical-physical formulations used in the UNIBEST_TC module is given than presented here.

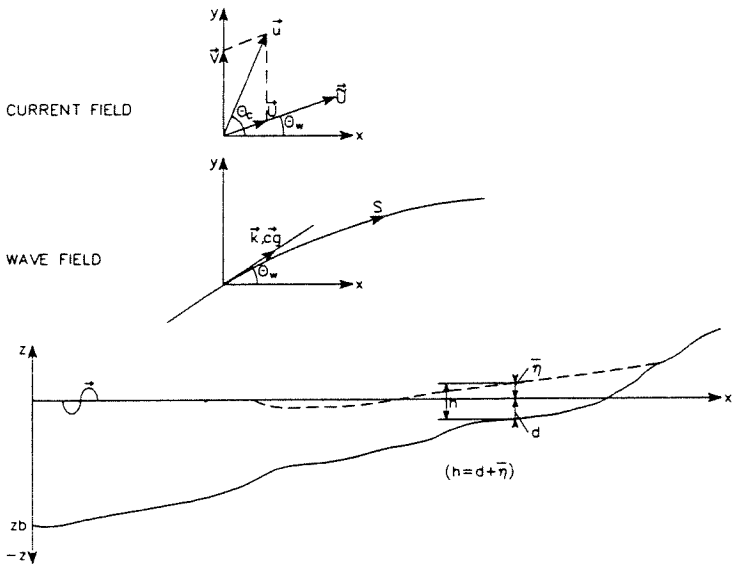

Figure C.1 Definition of coordinate system and domain

Wave propagation model

The wave energy decay model of Battjes and Janssen [1978] is used. It includes the wave energy changes due to bottom refraction, shoaling, bottom dissipation and wave breaking. The current refraction due to the longshore velocity component in the short-wave propagation direction is included as well:

$$\frac{d}{dx}\left[c_g \cos\theta_w \frac{E}{\omega_r}\right] + \frac{D_b}{\omega_r} + \frac{D_f}{\omega_r} = 0$$

where:

$$E = \frac{1}{8} \rho g H_{rms}^2$$

$$c_g = \frac{\partial \omega_r}{\partial k}$$

$$\omega_r = \omega - k \sin\theta_w V \ , \ \omega = 2\pi/T$$

$$\omega_r^2 = gk \tanh(kh)$$

$$D_b = \frac{1}{4} \rho g \alpha_c Q_b (\omega_r/2\pi) H_m^2$$

and:

$$Q_b = \exp\left(-\frac{1 - Q_b}{(\frac{H_{rms}}{H_M})^2}\right)$$

calibration coefficient $\alpha_c = O(1)$

$$H_m = (0.88/k) \tanh(\gamma kh/0.88)$$

$$D_f = \frac{1}{8} \rho f_w \pi^{-1/2} \left(\frac{\omega_r H_{rms}}{\sinh(kh)}\right)^3$$

and:

$$f_w = \exp\left[-5.997 + 5.213 \left(\frac{a_b}{r}\right)^{-.194}\right]$$

a_b is the amplitude of the hor. orbital excursion near the bottom

r is $2.5 \cdot D_{50}$

The turbulent dissipation is derived from the following equation:

$$D = D_b - \rho\beta_f \frac{\partial}{\partial x}(k_s hc \cos\theta_w)$$

where:

$$D = \rho\beta_d k_s^{\frac{3}{2}}$$

The cross-shore momentum equation which is used to calculate the wave induced set-up:

$$\frac{d}{dx} S_{xx} + \rho g h \frac{d\bar{\eta}}{dx} = 0$$

where:

$$S_{xx} = E\left(n(1 + \cos^2\theta_w) - \tfrac{1}{2}\right)$$

$$n = \frac{kh}{2\sinh(2kh)}$$

The wave angle with the shore normal is after Snel's law:

$$k \sin\theta_w = \text{constant}$$

The longshore momentum equation, which describes the balance between the driving forces of the longshore current due to the tide and waves and the bottom friction:

$$\rho g h i_y - \frac{D}{\omega} k \sin\theta_w = A\rho \frac{(1 + \sin^2\theta_w)}{\sqrt{\pi}} \sqrt{(f_w f_c)}\, \tilde{U}|_{H_{max}} V$$

Secondary current

The secondary current is due to the vertical non-uniformity of the driving forces in the nearshore zone. This is modelled according to the formulations given by Stive and de Vriend [1987]. They use a profile function technique in combination with a horizontally two-dimensional current to describe the three-dimensional current system in the coastal zone. The secondary current velocity is estimated using a three-layer concept.

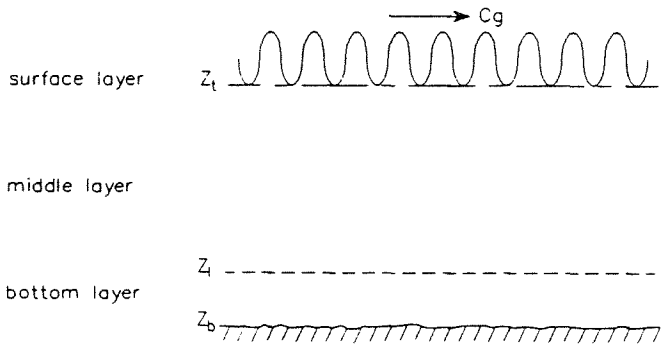

Figure C.2 Three layer concept

The influence of the surface layer on the underlying layers is accounted for by an effective shear stress at trough level [Stive and Wind, 1986]. This compensates for the momentum decay in the surface layer due to viscous dissipation and momentum loss due to wave breaking. The effective shear stress is at wave trough level is given by:

$$\tau(t) = \rho \nu_t \frac{u_b^2 k}{c} \sinh(2kh) + \frac{D}{c}$$

The use of the turbulent dissipation instead of the wave energy dissipation results in a spatial lag between the wave breaking and the offshore directed secondary current.

The horizontal wave-average momentum balance for the middle layer in the cross-shore direction reads:

$$\frac{\partial}{\partial z}\left(\nu_{th} \frac{\partial U}{\partial z}\right) = \frac{\partial}{\partial x}\left(\langle u^2 \rangle - \langle w^2 \rangle\right) + g \frac{\partial \langle z_s \rangle}{\partial x}$$

For the bottom layer the horizontal wave-average momentum equation in the cross-shore direction is given by:

$$\frac{\partial}{\partial z}\left(\nu_t \frac{\partial U}{\partial z}\right) = \frac{\partial}{\partial x}\left(\langle u^2 \rangle - \langle w^2 \rangle\right) + g \frac{\partial \langle z_s \rangle}{\partial x} + \frac{\partial}{\partial z}\left(\langle uw \rangle\right)$$

where the last term on the right-hand side is no longer negligible compared to the Reynolds stress term given on the left-hand side of the equation. With the shear stress condition at the trough level and a no slip condition at the bottom, the solution for the secondary current is obtained by patching the velocities and shear stresses at the bottom boundary z_i. Using the integral condition of continuity:

$$\int_{z_b}^{z_t} Udz = -\frac{m}{\rho}$$

where:

$$m = \left(1 + Q_b \frac{7kh}{2\pi}\right) \frac{E}{c}$$

and m represents the mass flux in the surface layer due to breaking waves yields the final expression for the secondary current.

Long waves

In the case of a random wave field the grouping of the short waves will generate long waves. The assumption is made that the wave-group related features of a random wave field may be represented by a bichromatic wave train with accompanying bound long wave. For the amplitude of the bound long wave is used:

$$\xi_a = -G_{nm} \frac{a_m a_n}{h}$$

The short wave amplitudes are given by:

$$a_n = a_m = \frac{1}{8} H_{rms}^2 - \frac{1}{2} \xi_a^2$$

where the condition that the schematized wave train has the same surface variance as the random wave has been used. The individual velocities are obtained using linear wave theory.

For the long wave component is taken:

$$u_l = \xi_a \frac{\sqrt{gh}}{h}$$

The near bottom time-varying flow due to short and long waves is given by:

$$u_{bi} = \hat{u}_m \cos(\omega_p t) + \hat{u}_n \cos(\omega_p + \Delta\omega)t + \hat{u}_l \cos((\Delta\omega)t + \phi)$$

The beat frequency $\Delta\omega = \frac{1}{5} \omega_p$

Short-wave orbital velocity

The orbital velocities near the bed due to short waves, which determine the strength of the onshore directed wave assymetry transport, have been computed using the model RFWAVE, developed at Delft Hydraulics [G. Klopman, 1989]. It is based on the Fourier approximation of the stream function method as developed by Rienecker and Fenton [1981], using wave energy as input.

Sediment transport

The sediment transport is calculated according to the formulations given by Bailard [1981], of which only the cross-shore component is used for the time-dependent morphological computations. This formulation includes transport due to the combined actions of steady current, wave orbital motion and bottom slope effect. The Bailard transport model in 2 horizontal dimensions is given by:

$$\vec{q}_x = \frac{c_f}{\Delta g N}\frac{\epsilon_B}{\tan\phi}\left[<|\vec{u}|^2\vec{u}_x> - \frac{\tan\beta_x}{\tan\phi} <|\vec{u}|^3> \right] +$$

$$+ \frac{c_f}{\Delta g N}\frac{\epsilon_s}{w}\left[<|\vec{u}|^3\vec{u}_x> - \frac{\epsilon_s}{w}\tan\beta_x <|\vec{u}|^5> \right]$$

$$\vec{q}_y = \frac{c_f}{\Delta g N}\frac{\epsilon_B}{\tan\phi}\left[<|\vec{u}|^2\vec{u}_y> - \frac{\tan\beta_y}{\tan\phi} <|\vec{u}|^3> \right] +$$

$$+ \frac{c_f}{\Delta g N}\frac{\epsilon_s}{w}\left[<|\vec{u}|^3\vec{u}_y> - \frac{\epsilon_s}{w}\tan\beta_y <|\vec{u}|5> \right]$$

where:

c_f : $0.5\ f_w$

f_w : $\exp\ [-5.977 + 5.213\ (a_b/r)^{-.194}]$

$< >$ indicate averaging over time.

The longshore transport is defined as the component of the total transport vector in longshore direction.

The transport formulation contains several velocity moments. The time-averaged total near bed velocity is split up into a mean and a time varying velocity component:

$$u = \bar{u} + \tilde{u}(t)$$

where $\tilde{u}(t)$ stands for the velocity variation on the time scale of the wave groups and that of the individual waves. With these separate terms for the wave-orbital motion and the steady current the terms $<|\vec{u}|^m u_i^n>$, with m = 2, 3, 5 and n = 0,1 can be approximated by a Taylor series. In these series the angle between waves and currents has also been included.

Two Taylor expansions are possible: one with the orbital motion small compared to the steady current and vice versa.

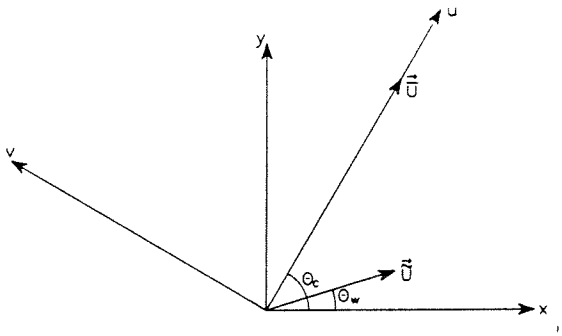

Figure C.3 Velocity directions

The first yields the following expressions for the odd velocity moments in u-direction:

$$<|u_t|^2 u> = \bar{u}^3 + \bar{u} <\tilde{u}^2> (1 + \cos^2\varphi) + <\tilde{u}^3> \cos\varphi$$

$$<|u_t|^3 u> = |\bar{u}|^3 \bar{u} + |\bar{u}| \bar{u} <\tilde{u}^2> (3 + 9\cos^2\varphi)/2 + |\bar{u}| <\tilde{u}^3> (3\cos\varphi + \cos^3\varphi) + \\ + \frac{\bar{u}}{|\bar{u}|} <\tilde{u}^4> (3 + 6\cos^2\varphi - \cos^4\varphi)/8$$

the odd velocity moments in v-direction:

$$<|u_t|^2 v> = \bar{u} <\tilde{u}^2> (2\sin\varphi\cos\varphi) + <\tilde{u}^3> \sin\varphi$$

$$<|u_t|^3 v> = |\bar{u}| \bar{u} <\tilde{u}^2> (3\sin\varphi\cos\varphi) + |\bar{u}| <\tilde{u}^3> (3\sin\varphi + 3\sin\varphi\cos^2\varphi)/2 \\ + \frac{\bar{u}}{|\bar{u}|} <\tilde{u}^4> (3\sin\varphi\cos\varphi - \sin\varphi\cos^3\varphi)/2$$

and the even velocity moments:

$$<|u_t|^3> = |\bar{u}|^3 + |\bar{u}| <\tilde{u}^2> (3 + 3\cos^2\varphi)/2 + \frac{\bar{u}}{|\bar{u}|} <\tilde{u}^3> (3\cos\varphi - \cos^3\varphi)/2$$

$$<|u_t|^5> = |\bar{u}|^5 + |\bar{u}|^3 <\tilde{u}^2> (5 + 15\cos^2\varphi)/2 + |\bar{u}| \bar{u} <\tilde{u}^3> (15\cos\varphi + 5\cos^3\varphi)/2 \\ + |\bar{u}| <\tilde{u}^4> (15 + 30\cos^2\varphi - 5\cos^4\varphi)/8 \\ + \frac{\bar{u}}{|\bar{u}|} <\tilde{u}^5> (15\cos\varphi - 10\cos^3\varphi + 3\cos^5\varphi)/8$$

Where:

$\varphi = \theta_w - \theta_c$.

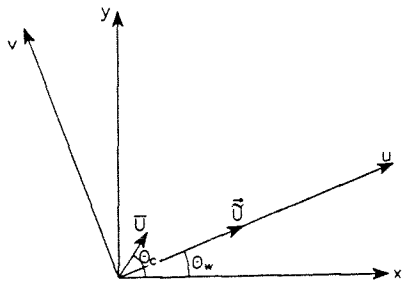

Figure C.4 Velocity directions

If the mean velocity component is small compared to the orbital velocity the Taylor expansion yields for the odd velocity moments:

$$<|u_t|^2 u> = <\tilde{u}^3> + \bar{u} <\tilde{u}^2> (3\cos\varphi) + \overline{u^3} (\cos\varphi)$$

$$<|u_t|^3 u> = <|\tilde{u}|^3 \tilde{u}> + \bar{u} <|\tilde{u}^3|> (4\cos\varphi) + \overline{u^2} <|\tilde{u}|\tilde{u}> (3 + 9\cos^2\varphi)/2 +$$

$$+ \overline{u^3} <|\tilde{u}|> (3\cos\varphi + \cos^3\varphi)$$

the odd velocity moments in v-direction:

$$<|u_t|^2 v> = \bar{u} <\tilde{u}^2> (\sin\varphi) + \overline{u^3} (\sin\varphi)$$

$$<|u_t|^3 v> = \bar{u} <|\tilde{u}^3|> (\sin\varphi) + \overline{u^2} <|\tilde{u}|\tilde{u}> (3\sin\varphi\cos\varphi)$$

$$+ \overline{u^3} <|\tilde{u}|> (3\sin\varphi + 3\sin\varphi\cos^2\varphi)/2$$

and the even velocity moments:

$$<|u_t|^3> = <|\tilde{u}|^3> + \bar{u} <|\tilde{u}|\tilde{u}> (3\cos\varphi) + \overline{u^2} <|\tilde{u}|> (3 + 3\cos^2\varphi)/2$$

$$<|u_t|^5> = <|\tilde{u}|^5> + \bar{u} <|\tilde{u}|^3\tilde{u}> (5\cos\varphi) + \overline{u^2} <|\tilde{u}|^3> (5 + 15\cos^2\varphi)/2$$

$$+ \overline{u^3} <|\tilde{u}|\tilde{u}> (15\cos\varphi + 5\cos^3\varphi)/2$$

$$+ \overline{u^4} <|\tilde{u}|> (15 + 30\cos^2\varphi - 5\cos^4\varphi)/8$$

where:

$\varphi = \theta_c - \theta_w$.

A smooth transition from one formulation to the other is taken care of.

The orbital velocity component is split up into a short-wave and a long-wave component:

$$\tilde{u} = \tilde{u}_s + \tilde{u}_l$$

The long-wave velocity is assumed to be significantly smaller than the short-wave component. A second assumption is that there is no correlation between u_s and $|u_l|^n$. With these assumptions we can write for the following odd velocity moment:

$$\langle \tilde{u}|\tilde{u}|^2 \rangle = \langle u_s|u_s|^2 \rangle + 3 \langle u_l|u_s|^2 \rangle$$

Where the first term on the right is non-zero in the case of an assymmetry about the horizontal plane caused by the non-linearity of the short waves. As mentioned before, this part is calculated with RFWAVE.

The second term on the right is nonzero if there is a correlation between u_l and u_s^2. This correlation is present in the case of long bound waves accompanying a short-wave group, resulting in a negative correlation. In that case the velocity moment is approximated by:

$$3 \langle u_l|u_s|^2 \rangle \approx \langle u_{bi}^3 \rangle$$

where the bi-chromatic velocity component is calculated as described previously. The other velocity moments are expanded in a similar way. In order to reduce computing time, the results have been tabulated as function of two dimensionless variables:

$$f\left(\frac{H_{rms}}{h}, T_p\sqrt{\frac{g}{h}}\right)$$

Morphology

The bottom level changes are computed from the mass balance:

$$\frac{\partial z}{\partial t} + \frac{\partial S_x}{\partial x} = 0$$

APPENDIX D

- CALCULATION OF TRANSPORT WITH THE BAILARD FORMULA

CALCULATION OF TRANSPORT WITH THE BAILARD FORMULA.

Example of calculation of the transport through vertical 9 of experiment A (all the values are taken at Delft scale).

In the Bailard formula applied in UNIBEST_TC the friction factor is given as:

$f_w = \exp((-5.977+5.213(a_b/r)\text{^}-0.194)$

with $r = 2.5*d_{50}$
$A_d = (T_p/2*\pi)*U_d$
$U_d = \pi*H_s/(T_p*\sinh(2*\pi*h/L))$

Applied to experiment A vertical 9:

h = 0.282 m
d_{50} = 0.000095 m
T_p = 2.07 s
H_s = 0.1 m
L = 6.69 m
g = 9.81 m/s^2

$$U_d = \frac{\pi * 0.1}{2.07 * \left(\frac{e^{2*\pi*0.282/6.69} - e^{-2*\pi*0.282/6.69}}{2} \right)} = 0.5654 \text{ m/s}$$

$$A_d = \frac{2.07}{2*\pi} * 0.5654 = 0.1863 \text{ m}$$

$r = 2.5 * 0.000095 = 0.0002375$ m

$$f_w = e^{\left(-5.977+5.213*\left(\frac{0.1863}{0.0002375} \right)^{-0.194} \right)} = 0.0106$$

The instanteneous bed load and suspended load transport rates are expressed as:

$$q_{b,w} = \frac{c_f}{\Delta g N} \frac{\varepsilon_b}{\tan\varphi} \left[\langle |u|^2 u \rangle - \frac{\tan\beta}{\tan\varphi} \langle |u|^3 \rangle \right]$$

$$q_{s,w} = \frac{c_f}{\Delta g N} \frac{\varepsilon_s}{w_s} \left[\langle |u|^3 u \rangle - \frac{\varepsilon_s}{w_s} \tan\beta \langle |u|^5 \rangle \right]$$

in which:
$q_{b,w}$ = instanteneous wave-induced bed-load transport (m^3/m'/s)
$q_{s,w}$ = instanteneous wave-induced suspended load transport (m^3/m'/s)
u = instantaneous near-bed orbital velocity (m/s)
ε_b = efficiency factor for bed-load transport (0.1-0.2)
ε_s = efficiency factor for suspended load transport (0.01-0.02)

c_f = friction factor based on the particle diameter = ½ f_w, (-)
β = bottom slope (o)
φ = dynamic friction angle (tanφ = 0.6), (o)
w_s = fall velocity of bed material (m/s)
N = ratio of sediment volume to total volume bed material (-)

Applied to experiment A vertical 9:

f_w = 0.0106
ρ = 1000 kg/m^3
ρ_s = 2650 kg/m^3
g = 9.81 m/s^2
ε_b =0.15
ε_s =0.02
tanφ = 0.63
tanβ = 0.0667
w_s = 0.01 m/s
N = 0.4

$\langle|u|^2u\rangle$ = -0.000399 m^3/s^3 (*)[1]
$\langle|u|^3\rangle$ = 0.004833 m^3/s^3
$\langle|u|^3u\rangle$ = -0.0001564 m^4/s^4
$\langle|u|^5\rangle$ = 0.000345 m^5/s^5

$$q_{b,w} = \frac{½ * 1000 * 0.0106 * 0.15}{(2650-1000) * 9.81 * 0.4 * 0.63}\left[-0.000399 - \frac{0.0667}{0.63} * 0.004833\right]$$

= -1.7749e-07 m^3/m'/s

$$q_{s,w} = \frac{½ * 1000 * 0.0106 * 0.02}{(2650-1000) * 9.81 * 0.4 * 0.01}\left[-0.000156 - \frac{0.02}{0.01} * 0.0667 * 0.000345\right]$$

= -3.3075e-07 m^3/m'/s

$$q_{tot} = q_{b,w} + q_{s,w} = -1.7749e-07 + -3.3075e-07 = -5.0823e-07 \text{ m}^3\text{/m'/s}$$

At t1(=30 min) the total transport is:
S_{xx}= 30 * 60 * -5.0823e-07 = -9.1482e-04 m^3/m'

The transport measured in Delft through vertical 9 experiment A is -1.0085e-03 m^3/m'.
The ratio is -1.0085e-03 / -9.1482e-04 = 1.1024

(*)[1] Velocity moments include only the oscillatory contributions.

APPENDIX E

- **INPUT PARAMETERS UNIBEST_TC**

INPUT PARAMETERS UNIBEST_TC

Definition of the profile

mean sea level: h_0 = 0.65 [m]

Definition of gridpoints (see table E.1)

The grid is made taking into account the positions where the velocity measurements in Barcelona have been taken, because values at these points are needed to be able to make a comparison. The first part of the slope is constructed from concrete and there is not a lot of transport down the slope, so the grid is taken quite wide. In the area near the breakwater and the first part shoreward of the breakwater where the most transport is taking place the grid is fine. In the last part the changes are rather small and the grid is taken larger.

Number of Δx [-]	Δx [m]	From / until [m]
10	0.50 m	-3.00 m - 2.00 m
1	0.15 m	2.00 m - 2.15 m
2	0.40 m	2.15 m - 2.95 m
1	0.55 m	2.95 m - 3.50 m
14	0.05 m	3.50 m - 4.20 m
4	0.04 m	4.20 m - 4.36 m
7	0.05 m	4.36 m - 4.71 m
8	0.09 m	4.71 m - 5.43 m
1	0.08 m	5.43 m - 5.51 m
8	0.09 m	5.51 m - 6.23 m
1	0.08 m	6.23 m - 6.31 m
1	0.09 m	6.31 m - 6.40 m
16	0.10 m	6.40 m - 8.00 m
1	0.30 m	8.00 m - 8.30 m
1	0.20 m	8.30 m - 8.50 m
14	0.25 m	8.50 m - 12.00 m

Table E.1 Definition of gridpoints in UNIBEST_TC

Wave conditions

For the wave height is taken the average value of H_{rms} measured at x = -3.00 meter over the whole duration of the experiment in Delft (see table E.2).
For the period is taken the peak period of the input of the wave board (see tableE.2)

General parameters

wave breaking parameter	gamma	=	0.75 [-]
wave breaking parameter	alfac	=	1.00 [-]
friction factor	fw	=	0.01 [-]
bottom roughness	rkls	=	0.05 [m]

experiment	H_{rms} [m]	T_p [s]	ε_b [-]	ε_s [-]
exp A without breakwater	0.069 m	2.07 s	0.15	0.02
exp B without breakwater	0.071 m	1.55 s	0.20	0.03
exp C without breakwater	0.069 m	1.29 s	0.10	0.01
exp D without breakwater	0.100 m	1.81 s	0.20	0.03
exp E without breakwater	0.048 m	1.29 s	0.10	0.03
exp A with breakwater	0.080 m	2.07 s	0.20	0.03
exp B with breakwater	0.084 m	1.55 s	0.20	0.03
exp C with breakwater	0.074 m	1.29 s	0.20	0.03
exp D with breakwater	0.101 m	1.81 s	0.20	0.03
exp E with breakwater	0.049 m	1.29 s	0.20	0.03

Table E.2 Input values of the wave characteristics and transport coefficients per experiment.

Sediment parameters

Coefficient bottom transport	epsb (ε_b)	=	depending on the experiment (see table E.2) [-]
Coefficient suspended transport	epss (ε_s)	=	depending on the experiment (see table E.2) [-]
sediment fall velocity	wee (w_s)	=	0.01 [m/s]
tangent of internal friction angel	tanf ($\tan\varphi$)	=	0.63 [-]
50 % grain diameter	dsed (d_{50})	=	95 e-06 [m]
sediment density	rhos (ρ_s)	=	2650 [kg/m^3]
sediment porosity	por (N)	=	0.4 [-]

Run parameters

The smallest possible timestep is taken (t = 0.01 day). The in Delft performed experiments lasted 7.5 hours, so the number of timesteps is 32.

Optional parameters

definition of 'dry' Tdry = 21 [-]

(T_{dry} = computations carried out up to the point where the relative wave length becomes too great; depth < g * $(T_p/T_{dry})^2$; depth ≈ 0.05 m)